Modelling of planimetric/historical changes of the Geul river (The Netherlands)

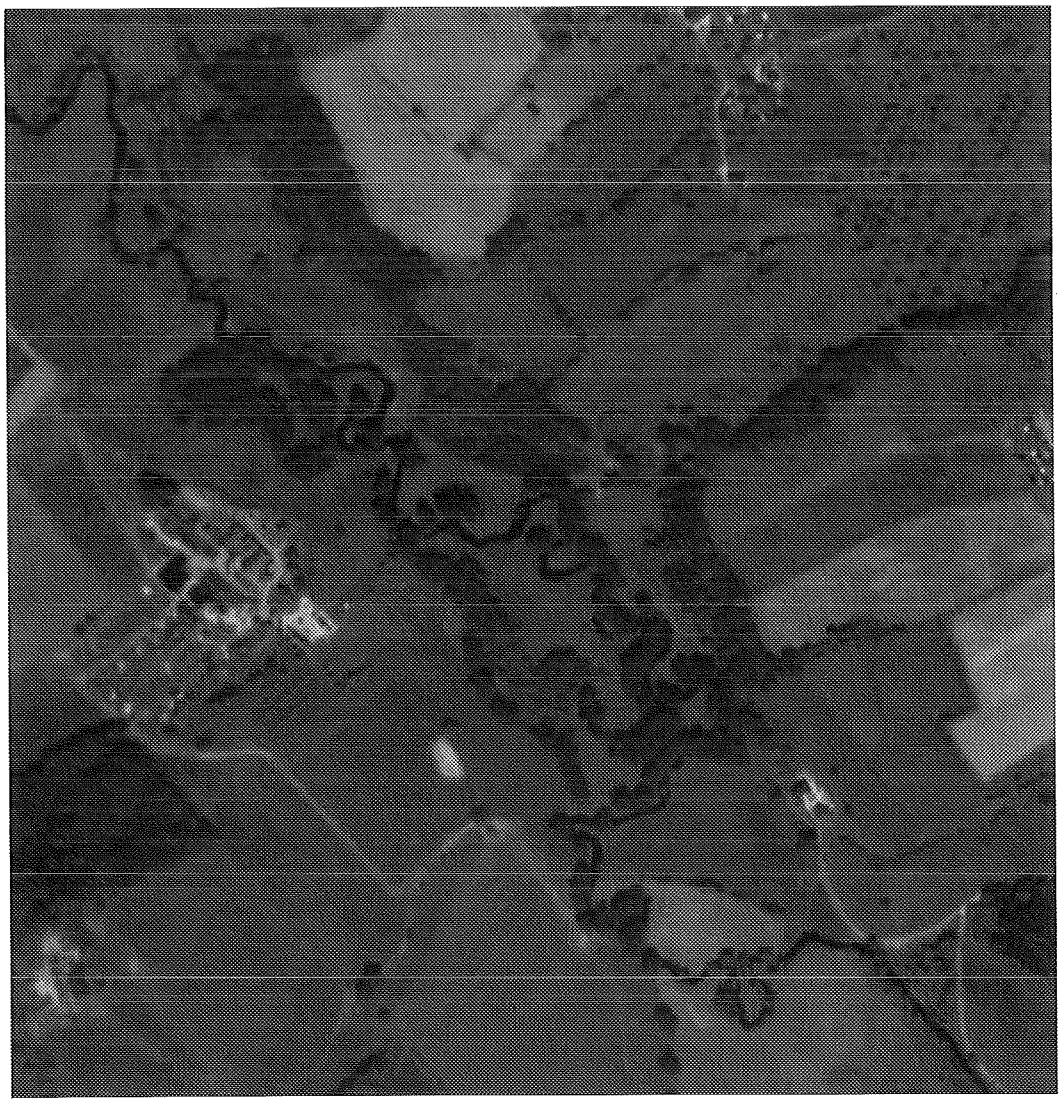

Eva Miguel Alfaro
August 2006

Delft University of Technology

Preface

This report will be the guiding line of the Msc. thesis "Modelling of planimetric/historical changes of the Geul River".

The thesis is a part of the graduation program of the Civil Engineering School in the UPC (Universitat Politècnica de Catalunya, Barcelona, Spain) and in the Ecole de Ponts et Chaussées (ENPC, Paris, France), and will be finalised in an exchange program in the Hydraulic Engineering Department, faculty of Civil Engineering and Geosciences, Delft Technical University, in cooperation with the Vrije Universiteit Amsterdam (VUA).

In this study the meandering processes of the Geul river (The Netherlands) have been examinated using the river migration model Miandras. The applicability of the model to simulations of the planform changes of this river has been analysed.

Many people have been involved in different ways to the successful accomplishment of this work. I would like to express my gratitude to ir. Alessandra Crosato for her explanations, comments, answers and advices. I also thank ir. J. de Moor for providing all the necessary inputs and for his answers and for his guiding during the site visit. Prof.dr.ir. H.J. de Vriend, dr.ir. I. Overeem and dr. R.T. van Balen for their assistance. I would also like to thank ir. M. Baptist for his help in the research of articles. I express my gratitude to Delft Hydraulics and especially to J. Overmaas for his help with ArcGis program.

I especially thank my family and Ricardo for their encouragement and support through these months.

Eva Miguel Alfaro
Delft
August 2006

Abstract

This report presents the analyses and conclusions of a study on the planform evolution of the Geul river in the last 80 years. The results are compared with those of studies carried out by the Vrije Universiteit Amsterdam (VUA).

The Geul river is to tributary of the Meuse River (The Netherlands). It has been straightened and protected against the erosion in the past, but since 1980 some stretches are allowed to meander freely. A meandering stretch near the Belgian border has been analysed.

Historical planform changes are analysed with aerial photographs between 1935 and 2003. Channel migration is observed through the movement of the centreline of the river for each photograph. Channel width evolution, the presence of trees and its effects are also studied from the photos.

In order to simulate the planform changes of the Geul river, the river planform model Miandras (Crosato, 1990) has been applied.

Flow parameters (discharge, Chézy factor...) are analysed and discussed. After the calibration of some of them, erodibility coefficients needed for Miandras computations are obtained.

The results of the aerial photos analysis show that bank erosion and channel width increase with time, as expected, due to the bank protection removal. Bank stability analysis is more affected by the properties of riverbanks than by the flow properties. The flowing ground water from the hills to the rivers and though the valley has an importance influence of the stability.

Centreline coordinates obtained from the aerial photos are affected by inaccuracies in the photos, and the river migration obtained from them does not correspond with the one observed in field analysis. This renders aerial photos unsuitable to monitor small displacements of this type of rivers.

The results obtained with Miandras reproduce the migration trend as derived from the field observations for a short scale of time. This means that a prediction for a period of few years is possible.

Contents

1- Literature review

This chapter summarizes the most important ideas and results from the literature study. The chapter deals with:

- Types of rivers and description of meandering rivers
- Meandering river process
- Theories on river meandering
- Effects of vegetation

1.1- Types of rivers and description of meandering rivers

1.1.1-Meandering rivers

Water flowing in an alluvial channel tends to be sinuous, not to flow in a straight line. A meander is a bend in the river; since a meander is formed, its presence only influences more meandering.

Meandering rivers have alternating bends that are characterised by a point bar at the inner bank and a deep pool at the outer bank.

Erosion takes place along the concave (outer) banks whereas deposition occurs along the convex (inner) banks (Figure 1.1). This bank erosion process is a combination of particle entrainment by the water flow and bank failure of the outer bank. Eroded material is transported and deposited farther downstream.

This process of erosion and deposition causes the typical migration phenomenon of river meanders, which consists of downstream translation, lateral extension and set-backs by meander cut-offs.

Channel migration is a slow process visible only in the time span of years.

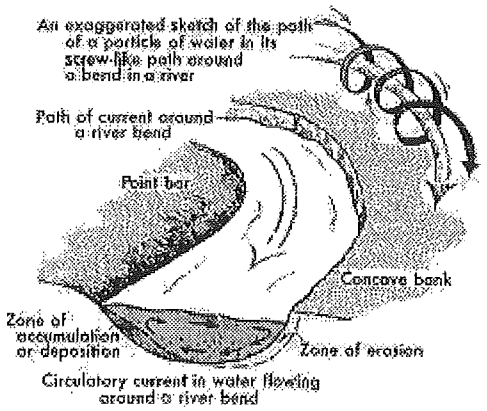

Figure 1.1: The effect of curved channel (Colorado Water Resource, 1995)

Meander bends are eventually cut off when the curvature becomes very tight. The result is oxbow lakes throughout a valley.

1.1.2-Channel Patterns

Channel pattern is the planimetric geometry or the form of the channel when viewed from above. This pattern represents a form of adjustment in the horizontal plane and influences the resistance to the flow.

The major planform properties are: channel sinuosity, presence of point bars, degree of braiding and anabranching (Figure 1.2).

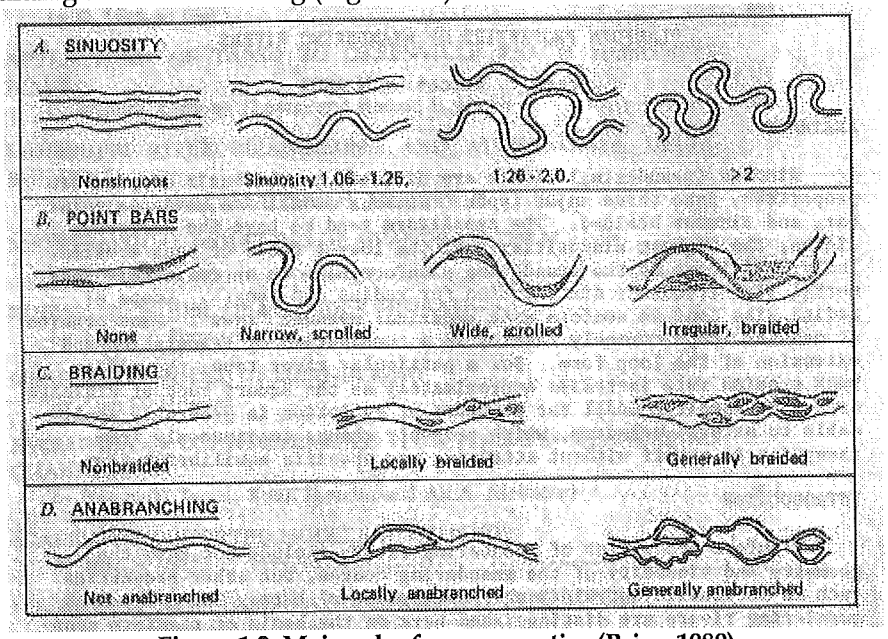

Figure 1.2: Major planform properties (Brice, 1980)

The sinuosity is the ratio between the channel length and the valley length. Channels sinuosity can be a function of river discharge, channel gradient, sediment flux, and substrate erodibility, and rivers remain straight if little or no lateral erosion is possible.

Two important parameters to describe a meander are the length and the amplitude, which permit to set the sinuosity. Leopold (1964) suggested that the sinuosity values are situated between one and four.

A point bar is a non-migrating deposit of sediment at the inner side of river bends. In meandering rivers the point bar tends to increase with the erosion along its opposite bank.

A braided river is divided by small mid channel bars or islands. Their characteristic feature is the repeated division and joining of channels (Robert, 2003). Following patterns of convergence and divergence, the planimetric configuration of braided rivers changes rapidly. Braided rivers have a high width/depth ratio and their cross sections are wide and shallow.

Braiding has been attributed to many causes (Tierney, 2001):

- highly erodible banks,
- steep river gradients,

- lack of river competence, due to an abundant and coarse bed load,
- highly variable discharge.

If the width of these bars is large in relation with the channel width, then the river is considered an anabranched river. A characteristic of anabranched rivers is that their planimetry is more stable than that of braided rivers.

An anabranching river consists of multiples channels separated by stable islands, which usually persist for decades or centuries, unlike the more transient bar of braided systems, and they are at the same level as the surrounding floodplain. Each channel of anabranching systems behave as independent channels. Characteristics of these systems can be assessed in relation to the continuum of the river channel patterns by using three variables: flow strength, bank erodibility and relative sediment supply (Knighton and Nanson, 1993).

1.1.3-River classification based on planform

According to planimetric properties, four major river types can be distinguished (Brice, 1980): sinuous canaliform, sinuous point bar, sinuous braided and non-sinuous braided (Figure 1.3).

A typical sinuous canaliform river is characterized by narrow crescent-shaped point bars, a uniform width, a lack of braiding, and a moderate to high sinuosity. This river type tends to be associated with a substantial degree of bank resistance (owing either to bank vegetation or to clay content) relative to slope and discharge. The bed material is typically sand or silt, but it may be gravel.

Sinuous point bar rivers tend to increase in width at the apexes of bends, and to have prominent bare point bars that are visible at normal stage. Point bars are typically scrolled, although the prominence of these scrolls is highly variable from one river to another. Bank resistance (relative to slope and discharge) is lower than for canaliform rivers. Bed material is commonly sand or gravel, but with an increasing proportion of gravel bends tend to become more irregular.

As bank resistance decreases or the quantity of bed-material load increases, the degree of braiding tends to increase, the point bars become more irregular, and the river type changes to sinuous braided. The river is wider with increased sandbars or depositional areas.

With a further decrease in bank resistance or increase in bed material load, the channel becomes less sinuous and more braided; no point bars are visible along the sides of the channel, and the river becomes non-sinuous braided.

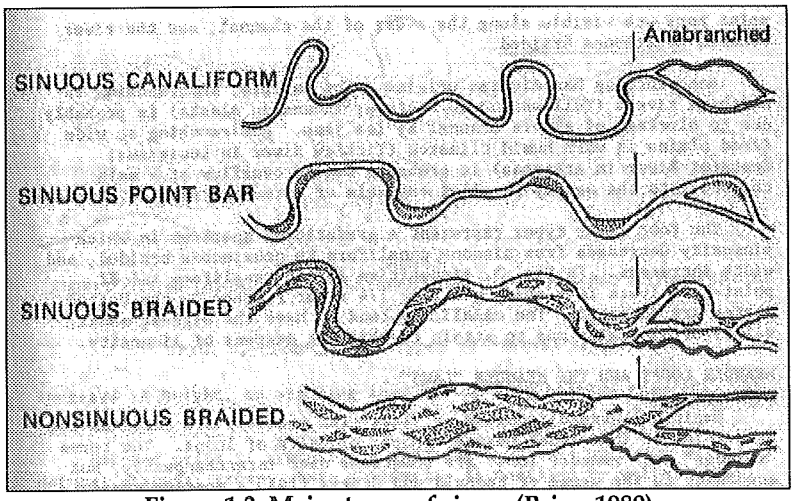

Figure 1.3: Major types of rivers (Brice, 1980)

1.1.4-Meander planform characteristics

Leopold and Wolman (1957) related the channel patterns to the channel slope and the bankfull discharge. The empirical relation that they found suggests that one river can develop either meandering (single channel) or braided (number of channel).

Anderson (1967) and Werner (1951) suggested that the meander initiation surges of a straight channel. The transverse velocity in some section produces a rise in bed level in one bank. Then main current causes the surge thus initiated to move obliquely to the opposite bank in attenuated form. The natural period involved is:

$$\theta = 2\pi\sqrt{MK}$$

with θ: related with Froude number; M: water mass involved; K: spring force

Planform studies have attempted to characterize the shape of an individual bend or pair of bends when viewed from above using a variety of mathematical functions. Early investigators examined circular, parabolic, and sine curves before deciding that a sine-generated curve best resembles an idealized meander (figure 1.4).

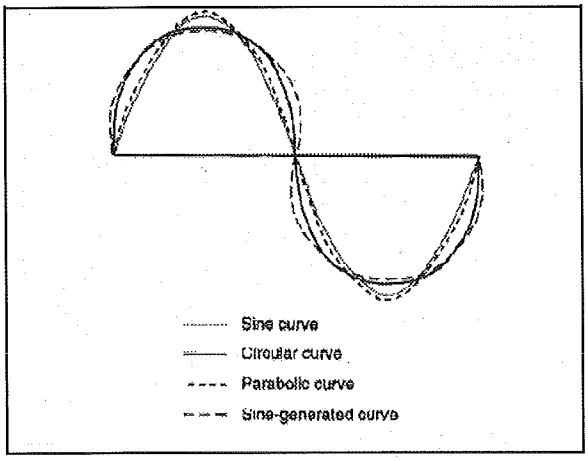

Figure 1.4: Mathematical functions used to represent meander shape

However, Leopold and Langbein also noted that, unlike the simple geometric shapes they investigated, real meander bends are rarely symmetrical. Much subsequent work has failed to produce a function that describes meander form to the general satisfaction of academics (Ferguson, 1973; Carson and Lapointe, 1983). It is recognized that attempts to find a complex function capable of accurately representing idealized planform for a meander are probably futile. Carson and Lapointe recommend that sine-generated models of meander shape should be discarded but do not suggest an alternative function to be used. Although Chang reports on flow paths and migration of symmetrical bends, Whitesell concluded that asymmetry is inherent to meander bends.

Few natural meanders display a classic or idealized planform in any case, due to non-uniformity in the bed and bank materials or variation in entrance flow conditions.

Studies of planform of meandering reaches were initially based on mapping, and Dort's investigation of historical changes to the Kansas River and its tributaries from 1857 to 1868 and 1976 provides an excellent example of what can be achieved. Analytical work based on historical maps is hampered by uncertainties concerning the accuracy of the maps and the criteria used. Planform studies using maps and aerial photographs have yielded a number of empirical relationships for a reach-scale meander geometry and scale.

Based on their results, Chang and Toebes (1980) concluded that the geological history of channel development, as well as the current flow regime, influences equilibrium meander form and they suggested that bend radius better represents meander geometry than wavelength. They also found that average discharge better represents river size than bankfull discharge.

Brice (1974) has proposed using the aerial photographs for meander planform analysis, amassing a large collection of historical aerial photographs for over 350 rivers. He used his collection to develop a classification of meander forms and a method to assess channel stability based on aerial photographs. Brice's work is significant because it both founded and established the practical utility of contemporary and historical aerial photographs for meander classification, stability analysis and migration prediction. Of particularly relevance to the study of meander migration was Brice's discovery that it permits to observe that the width of actively meandering channels varies systematically with planform position. Active meanders tend to be wider at bends than at crossing, while meandering channels that do not exhibit this trait are static for long periods.

Hickin & Nanson (1975), conducted important studies of bend form and evolution based on historical analysis of the Beatton River in North Eastern British Columbia (Canada). Initially, the history of meander evolution was inferred from scroll bars left on the floodplain. They suggested the existence of a relationship between bed migration rate and the ratio of half width to centre-line radius of curvature of river bends.

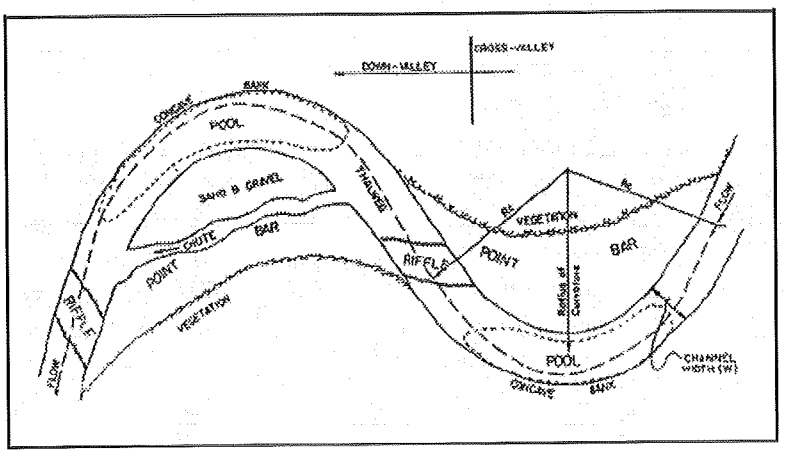

Figure 1.5: Planform features and geomorphic surfaces

Many subsequent studies have reinforced their basic description of the stages of bend development. Ferguson (1983) developed a simulation model of which the empirical support comes from the work of Hickin & Nanson (1975). He demonstrated that asymmetric beds and secondary loops can develop from a regular waveform, such as the sine-generated curve, through the operation of relationship between local channel curvature and migration rate. Since it involves only time and geometry, and not mass or force, Ferguson's meander migration model is a cinematic rather than a dynamic model.

Some of the variability may be explained by boundary conditions, such as the erodibility or mass stability of the outer bank of the bend. Biedenharn (1989) showed that bends on the Red River in Arkansas that encountered clay plug, backswamp or Pleistocene materials migrated much slower than those eroding banks formed in meander belt sediment.

A further source of variability was revealed by observations of channel evolution on the Lower Mississippi River by Larsen and Shen (1989). They found that the sinuosity of 55 bends increased progressively over long periods of time. When sinuosity became large, the bend was cut off, with the life span of a bend being of the order of 600 years. However, the occurrence of a cut-off not only reduces the sinuosity of the cut-off bend, it also influenced adjacent bends upstream and downstream.

This phenomenon was also observed by Hooke (1995) following both neck and chute cut-offs on the meandering River Bollin in England. These studies demonstrate that the rate of erosion at a given bend is determined not only by geometry of that bend, but also the evolution of the bends immediately upstream and downstream (Howards, 1996).

1.1.5-Style of meander change

The points of maximum bank erosion within a bend change as the bend evolves and so does the primary direction of meander movement. The complexity of meander growth, migration and distortion is codified in a number of styles of change.

Bends grow in a direction that is transverse to the valley axis (Leeder, 1975); it has been referred to as "extension" (Knighton, 1984). This pattern of development occurs because maximum erosion is located close to the bend apex.

Bend migration is referred to as "translation" (Bagnold, 1960; Knighton, 1984). Under these circumstances, the zone of maximum bank erosion is located downstream of the bend apex. However, meander bend activity is by no means limited to growth and migration; bends also display changes described in terms of rotation and combinations of extension, translation and rotation. Hooke (1977) synthesized the results of several previous studies to suggest the following styles of meander changes (Figure 1.6):

Simple	Combined
Extension	Extension and Rotation
Translation	Extension and Translation
Rotation	Rotation and Translation
Enlargement	
Complex	

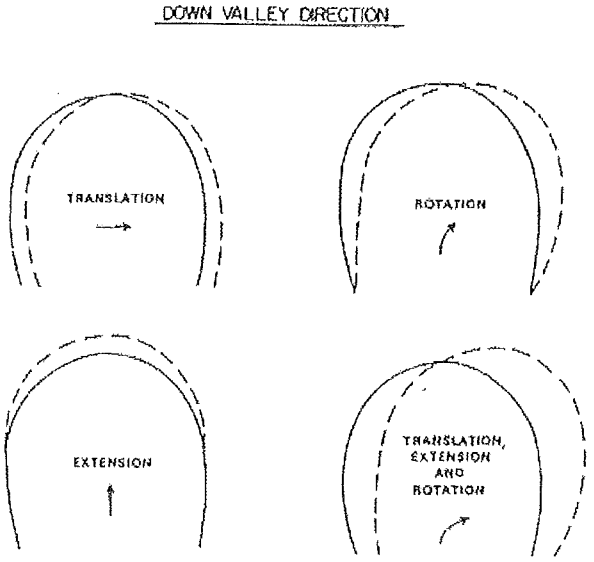

Figure 1.6: Style of change displayed by meander bends (Adapted from Knighton, 1984).

Stable reaches, unstable reaches and reaches with changing channel pattern within a given stream co-exist, so that there is no single style of meander change that can be applied to describe planform change in the system.

Meander bends eventually cut-off when two bends become in contact with each other or during flow when the stream takes another course by excavating a new channel.

There are four types of cut-offs (Erskine et al., 1992): neck cut-off, chute cut-off, mobile bar, and bend flattening (Figure 1.7).

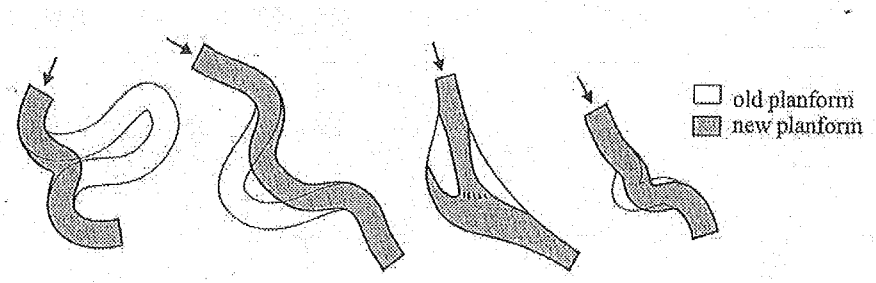

Figure 1.7: Sketches illustrating the four cut-off types: (1) neck cut-off, (2) chute cut-off, (3) mobile bar cut-off, (4) bend flattening (van Houter, 2003)

Neck cut-off is defined as a cut-off that connects two parts of the river that are separated by less than one channel width. There are two types of neck cut-offs depending on the process that creates the final gap. In both cases the point bar progressively narrows in one place due to lateral migration of the upstream and downstream meander bends. The first type consists of the migration of the two limbs of the meander that finally meet leading a breach (bank erosion). This neck cut-off is the dominant shortening process for meandering river with narrow channels, vegetated banks and low gradients (Howards and Knutson, 1984). The second type considers the case that cut-off may form during high flow a new channel by incising across the narrow meander neck.

A chute cut-off is a cut-off resulting from local flow acceleration. It may occur along the inside of a meander bend. This kind of cut-off occurs most frequently where curvature is strong, during high flood discharges, especially in rivers with wide channels, poorly cohesive, weakly vegetated banks and high gradients (Howards and Knutson, 1984).

The mobile bar cut-off can be interpreted as a submerged chute cut-off (Lewis and Lewin, 1983).

Bend flattening is related to the formation of the concave bank benches and the associated reduction in channel curvature due to point bar erosion (Matthes, 1948; Erskine and Melville, 1982). This process is not associated with a discrete shift in channel course, but a change in migration direction. It will reduce the river length, but it does not lead to a new cut-off channel.

1.1.6-Channel cross section

Along the entire length of a river, shape and size of cross sections are in constant variation, adapting to discharge, sediment load contributed by the reach upstream and bank erodibility.

Cross section definition can be based on morphology (guided by minimum width/depth ratio, bend index, definition of active channel, height of point and alluvial bars), sediment and ecological character using trees, grass, shrubs, indicator species, and evidence from recent floods events.

In meandering rivers the cross-sectional profile can present a nearly symmetric rectangular shape, in the transition stretch between two bends (section B), and more asymmetrical shape inside bends (sections A and C) (Figure 1.8).

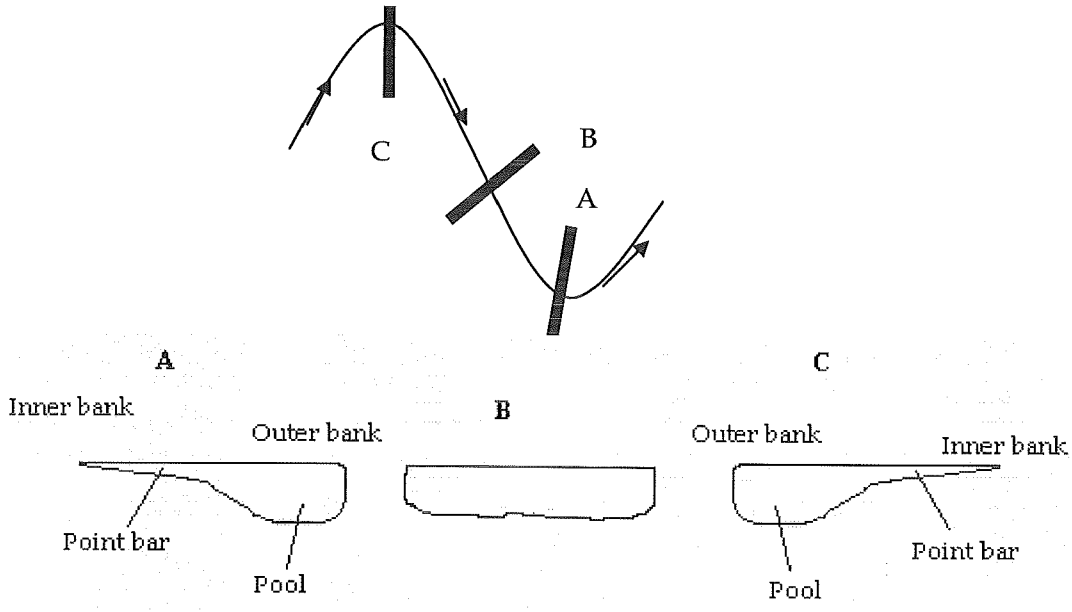

Figure 1.8: Cross section profile

In the scheme, sections A and C represent a bend cross section. In C section, the pool is situated on the left (according to the flow direction), where flow erodes bed and bank. In A section, the same situation occurs on the right.

This cross-sectional shape is caused by the flow, as an interaction of a main flow (which is the responsible of the erosion) (Farther in 1.1.5) and of a secondary flow (circular motion), which tends to deposit the material at the inner side of bends (Figure 1.1). The effect of the secondary flow in relation with bank erosion is negligible when it is compared to the effects of the primary flow.

Asymmetric sections occur at river bends, where the current is concentrated near to the outer bank of the meander, creating a deep-water pool, where the highest velocity and gradients are located. In the inner bank, the channel is less deep and the sediment is deposited forming a slope from the point bar towards the outer bank.

The symmetric sections occur at the cross-overs. The highest flow velocities and the highest velocity gradients are located near the centre of the channel, with the lowest gradients occurring near the margins.

The bottom in these "rectangular" sections consists of a series of undulations, which represent the transverse cross-sections of several longitudinal ridges.

Flow velocity across symmetric sections is controlled by a complex of factors. If the longitudinal gradient of the bed increases, the flow velocity should also increase. But if the channel is broad and shallow, the ratio of wetted perimeter to cross-sectional area

increases and the roughness of the channel bed are slightly greater than in the meander bends. Then the current slow down.

Studies show that width and depth tend to vary regularly with stream discharge. If discharge is held constant and width decreases then the channels hold deepen by scouring. This occurs as a result of the increased velocity and transportation power which accompanies the narrowing of a channel.

1.1.7-Flow in river bends

The dominant flow structure in a river bend is the helical flow (Jansen, 1973), which appears as a result of interaction of centrifugal force and the pressure gradients.

Due to the curvature, water level is higher at the outside (Figure 1.9). This creates a uniform pressure gradient from the outside to the inside.

This pressure interacts with centrifugal force (function of velocity). This velocity is higher at top levels, which causes a non uniform distribution along the vertical.

The result is a distribution inside the channel as shown in Figure 1.8, and the origin of the transverse (circular) flow, which combined with the longitudinal flow, gives rise to the helical flow. Near river banks the flow is vertical which means that the flow in river bends is three-dimensional (Figure 1.10).

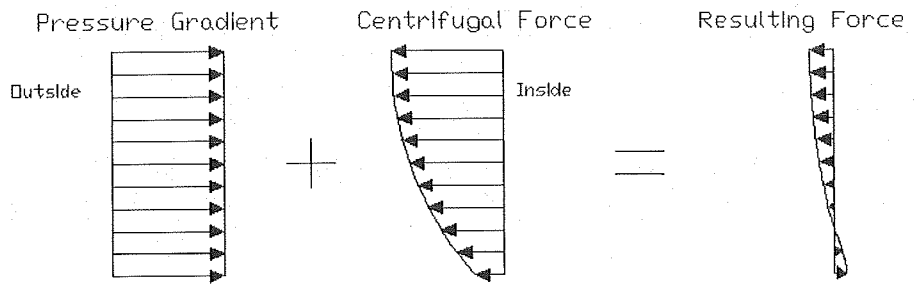

Figure 1.9: Schematization of forces in transverse direction

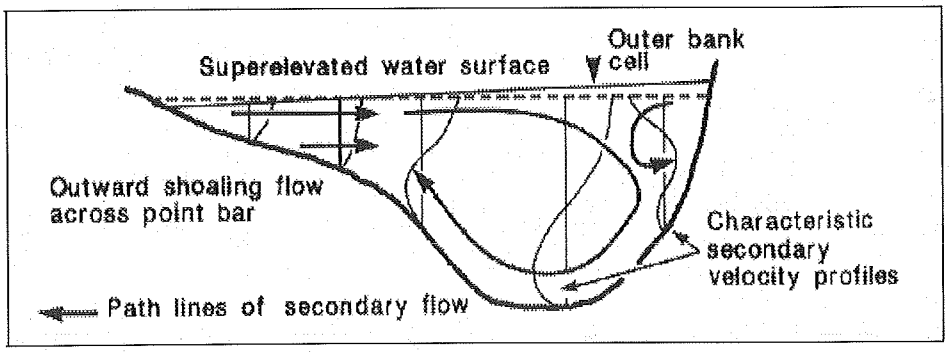

Figure 1.10: Secondary flows in a cross section (sharp curvature) (Powell, 1998)

The distribution of flow field in a curved open channel is represented in Figure 1.8. The "primary flow" is the depth-averaged flow or the flow computed with a two-dimensional model in which a logarithmic velocity profile is imposed

The so-called "secondary flow" is all derivations from this flow, with longitudinal and transversal components.

In highly curved bends, the secondary flow covers a large part of the cross-section and, in the non-covered part, there are some secondary circulation cells (Figure 1.11), which flow in the opposite direction and generally take place near the outer bank. Although relatively weak and small, these circulation cells are important as they protect steep outer banks from erosion (Christensen et al., 1999; Blanckaert & Graf, 2004).

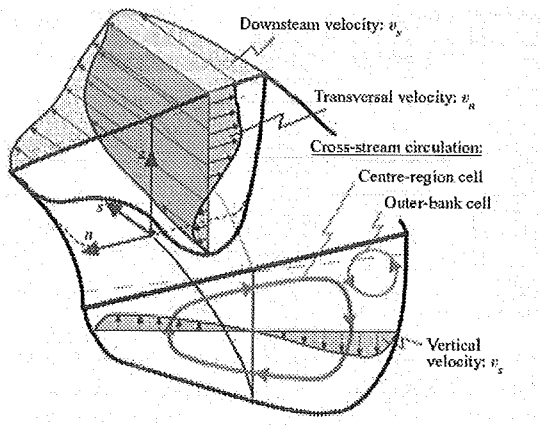

Figure 1.11: Definition sketch of sharp curved open-channel flow (Blanckaert and de Vriend, 2003)

Improved understanding of the flow pattern is important, because it explains the characteristic cross profile of the point bar. Natural point bars consist of a flat upper surface, which is dominated by outward flow, separated from a steep lower surface, which is dominated by helical flow and by a sharp depositional edge.

1.1.8-Mathematical description of flow in river bends

The complexity of mathematical procedures needed for the description of the river flow depends strongly on the number of dimensions involved. Flow in rivers is generally variable in time: it is unsteady. For practical applications, however, the variation may be considered so slow that a steady (or quasi-steady) flow situation can be assumed for low-land rivers. Considering the spatial distribution of flow, it can be concluded that it is essentially three dimensional and that direction and magnitude of the flow vary from one point to another.

The two-dimensional description involves a kind of averaging, which may influence the results.

The motion equations describe the conservation of mass and the conservation of linear momentum (as expressed by Newton's second law) using the Navier-Stokes equations:

Conservation of mass:

$$\frac{d}{dt}\int_V \rho dV = 0$$

Conservation of linear momentum:

$$\frac{d}{dt}\int_V \rho v dV = \int_S t dS + \int_V \rho f dV$$

in which: ρ : water density
v : fluid velocity
t : traction vector
f : body force density

1.2- Bank erosion and accretion

1.2.1-Riverbank erosion

Riverbank erosion consists of the detachment and removal of bank material. It is often caused by a combination of two different mechanisms: mass failure and hydraulic action (fluvial entrainment and subaerial weakening) (Richards, 1982; Knighton, 1998; Thorne, 1998).

The nature of the responsible processes depends on the geotechnical properties of the bank material. The presence or absence of cohesion has particular importance. Two kinds of banks are distinguished: non-cohesive and cohesive.

Non cohesive banks: material is usually detached and entrained grain by grain. Stability depends on the balance of the forces acting on superficial grains. The forces governing the process are the downslope component of submerged weight and the applied fluid forces of lift and drag. Resisting forces are the slope-normal component of submerged weight and inter-granular forces due to friction and inter-locking, which can be a major source of erosion resistance in alluvial deposits.

Cohesive banks: material is usually eroded by the detachment and entrainment of aggregates or crumbs of soil. The forces governing the process are the same as those for non-cohesive banks, but the resisting forces are primarily the result of cohesive bonds between particles and aggregates. The bonding strength and therefore the bank erosion resistance, depends on the physico-chemical properties of the soil and the chemistry of the pore, and eroding fluids.

Mass failure is the slumping or collapsing of the riverbanks under the influence of gravity (Figure 1.13and 1.14) It is influenced by bank geometry, structure and material. It is typical on cohesive banks.

Some of the particular processes which reduce the strength of the bank are:

- toe erosion by the flow or increased bank height and verticality due to higher erosion in the lower part of the bank or to near bank bed erosion.

- wetting and drying factors: the swelling and shrinking of clay particles can weaken the bank (reduces shear stress needed for the bank to fail),

- freezing and thawing cycles: water freezes and expands slightly, opening up pores. When the water melts the pores remain open; this is an important process in creating aggregates,

- pore water movement: it consists of the creation of soil water pipes,

- saturation and slaking: within the river bank, pore spaces are filled by water and air. As the bank is submerged in water, the water from the river forces its way into the bank. This water compresses the water and air already in the soil pore spaces. As the water in the channel decreases, water and air are still under pressure, which is released through the bank itself, forcing the surface material off the bank.

In figure 1.12, we can observe some different types of failure.

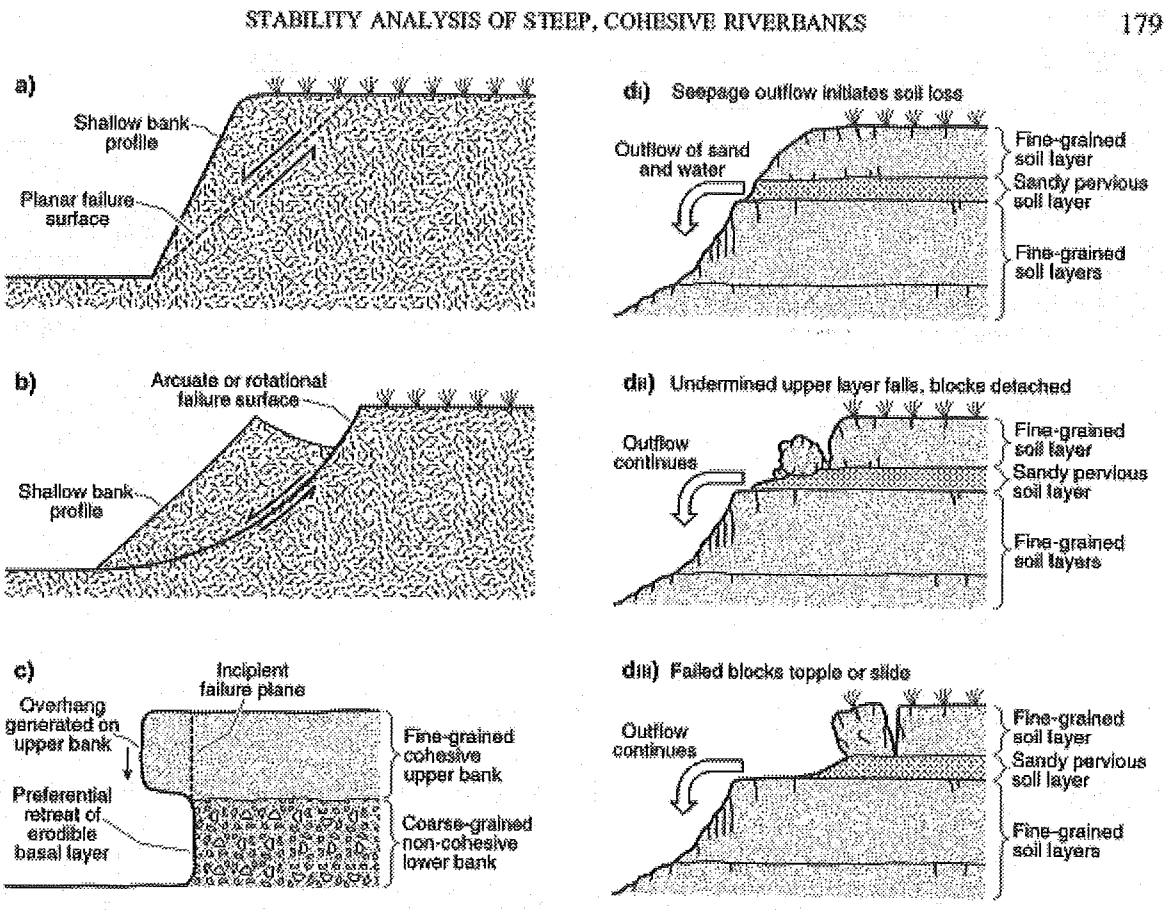

Figure 1.12: Examples of different types of failure. a) planar failure as analysed by Darby (1999); b) rotational failures can be analysed using Bishop (1955); c) cantilever failures can be analysed using Thorne and Tovey (1981); d) piping/sapping type failures (modified after Hagerty, 1991)

Figure 1.13: Mass failure in the Geul river (April 28, 2006)

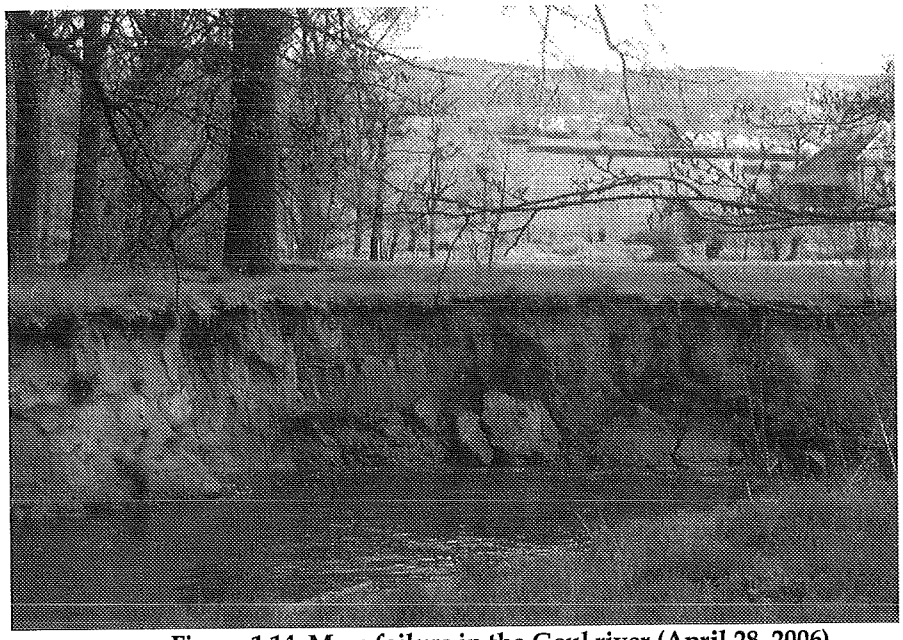

Figure 1.14: Mass failure in the Geul river (April 28, 2006)

Fluvial entrainment is the direct removal of bank material by the physical action of the flowing water. Water flowing in the channel exerts a drag force on the river banks, which may lead to the detachment and entrainment of surface particles.

This action is most important at higher discharges. In that case there is an increase in water velocity, an increase in shear stress and an increased potential of erosion processes to operate over the entire wetted perimeter.

Velocity tends to be high in the concave outer bends of a river and it is where bank erosion is most common.

Near banks scour contributes to bank erosion by facilitating mass failure.

Subaerial weakening is caused by external factors and not by fluvial processes. It can lead to direct erosion and can also weaken the riverbanks which may increase scour and mass failure.

The principal factors that cause these mechanisms are:

- climate: the frequency and duration of freezing, and the amount, intensity and duration of rainfall.
- subsurface conditions: piping, soil moisture levels, pore water pressures...
- biology: type, density and root system of vegetation; animal burrows and trampling
- man-induced factors: urbanisation, land drainage, reservoir development, boating, bank protection structures...

The rate of bank migration is influenced by some factors, including: discharge (magnitude and frequency of channel forming flows), bed material mobility (ability of curved flow to produce bend scour), supply of sediments (availability of sediment to fuel point bar growth), bank erodibility (ability of banks to withstand fluvial shear stress), bank geotechnics (bank stability related with the slope failure), bank vegetation (through affects on flow erosivity, bank erodibility and bank stability), near-bank hydraulic and morphological characteristics (velocity, shear stress, bed topography...), physical characteristics of the banks (bank elevation, cross-sectional shape, soil composition, presence of vegetation, water content...), and properties of eroding water (temperature, electrochemical qualities...).

We can distinguish two approaches for measuring bank erosion: the indirect approach and the direct approach.

The indirect approach uses archive sources to calculate the rate of channel shift. In this group, we can find 3 different ways of determining the erosion: analysis of the aerial photography, satellite imagery and sedimentary evidence.

(1) Aerial photographs are used to measure planform river channel change. The analysis consists of the comparison of pictures of the same stretch of the river from different years and observing the changes of channel location.

(2) Satellite imagery was developed in the mid 70's. The analysis of satellite images is very useful if erosion rates are very high, but, as aerial photographs, spatial errors are inevitable and can lead to inaccuracies.

(3) The sedimentary evidence requires going to the site and reconstructing channel pattern from evidence of the past. These are former river courses which can be dated using carbon-14 (C^{14}).

This method is not useful to determine present bank erosion rates, but only ancient trends.

The direct approach is field based and involves taking measurements. There are two ways to carry out these measurements: taking point measurement of erosion and taking area and volume measurements.

For the point method, there are two ways to obtain the information. An erosion pin is a steel rod (0,5-2m long) and it is driven horizontally into the river bank. As the bank is eroded, more of the pin is exposed, which gives an idea of the erosion rate. The pin has some disadvantages: it can create turbulence within the water and thus,

accelerating erosion around the pin; and it does not show the moment at which erosion occurred.

The photo electronic erosion pin is an automated erosion monitoring system (1990's), which aids measurements of bank erosion and deposition. The sensor consists of a series of photo electric cells, enclosed within a transparent, acrylic tube. Sensors are inserted horizontally into a river bank and connected to a data logger. As the face of the bank is eroded, more cells are exposed to light, and so the sensor voltage output is increased. Deposition reduces the voltage output. The sensor voltage output is sent to the data logger which records magnitude, frequency and timing of individual erosion and deposition events.

Area and volume measurements can be also analysed by two methods. A survey river bank can be carried out using Geographical Information Systems (GIS). Channel cross sections can be surveyed frequently, and channel elevation and incision can be monitorised. Area and volume measurements strictly speaking, which consists of studying an entire reach of river, and measuring the area and volume loss.

1.2.2-Theories on bank erosion processes

On the basis of his field observations, Hickin (1978) suggested that the physical process which causes bank erosion is the shear stress exerted on the bank by the main flow. Kitanidiis & Kennedy (1984) suggested that it is the secondary flow. The intensity of this secondary flow is smaller than that of the main flow, which implies that the theory holding the main flow responsible of bank erosion is more likely to be true.

Eroded materials from the bank participate in the sediment transport process, therefore, they also influence the erosion process (Neil, 1987).

The rate of bank retreat is directly proportional to the difference between the flow shear stress on the bank and the critical value, below which no erosion occurs. This makes it possible to develop a simple relation for the rate of erosion in cohesive banks (Arithuri & Arulanandan, 1978).

Some relations to assess the critical shear-stress and the coefficient of erodibility for cohesive soils have been defined (Arulanandan, 1980).

The geometry evolution of particular bends was explained qualitatively by among others: Daniel (1971), Hickin (1974) and Brice (1974).

More recently various models have been developed to simulate the meander migration processes of which the first ones are based on empirical relationships.

These firsts approaches had severe limitations; for example, an idealised representation of the river planform, such as the sine-generated curve (Leopold, 1966; Thakur and Scheidegger, 1970), or a neglected adjustment of the channel width, which is considered constant (Nelson, 1989; Bridge, 1992; Alabyan, 1996; Sun et al., 1996, 2001). The aim of taking into account these limitations has entailed further analysis and new approaches.

Osman and Thorne (1988) studied a more mechanistic approach that simulates changes in bank stability conditions resulting from deformation of the bank profile caused by direct fluvial shear erosion of bank materials and near-bank bed degradation.

Some studies takes account of the geotechnical characteristics of the bank materials, the shape of the bank profile and the relative position of the ground and surface water elevations to estimate stability with respect to mass failure along a planar-type failure surface (Darby et al., 1999).

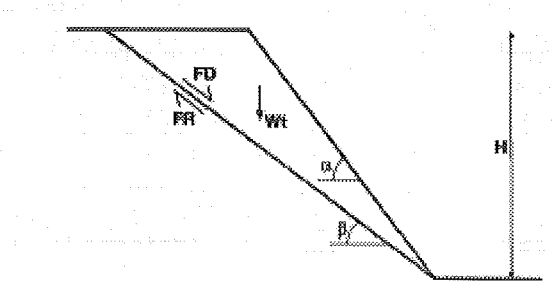

Figure 1.15: Bank failure along a planar type failure bank (Darby, 1999).

Planar failures often occur earlier in the adjustment sequence than do rotational failures hen banks are lower (Simon, 1989) and can occur along any critical failure plan

Fluvial processes erosion at the bank toe are shown to occur mainly at the beginning and at the end of flow events (Mengoni and Mosselman, 2006), when discharge are low and the flow is manly concentrated in the low water bed. This could explain interactions with mass failure processes and timing of bank collapse.

Some group of scientifics are still working on the approaches to calculate the bank erosion rate (for example Duan, 2005).

1.2.3-Bank accretion

Sedimentation occurs when flow falls below the settling velocity of a particle in the stream. In meandering river systems it can be divided into channel deposits and flood deposits.

Channel deposits can occur as bed deposits or in the form of bars.

Point bars are generally the main depositional features in meandering channels. They develop near convex river banks where flow velocity is low. Point bars accrete laterally and in meandering rivers compensate the erosion of the concave banks. They also grow vertically once inundated and slowly build up to floodplain level due to the presence of vegetation. The size of the particles in the deposit is determined by the water velocity.

Bars may also develop as an island in the channel, which will be either eroded or incorporated into point bars as the river migrates (Knighton, 1998).

Flood deposits build up when water flows over the river banks onto the floodplain. Fine sediment is deposited there because flow velocities are very low. The amount of sediment deposited on the floodplains does not only depend on the frequency and duration of flooding, but also on the grainsize distribution of the

sediment in the river (Knighton, 1998). When there is a high content of fine particles, vertical accretion during flooding will be higher.

The fluvial deposits exhibit a fining-up trend. There is often also a downstream trend in grainsize along a river's course. The coarser grains are deposited first and therefore the proportion of finer grains will increase further down the river. This is reflected in the deposits.

River point bars are divided into three classes of different activity: active bars, vegetated active bars and inactive bars. Their "activity level" has to do with the frequency of "reworking" of bars. The most "active bars" consist mainly of gravel and coarse sands. Their top is usually around, or just above, mean low-water-level.

The "vegetated active" bars are all above mean low-water-level. They are often flooded and mainly sand or silt is deposited on them. Vegetation on these bars is a mixture of grasses, herbs and occasionally small shrubs on the highest parts.

The "inactive" bars are well above mean low water level and they are only inundated during high discharges. They are densely vegetated with grasses, herbs, shrubs and trees (mainly fast growing willow). Sedimentation consists of fine sands, silts and clarp.

Lateral accretion appears when the point bar grows. Lateral accretion is driven by general bed aggradation. The quick and large erosion occurring during a flood creates a wider main channel. At lower discharges this profile is too wide, which causes inner bend accretion, but no further erosion of the outer bank. This way the point bar is built out discontinuously.

Towards the centre of the channel this process together with erosion at the other side of the channel may lead to the development of a sinuous channel from an initially straight one.

Vertical accretion takes place when rivers overtop their banks, they deliver water and suspended sediment to the surrounding floodplain. Flows in the floodplain are shallower and encounter roughness in the form of vegetation. As a result, the suspended sediment in the flood water gradually falls out away from the river. This creates a ridge or levee of silt-to-sands along the river banks. Sands fall nearer the river banks, while silts and muds are deposited further away. Material is generally dropped out of suspension, but can get ripple beds and lamination from currents.

Vertical accretion is enhanced by the presence of vegetation.

1.3- Theories on meandering river

The origin of meandering and the meander processes have been studied and analysed since long, and theories on river meandering and bank erosion have been developed.

1.3.1-Theories on cross-sectional geometry

The most important theories on cross-sectional geometry of alluvial channels, not only meandering rivers, are described in this section.

The regime theory studied the cross-sectional geometry of single channel rivers. It's based on field observations of irrigation canals in India (Kennedy, 1895; Lacey, 1930; Lane, 1955; and Blench, 1966) to define the geometry of alluvial channels.

At the beginning, the equations were only related to a "formative" discharge. The radius of curvature for the meander was related to the square root of the water discharge. The formulas were, however, difficult to apply, as it was problematic to obtain values for their constants since these constants were different for different rivers.

Later versions have included another important input parameter in the regime theory formula: the bed load transport (Blench, 1966). This has shown to be very difficult to estimate, because a large number of bed load formulas have been developed over the last 100 years, giving very different results.

The theory of minimum stream power (MSP) is used to determine the optimum channel width of one channel river and geometry for a given set of constraints. This theory suggests that the geometry and slope of an alluvial river are dependent variables. The water discharge and sediment load imposed upon the river by the drainage basin have influence on the alluvial river formation in a long term.

MSP states that the width, depth and slope are so adjusted that the stream power per unit of channel length is a minimum, consistent with physical relations of flow continuity, resistance and sediment transport. This theory includes the statistical analysis known as the "Theory of Minimum Variance" (Langbein and Leopold, 1966). Yang (1976) stated that the time rate of energy expenditures explains the formation of meandering streams. Chang (1984) developed an analysis that establishes the maximum curvature for which a river does the least work in turning and explains meandering development by river tendency to seek minimum channel slope for the given conditions.

This is a discussed theory, because these statements are in conflict with accepted theory and field observation.

1.3.2-Theories on meandering rivers origins

An approach to explain while alluvial rivers do not remain straight but end to meander or braid is based on a stability analysis. It considers the origin of meanders as a stability problem: small perturbation of the channel bed or of channel bends may grow to a meandering pattern.

There are different analyses, based on two theories: Bar and Bend theories.

The "Bar Theory" is based on the assumption that the development of migrating alternate bars in a straight channel would eventually lead to the formation of meanders or braids. The basic idea is that the flat alluvial bed of a straight channel, under certain conditions, becomes unstable. Bed instability is assumed to be the cause of the alternate bar formation. Fluvial instability analyses are carried out by examining submerged bed forms in a shallow channel with straight non-erodible banks. Meandering and braiding are treated as different manifestations of the same instability phenomenon (Hansen, 1967; Callander, 1969; Engelund, 1970; Parker, 1976; Fredsie, 1978).

Ikeda, Parker and Sawai (1981) introduced the point of view of being bend instability at the origin of meandering. They analysed the growth rate of lateral bend amplitude in a mildly curved channel with erodible banks (Bend theory). Bend instability does not occur in straight channels and differs from the alternate bar instability. However, they found that the two mechanics operate at similar wavelength of the incipient meanders, which led to the conclusion that migrating alternate bars gradually evolve into river bends.

Blondeaux and Seminara (1985) demonstrated that bend growth and migrating alternate bars development are caused by two different phenomena: resonance, forced by the development of the channel sinuosity, and channel bed instability. Resonance occurs when a flow disturbance is varying in a periodical way with s (like the curvature in a sinuous channel) and when appropriate conditions are satisfied.

Given the linear relationship assumed to hold lateral migration rate of the channel and flow perturbations, such findings imply that meanders migrate downstream under sub-resonant conditions, whereas super-resonant conditions are associated to upstream migration (Seminara et al., 2001).

Another approach to explain why rivers tend to develop a sinuous planimetry consists of assuming that upstream flow disturbances, causing steady bed deformations of the alternate bars type, rather than migrating alternate bars, are at the origin of river meandering. Alternate bars migrate much faster than meander bends. This assumption implies that meandering can be initiated by any flow disturbance, like an obstacle.

Olesen (1983) and Struiksma et al. (1985) also found that the wave lengths of the steady bed oscillation were more or less in accordance with those of meanders at their initial stage. Seminara and Tubino (1988) have demonstrated the existence of interactions between migrating alternate bars and meander formation.

Analytical and numerical analysis (Lanzoni, Federici & Seminara, 2005) provided some results that imply that, in the absence of a fixed disturbance (such as, for example, a partial obstruction of a given section, or the presence of a curved channel reach characterised by non erodible banks), a non negligible upstream or downstream migration portion of the channel is invariably bound to straighten.

All these theories are based on the assumption that bank accretion is equal to bank erosion. Further studies on why bank accretion acts like that have not been published.

1.3.3-Mathematical description of meandering rivers

Theoretical work has also been done starting with physic description in a mathematical way of water, sediment transport and of bank erosion in a one, two and three-dimensions. A large number of simplifications are necessarily introduced, resulting in formulas for the meander location and downstream velocity of the meander movement.

The simplifications depend for example on the number of dimensions used to describe the processes. For a two-dimensional description simplifications include:

removing all terms that included the vertical velocity; assuming a hydrostatic pressure distribution in the vertical direction; assuming a vertical velocity profile of the stream wise velocity that follows a power-law formula; assuming an empirical vertical distribution of the transverse velocity; assuming isotropic distribution of the eddy-viscosity; and assuming that the bed shear stress direction is the same as the depth-averaged water velocity (when secondary currents don't have any effect).

The model of Ikeda calculates river migration by relating the bank erosion rate to the near-bank primary flow velocity excess. Some models were developed using this approach to predict channel migration (Ikeda, 1981; Blondeaux and Seminara, 1985; Odgaard, 1986, 1989; Crosato, 1987; Johannesson & Parker, 1989).

The mathematical modelling has its physical foundation in the fluvial process-response, which is characterized by the river constant adjustment toward dynamic equilibrium subject to the physical constraints. In response to a natural or human-made change, the transient behaviour of an alluvial river is reflected in its adjustment towards a new dynamic equilibrium, although the dynamic equilibrium may never be attained in nature.

Another approach to studies of meandering rivers has been to use physical laboratory flumes (Schumm, 1987; Zimpfer, 1975). The physical models make it possible to simplify the meandering process and eliminate geometric inhomogenities often found in the field. Zimpfer (1975) showed that repeated flume tests on the same conditions would give very similar results for the meandering pattern. The tests started with a straight channel in a sand box, and an initial upstream instability. After 1-5 hours, a meandering channel formed. This channel was, however, not stable, and a braided channel was formed some hours later. The same observation was found for repeating runs over a number of different water discharges and slopes. It was suggested that stable meandering channels would require some cohesion in the banks (Schumm, 2001).

Mosselman (1989) analysed the influence of bank erosion products on the bed development. His main conclusion is that in most cases the computations of river bed topography and bank erosion can be decoupled: for most rivers the input of bank erosion products does not significantly affect the bank erosion process. He also developed a model to compute the retreat of cohesive banks in which width variation has also been taken into account (Mosselman, 1990).

Many models stem from the early work of Engelund (1974) who produced a simplified set of equations describing flow at a bend that were amenable to analytical solution. In particular, Engelund's approach was developed and refined by Odgaard (1989) to produce a model that could be applied in the context of engineering analysis of meandering rivers. Odgaard's work is particularly significant because he went on to use the implications of his analytical bend-flow model to underpin an empirical model for bank retreat at bends (1987).

However, Engelund's approximations of the equations of motion for curved flow were heavily criticized by Dietrich et al. (1984) because he ignored certain terms for convective accelerations, which turned out to be crucial to generating outward secondary flow near the inner bank.

The model of Smith and McLean (1984) demonstrated that these terms were not negligible and their omission seriously limited the capability of Engelund's model (or other models derived from it) to represent bend flow properly. However, application of the Smith and McLean model demands very accurate data on water surface topography. It is sensitive to errors of only ±1mm in water-surface elevation, ruling it out as a tool for engineering analysis or design in real alluvial streams.

A number of authors have attempted to produce simpler models suitable for engineering applications by modifying more complex models. This approach can be illustrated by the work of Garcia et al. (1994) who developed the model of Ikeda et al. (1981) especially to provide a tool for stream management and engineering. They combined the two dimensional, depth- average St. Venant equations for shallow flow with the depth-average continuity equation to produce a function that gives the depth-averaged downstream velocity at every point in the channel. Knowledge of the spatial distribution of depth-average velocity can be used to drive a morphological model capable of predicting bed scour and the spatial distribution of bank retreat. However, the practical utility of Garcia et al.'s model comes at the price of accepting limiting assumptions that rule out its applications to many alluvial rivers. For example, boundary conditions specify a constant channel width maintained by parallel migration of inner and outer bank, a linear, steady-state, cross-stream bed slope, and a bend radius that is large compared to the channel half-width.

There are theoretical difficulties too. For instance, sediment continuity is neglected so that an important reality check is eliminated.

Cherry et al. (1996) evaluated the performance of Garcia et al.'s model in forecasting behaviour of bends at 26 sites selected from the Brice (1982) data set on planform shifting of meanders in alluvial streams. They discovered that additional data collection was essential to support application of the computational model, which would limit the applicability of the approach to sites where detailed data either pre-existed due to earlier academic research or could be collected through intensive fieldwork. The results of model application were not encouraging and they concluded that prediction of meander migration based on computational bend-flow model was not feasible at that time (mid - 1990's).

1.4- Effect of vegetation

Understanding and predicting the interactions between vegetation and the morphology of rivers is becoming important for river management.

Two analyses related with vegetation can be made: vegetation used to protect river bank erosion and the natural development of vegetation.

The development of vegetation is strongly determined by the morphology of the river. Gradual accretion will raise the point bars level, thus creating suitable conditions for dryer species and more protection against severe flow, leading to more mature vegetation types.

Then, vegetation affects the morphology through slowing down and diversion of flow. It can do that directly or indirectly. Indirectly, the increased resistance caused by the vegetation can change the water level gradient and discharge distribution, which at the same time turn change local flow conditions.

Directly, some mechanism might be determining. The roughness of vegetation might divert the flow towards the outer bend. This may accelerate outer bank erosion, causing larger width of the profile. The increased roughness may also cause different flow patterns downstream of the vegetation; for example, if flow velocity is lower, more sedimentation can appear.

Vegetation acts as a sediment trap, which affects sediment transport by the low flow velocity.

Flow deflection by vegetation also causes main channel bed erosion: the main channel becomes deeper with dense vegetation. The hydraulic resistance of dense point bar vegetation also decreases flow velocity in vegetated areas, resulting lower bed shear stresses and lower sediment transport. This means the point bar itself is morphologically less active.

The other analyses consist of studying the effect of planting trees in the riverbanks to deal with the erosion. Roots of trees bid the soil and introduce extra cohesion to the intrinsic cohesion that the bank material may have.

Soil is strong in compression, but weak in tension. En contrary, tree roots are weak in compression, but strong in tension. The theory of reinforced earth was established by Vidal (1969). Roots are effective in adding tensile strength to the soil and, through their elasticity, distributing stresses through the soil, so avoiding local stress build-ups and progressive failures.

Trees may entail an undesirable effect on the stability. The surcharge weight can reduce bank stability. However, depending on the slope angle and its position on the bank, surcharging can also be beneficial to bank stability.

1.4.1-Theories on vegetation effect

Due to vegetation effects in modifying hydraulic scour through changes in flow resistance and velocity, and its benefits to environmental quality, vegetation is widely believed to increase the stability of streambanks (Thorne, 1990; Simon, 1999).

Vegetation stabilizing effects include reinforcement of the soil by the root system and the reduction of soil moisture content.

However, studies of vegetation impact on the stability of hill slopes have highlighted the potential for some destabilizing effects (Greenway, 1987; Collison and Anderson, 1996). These include higher near-surface moisture contents during and after rainfall events due to increased infiltration capacity, and surcharge due to the weight of trees.

Although many authors have evaluated the mechanical benefits of vegetation on slope stability (Gray, 1978), few studies have specifically addressed the coupling of streambank processes and riparian vegetation (Abernethy and Rutherfurd, 2001; Simon and Collison, 2002).

Fewer studies have quantified the hydrologic effects of riparian vegetation, on considering the balance between potential stabilizing and destabilizing effects under different precipitation and flow scenarios (Simon and Collison, 2002).

2- Problem definition

2.1- Project site description

The Geul is a small, partly freely meandering, tributary to the Meuse River. It starts in Belgian near the border with Germany at Eynatten and joins the Meuse River near Itteren in The Netherlands (Figure 2.1). The river is 56 km long and the catchment area covers 280 km² (Spanjaard, 2004).

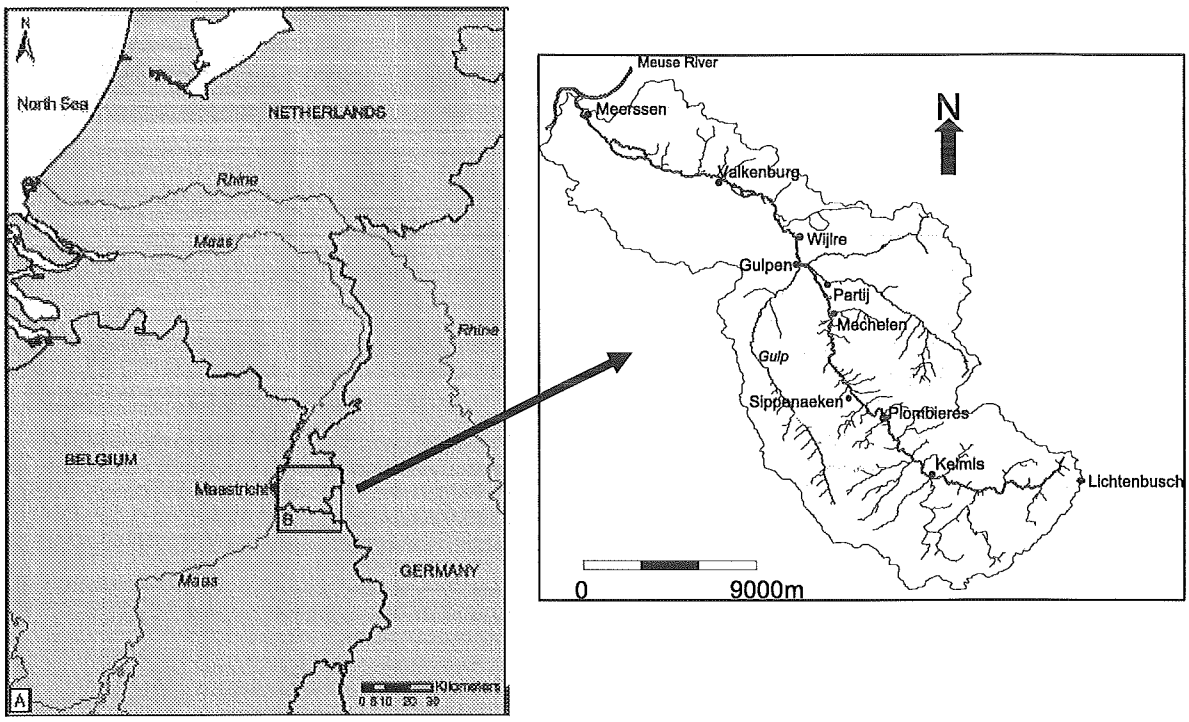

Figure 2.1: Location of the Geul river catchment (de Moor, 2006)

The catchment altitude varies from 50 m above the sea level at the confluence with the Maas River, to 400 m above see level in the source area (Figure 2.2). The valley gradient decreases from 0.02 m/m near the source to 0.0015 m/m in the Itteren (Meerssen). In the catchment area (Figure 2.3), the precipitation varies from 750-800 mm/y (near the confluence) to 1000 mm/y (near the headwaters) (Waterboard "Roer and Overmaas").

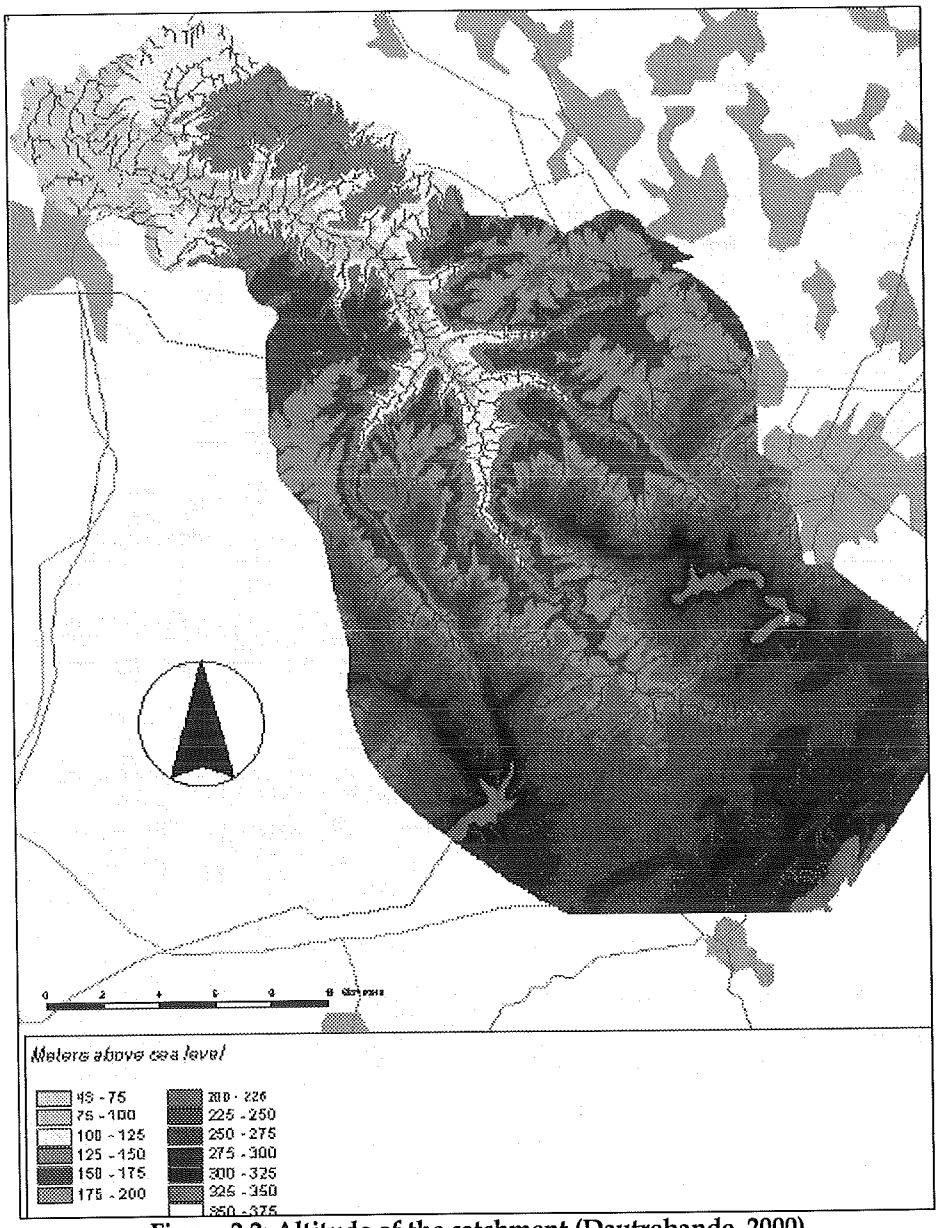

Figure 2.2: Altitude of the catchment (Dautrebande, 2000)

The annual rainwater is 300 mm/y, concentrated during wintertime, which produces an average discharge of 3.6 m^3/s. The actual discharge varies between 0.8m^3/s and 65m^3/s (Dautrebande et al., 2000).

The river valley is cut into Cretaceous and Palaeozoic rocks; the river itself only cuts through Holocene sediments which cover the valley floor.

The upper part of the catchment is formed by erosive soils derived from sandstone, shale and limestone; the middle part is formed by a limestone plateau covered by the deposits of the weithering products from the upper part and by aeolian deposited loess.

The right part of the valley is formed with a steep hill side that touches the river, with a lot of trees between the hill and the river. At the other side of the valley the hillside is mildly sloping.

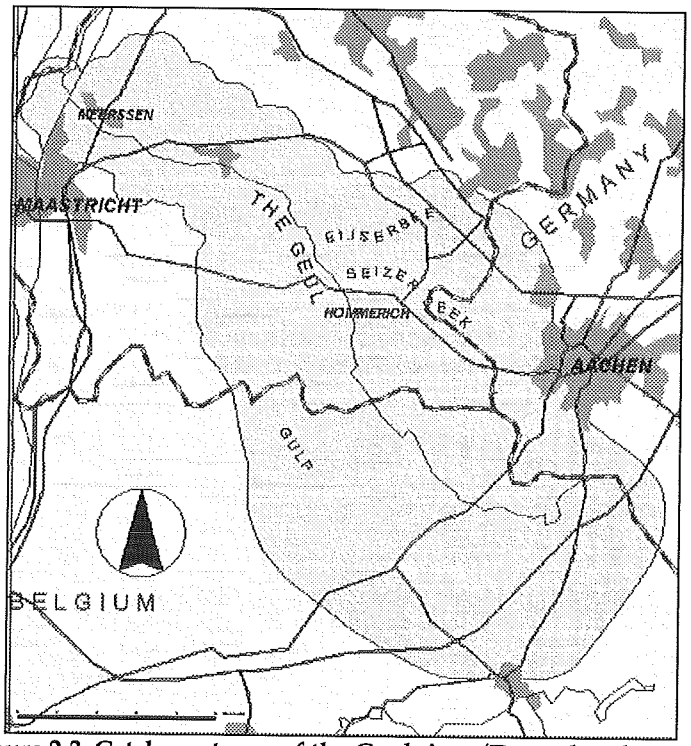

Figure 2.3: Catchment area of the Geul river (Dautrebande, 2000)

The Geul river is an incised river characterized by a 2-2.5 m thick silty floodplain, mainly deposited after large-scale deforestation phases in the Roman and Medieval periods (De Moor et al., 2004). In the 19th century, mining activities in the Belgian part of the catchment severely contaminated the sediments with lead and zinc which provided habitat conditions for odd flora in this region.

Nowadays, the dominating fluvial processes are lateral erosion and point-bar sedimentation.

During a long time, the Geul had been subject to management focussed on erosion prevention, channel straightening and quick water discharge, like all rivers in the Netherlands. Bank protection and straightening along several stretches of the Geul have been dated from 1937 (by visual interpretation of topographical maps; Spanjaard, 2004)

In 1988, this policy changed. Since then, a part of the river was allowed to meander freely: bank protection was removed and agricultural lands were turned into nature reserve, to allow river migration.

In the Geul, river migration is still localized, because of the presence of poplar trees along the banks. They haven't been removed, for ecological reasons, and they are

protecting much of the riverbanks. This will change in the future, because new trees won't be planted and existing trees will be removed by erosion.

The research project focuses on the river stretch that starts at the Belgian-Dutch border with a length of almost 1.6 km (Figure 2.4). This part is one of the more dynamic, with some protected and straightened, stable banks and also rapid lateral migration bends.

This stretch has a sinuosity of 1.67 and the valley slope is 0.004 m/m.

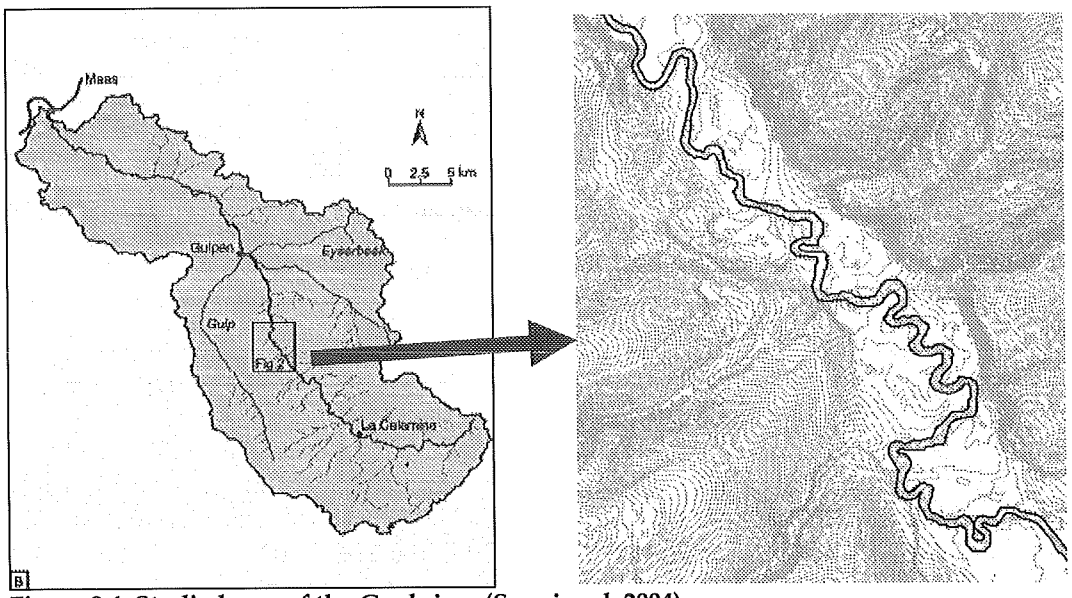

Figure 2.4: Studied area of the Geul river (Spanjaard, 2004)

2.2- Problem definition

Meandering rivers are single-channel rivers with a sinuous planform. They are characterized by an enlargement and migration of meanders through bank erosion and accretion processes. Generally speaking, concave banks tend to erode and convex banks tend to accrete.

Due to migration, freely meandering rivers can represent a problem to river valley management. The main problem is flooding, because man tends to build up infrastructures in the floodplains due to the relative stability of the single meandering channel (compared to braided rivers). Bank erosion can cause damage to roads and buildings, and in farmlands. To limit these problems, channels can be straightened, banks can be protected and flow is slowed down.

But, if we want to let a river take its natural course, we have to be able to analyse the situation by understanding river migration and making models predictions. Therefore, mathematical models have been developed to predict how the river will move and what will be its location.

2.3- Objectives

For the Geul river, a study has already been done at the Vrije Universiteit Amsterdam (Spanjaard, 2004; de Moor, 2006). This work is focused on the study of lateral erosion and accretion. These processes have been mapped and grainsize samples have been taken along a reach of the Geul.

According to the analyses of Spanjaard (2004), the conclusion is that bank protection placed in the early 1930's has effectively reduced bank erosion.

The group of scientists working at VUA has used the Lancaster & Bras model to analyse the planimetric evolution of the Geul river.

The present work lies in adding historical planimetric analysis to the VUA study, and in carrying out a new modelling study of the river migration using the model developed by A. Crosato (1987) at TU Delft, called Miandras.

Two different types of historical analysis are carried out. The first one consists of studying aerial photographs of the same stretch of the Geul studied by the VUA. River location and its evolution are analysed using photographs from different years.

The second one is the study of the effect of poplar trees on bank erosion. Vegetation affects the morphology through slowing down and diverging the flow. Poplar trees have shown to have an important role in protecting banks from erosion, as shown by the VUA study. These trees were planted on purpose to deal with the erosion.

The discharge evolution and channel width variation through the years will also be analysed, to understand the variation of the river migration rate with time and space.

Some data were provided by de Moor (VUA), based on the work of Spanjaard (2004) and de Moor (2006).

The study includes one site visit to get a better knowledge of the river and its environment. It is described in the Appendix A.

3- Model description: Miandras

In this thesis, simulations to model the planimetric evolution of the river Geul are done using a mathematical model (Crosato, 1987) and solved by the numerical code MIANDRAS, developed in TU Delft (Crosato, 1990).

3.1- General aspects and assumptions

The model combines a steady-state flow model and channel bed deformation model with a time-dependent river migration model, which computes the bank erosion rate as a function of near-bank hydraulic and morphological properties. Bank accretion rate is assumed equal to bank erosion rate at the other side of the river channel.

The flow and river bed is derived by fully coupling flow fields, bed topography and sediment transport and it accounts for the secondary flow momentum convection.

The model is appropriated for the simulation of the planimetric changes of rivers under the assumptions that:

- the bed development is not influenced by bank erosion.
- bank erosion is not influenced by the presence of migrating alternate bars.

These assumptions are true when the river has relatively low bank erodibility, lower than the river bed erodibility.

The first assumption leads to decoupling of the computation of flow and channel bed topography from the computation of channel migration.

The approach still allows for a varying discharge: a step-wise approximation of the discharge hydrograph gives a constant discharge during each computational time-step. However, the variation of discharge leads to a flow and bed deformation response which is lagging behind. Therefore, the model is provided with a simple decoupled time-adaptation formulation, which is governed by a characteristic time scale.

The models for the flow field and bed topography are based on a linear analysis of the 2-dimensional equations for water movement and bed topography. These equations are based on the approach that considers the interaction between steady water motion and time-dependent bed development (quasi-steady approach). It is valid in flows with small to moderate Froude number.

Time-dependent terms are neglected which means that the equations describe the equilibrium configuration.

The mathematical model describing flow and bed topography is a linear version of the more complete non-linear model developed by Kock & Flokstra (1980) and Struiksma et al. (1985).

The linear analysis of the model shows that under the assumption of a mildly curved channel the linearized set of equations still retains the main parameters

influencing flow and bed deformation. Furthermore, when computing the steady-state conditions the equations can be further simplified (linearized).

The prediction of flow and bed topography for finite amplitude meanders (strongly curved channel) has not been theoretically proved but with experimental measurements (Crosato, 1987).

This simplified linear version is appropriate for solving large-scale problems, while it still provides a fairly good prediction of the equilibrium configuration of flow and channel bed in meandering rivers.

This model assumes the rate of flow-induced bank erosion rate to be proportional to the near-bank main velocity deformation, like Ikeda et al. (1981). In this model, another term has been introduced to take into account the influence of bank elevation on the vertical failure of cohesive banks. This term is proportional to the near-bank water depth excess from the reach-average value, so as to produce a relatively greater instability for larger water depth.

In order to determine the rate of bank erosion, the near-bank velocity excess and bed deformation are calculated. Deviations in the flow field and water depth from uniform flow conditions (infinite long straight channel) can be caused by local conditions (flow deformations due to the curvature), upstream conditions (overshooting phenomenon) and back water effects (not accounted in MIANDRAS).

The following assumptions are made:

- the channel width is constant in space and time;
- the vertical pressure profile is hydrostatic;
- shallow-flow approximation is appropriate;
- mildly-curved channel approximation is appropriate;
- the spatial variation of the hydraulic roughness (Chézy coefficient) can be neglected;
- the rate of sediment transport is assessable by local conditions (dominant bed load);
- the influence of grain sorting is insignificant (uniform bed material);
- the Froude number is small to moderate (rigid lid approximation);
- the bed slope is mild;
- back water effects are negligible.

3.2- Mathematical description

3.2.1-Basic equations

The flow deformation is calculated by solving the 2-dimensional depth-averaged continuity and momentum equations, using the following co-ordinate system:

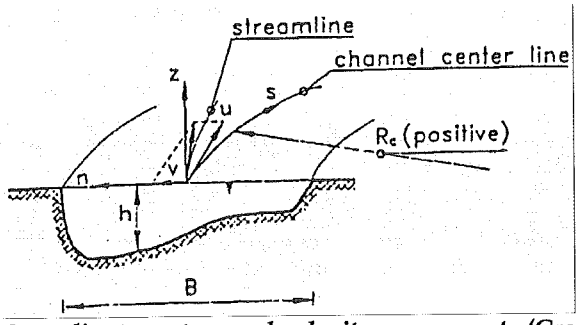

Figure 3.1: Co-ordinate system and velocity components (Crosato, 1990)

$$\frac{\partial(hu)}{\partial s}+\frac{\partial(hv)}{\partial n}+\frac{hv}{(R_c+n)}=0 \qquad [1]$$

$$u\frac{\partial u}{\partial s}+v\frac{\partial u}{\partial n}+\frac{uv}{(R_c+n)}+g\frac{\partial z_w}{\partial s}+\frac{g}{C^2}\frac{u\sqrt{u^2+v^2}}{h}=0 \qquad [2]$$

$$-\frac{u^2}{(R_c+n)}+u\frac{\partial v}{\partial s}+v\frac{\partial u}{\partial n}+g\frac{\partial z_w}{\partial n}+\frac{g}{C^2}\frac{v\sqrt{u^2+v^2}}{h}=0 \qquad [3]$$

in which:

s : longitudinal co-ordinate;
n : transverse co-ordinate;
u : depth-averaged tangential velocity;
v : depth-averaged transverse velocity;
h : water depth;
R_c : radius of curvature of the channel centre-line;
z_w : water level;
C : Chézy coefficient.

The stream-line curvature is approximated by (de Vriend, 1981):

$$\frac{1}{R_s}=\frac{1}{(R_c+n)}+c \qquad \text{with } c=-\frac{1}{u}\frac{\partial v}{\partial s} \qquad [4]$$

in which

R_s : stream-line radius of curvature;
R_c : centre-line of curvature induced;
c : curvature induced by the non uniformity of the flow.

Flow equations are combined with time-dependent depth-averaged equation for sediment transport, to take into account the interaction between flow and sediment:

$$\frac{\partial z_b}{\partial t}+\frac{\partial S_S}{\partial s}+\frac{\partial S_n}{\partial n}+\frac{S_n}{(R_c+n)}=0 \qquad \text{with} \quad \begin{aligned} S_S &= S_t\cos\alpha \\ S_n &= S_t\sin\alpha \end{aligned} \qquad [5]$$

in which:

z_b : bed level (m);

S_S :volumetric sediment transport, including pores, per unit of width in the s direction;

S_n : volumetric sediment transport, including pores, per unit of width in the n direction;

S_t : total volumetric sediment transport, including pores, per unit of width;

α : angle between s-direction and sediment transport direction.

Due to the gravity force acting on the grains moving along a transversally sloping bed, the direction of the sediment transport does not coincide with the direction of the bed shear-stress.

The expression for the deviation of sediment transport direction from s-direction, α becomes:

$$\tan\alpha = \frac{v}{u} - \frac{A}{R_s} - \frac{1}{f(\theta)}\frac{\partial z_b}{\partial n}$$

in which $f(\theta) = \frac{0.85}{E}\sqrt{\theta}$ and $A = \frac{2\alpha_1}{\kappa^2}(1 - \frac{\sqrt{g}}{\kappa C})$

with: θ : Shields parameter
E : calibration coefficient
κ : von Karman constant;
α_1 : calibration coefficient.

3.2.2-Linearization of the equations

For the linearization water depth, tangential velocity and sediment transport parameters are assumed to be given by the sum of two terms: the reach-averaged value (infinite long straight channel) and a deformation term:

$$h = h_0 + H' \qquad \text{being } \frac{H'}{h_0} = \varepsilon \qquad [6]$$

$$u = u_0 + U' \qquad \text{being } \frac{U'}{u_0} = \varepsilon \qquad [7]$$

$$S_s = S_0 + S_S' \qquad \text{with } S'_S \square S_0 \qquad [8]$$

$$\text{and } S_S' = S_0(b\frac{U'}{u_0}) \qquad [9]$$

The depth-averaged transverse velocity is assumed of first order:

$$v = V' \qquad \text{being } \frac{V'}{u_0} = \varepsilon \qquad [10]$$

with $\varepsilon \square 1$

in which:

h_0 , u_0 , S_0 : reach-averaged values of respectively water depth (m), depth-averaged tangential velocity (m/s) and volumetric sediment transport, including pores, per unit of width in s-direction (m^2/s);

H', U', S's : deformation terms respect to their reach-averaged values;

b : exponent in sediment transport formula.

The b exponent that comes from the linearization of the sediment transport formulas is kept constant. It implies that the formula is approximated by a power law in which b expresses the non-linearity if the sediment transport rate.

To carry out the linearization, the following equations are used:

Continuity equation: $$h_0 u_0 = \frac{Q}{B} \qquad [11]$$

Chézy equation $$i_{os} = -\frac{u_0^2}{C^2 h_0} \qquad [12]$$

in which

Q : discharge;

B : channel width (constant all along the river and with the time);

i_{os} : longitudinal water surface slope.

They apply for the conditions of uniform flow in an infinite long straight channel.

Linearization of flow equation:

The water level, z_w, is eliminated by cross differentiation of [2] and [3], applying the following differentiation rule (de Vriend, 1971):

$$\frac{\partial^2 z_w}{\partial n \partial s} + \frac{1}{(R_c + n)} \frac{\partial z_w}{\partial s} = \frac{\partial^2 z_w}{\partial n \partial s} \qquad [13]$$

Some more conditions are yield by the following assumptions:

- shallow water $\longrightarrow$ $\frac{h_0}{B} \approx \varepsilon$

- mildly curved channel $\longrightarrow$ $\frac{B}{R_c} \approx \varepsilon \rightarrow n \square \; R_c \; ; \; \frac{1}{R_c} \approx c$

- flow adaptation length is comparable with the channel width: $\lambda_W = \frac{h_0 C^2}{2g} = B$

Since non-linear terms are disregarded, the first order equation for the flow deformation, in a steady-state situation, is:

$$\frac{\partial^2}{\partial s \partial n}(U') + \frac{1}{\lambda_w}\frac{\partial}{\partial n}(U') = \frac{u_0}{2\lambda_w h_0}\frac{\partial}{\partial n}(H') - u_0\frac{\partial}{\partial s}(\frac{1}{R_c} + c') - \frac{u_0}{2\lambda_w}(\frac{1}{R_c} + c') \qquad [14]$$

Linearization of bed equation:

The bed equation is derived by combining the two dimensional depth-averaged flow continuity equations, [1], with the sediment balance equation taking into account the expression for the sediment transport direction.

The sediment balance equation is:

$$\frac{\partial z_b}{\partial t} + \frac{\partial S_S}{\partial s} + \frac{\partial S_n}{\partial n} + \frac{S_n}{(R_c + n)} = 0 \qquad [15]$$

in which z_b : bed level

The assumption of a small to moderate Froude number yields to consider:

$$\frac{\partial z_b}{\partial n} = -\frac{\partial h}{\partial n}$$
$$\frac{\partial z_b}{\partial t} = -\frac{\partial h}{\partial t}$$

Then, the first order equation in the steady-state situation for the channel bed deformation is:

$$\frac{\partial}{\partial s}(H') - \frac{h_0}{f(\theta_0)}\frac{\partial^2}{\partial n^2}(H') = (b-1)\frac{h_0}{u_0}\frac{\partial}{\partial s}(U') - Ah_0^2\frac{\partial}{\partial n}(\frac{1}{R_c} + c') \qquad [16]$$

in which

$f(\theta_0)$: weighing function for the influence of the sloping bed;

A : coefficient which weighs the influences of the spiral motion.

3.2.3-Analysis of the equations in a steady-state situation

The aim of the model is to estimate the near-bank flow velocity and water depth deformations to which the bank erosion rate is related. In order to make the equations one dimensional (function of s), a cross-sectional shape (sinusoidal) is imposed.

The total deformation of flow velocity and water depth is given by the sum of two terms, resulting of the non-homogeneous equations (zero-order) and the homogeneous equations (first-order).

The zero-order term $(\hat{u}_0, \hat{h}_0)$ is the deformation caused by the local channel curvature in fully developed bend flow conditions (Figure 3.2). The bed is sloping in transverse direction.

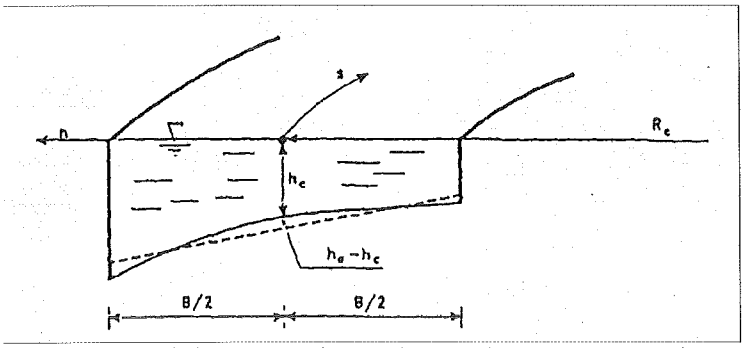

Figure 3.2: Water depth deformation due to the non-homogeneous solution (Crosato, 1990)

The first-order term $(\hat{u}, \hat{h})$ is the deformation coming from upstream. Crosato (1990) showed that the model gives an oscillating bed downstream (Figure 3.3).

The sinusoidal transverse shape that makes possible the one dimensional equations is described by the following equations (only function of s):

$$h' = \hat{h} \sin \frac{\pi n}{B}$$

$$u' = \hat{u} \sin \frac{\pi n}{B}$$

$$v' = \hat{v} \cos \frac{\pi n}{B}$$

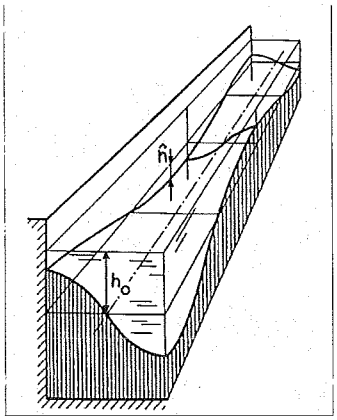

Figure 3.3: Channel's perturbed bed (Crosato, 1990)

Adding these two linear terms, the final expression describing the total near-bank deformation is:

$$\frac{\partial U}{\partial s} + \frac{U}{\lambda_w} = \left(\frac{1}{2\lambda_w} \frac{u_0}{h_0}\right) H - \frac{u_0}{k_B} \frac{\partial \Gamma}{\partial s} - \frac{(2-\sigma)}{2\lambda_w} \frac{u_0}{k_B} \Gamma \qquad [17]$$

$$\frac{\partial H}{\partial s} + \frac{H}{\lambda_s} = \frac{h_0}{u_0} (b-1) \frac{\partial U}{\partial s} + A h_0^2 k_B \Gamma \qquad [18]$$

with $U = \hat{u}_0 + \hat{u}$ and $H = \hat{h}_0 + \hat{h}$

With $k_B = \frac{m\pi}{B}$

$$\sigma = 1 + 90\frac{C}{\sqrt{g}}(\frac{h_0}{B})^2$$

$$\Gamma = \frac{1}{R_c}(\frac{m\pi}{2})$$

$$\lambda_s = \frac{1}{(\pi)^2} h_0 (\frac{B}{h_0})^2 f(\theta_0)$$

in which σ: coefficient weighing the momentum redistribution by the secondary flow; also used as a calibration coefficient.

For meandering rivers m (transverse perturbation mode or number the branches inside the channel) is equal to 1

The total bed deformation (depth water) in a curved channel obtained from the zero-order and first-order terms is represented in Figure 3.4.

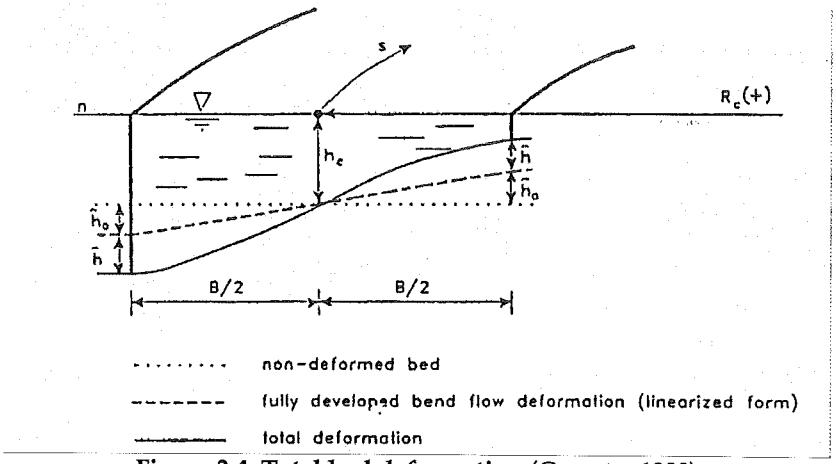

Figure 3.4: Total bed deformation (Crosato, 1990)

Equations [17] and [18] can be rewriting as:

$$\frac{\partial^2 H}{\partial s^2} + \frac{\partial H}{\partial s}[\frac{1}{\lambda_S} - \frac{(b-3)}{2\lambda_W}] + \frac{H}{\lambda_s \lambda_W} = F \qquad [19]$$

With F : curvature

$$F = -\frac{h0}{k_B}(b-1)\frac{\partial^2 \Gamma}{\partial s^2} + [Ah_0^2 k_B - \frac{(2-\sigma)(b-1)h_0}{2\lambda_W k_B}]\frac{\partial \Gamma}{\partial s} + \frac{Ah_0^2 k_B}{\lambda_W}\Gamma$$

in which Γ : curvature term

The importance of the coefficient (2- σ) has been demonstrated by Kalkwijk & de Vriend (1980), de Vriend (1981), and Johannesson & Parker (1987). In the case of bed friction term negative (σ>2; if σ=2, transverse bed friction is equal to zero), the effect is a transverse shift of the maximum velocity locus towards the outer bend, effect comparable to that of the secondary flow momentum convection.

3.2.4-Bank erosion model

The flow-induced rate of bank erosion is assumed proportional to the near-bank tangential velocity excess with respect to its reach-averaged value.

A second term can be introduced if the bank instability becomes important, to take into account the influence of bank elevation on the failure of vertical cohesive banks. This term is assumed proportional to the near-bank water depth deformation.

Bank accretion is assumed equal to bank erosion at the other side of the channel. In this way the channel width remains constant and bank erosion rate equal to $\frac{\partial n}{\partial t}$.

$$\frac{\partial n}{\partial t} = E_u U + E_h H \qquad [20]$$

in which

E_u :flow-induced bank erosion coefficient
E_h : bank-instability-induced bank erosion coefficients;
H : near-bank water depth deformation;
U : near-bank tangential velocity deformation.

3.3- Limitations of this model for the Geul river analysis

Some assumptions of the mathematical model do not apply to the Geul river. This can introduce errors in the channel migration prediction.

In the model, the channel width is assumed to be constant in space and time. In order to obtain a good representation of the river behaviour, this representative channel width has to be optimisated in order to find the value that gives the most realistic results.

Another assumption is the mild curvature. The Geul river is characterised by stretches of a high sinuosity where this assumption is not valid.

Some non-linear terms can be neglected in mildly curved channels, but not in the strong curved ones. These terms are negligible if $n << R_c$, which is not true in case of strong curvature.

The shallow water assumption assumes $\frac{h_0}{B}$ to be small. For the Geul river, this assumption is not valid (h≈2 m; B≈8 m for the formative discharge). Shallowness

influences the relative importance of secondary flows, thus the redistribution of the flow and the boundary shear stress (Blanckaert & de Vriend, 2003).

3.4- Numerical model

3.4.1-General

The program computes the equilibrium water depth and velocity at every time. Bank erosion is also computed every time, as a function of the near-bank velocity and water depth deformations.

It's is possible to take into account the variations of bank erodibility and presence of bank protection works along the river course. It's also possible to take into account the slower adaptation of the bed topography with respect to the flow field for varying discharge by means of a specific time scale for the bed development.

The longitudinal near-bank water depth profile is calculated by solving the equation [21]. It's solved at certain time-level with given boundary and initial conditions, and the numerical solution is based on the explicit Runge-Kutta method for second order differential equations.

The longitudinal near-bank tangential velocity profile is obtain by solving equation [19], when the near-bank longitudinal water dept profile is known and width a given boundary conditions.

Bank erosion relative to the duration of the last time-step is calculated by the equation [22], using the computed tangential velocity and water depth profiles. The computation of the bank erosion is improved by adopting a predictor-corrector method. Bank accretion equal to bank erosion at the other side, which implies that computing bank erosion is equivalent to computing the shift of the channel centre line ($\frac{\partial n}{\partial t}$).

At the new time level the cycle restarts.

The model predicts cross-sectional water depth and velocity (always with the assumption of anti-symmetric shape), the river planimetry and other channel characteristics.

The information necessary to start the simulation is:

- upstream boundary conditions,
- erodibility characteristics of the banks (erosion coefficients),
- initials channel axis co-ordinates (the river can start meandering also from a straight planimetry with non-uniform inflow),
- initial water depth and longitudinal profile (when using the time-scale of the bed development),
- discharges conveyed by the main channel (no-flood plains),
- and initials channel characteristics, valley slope, calibration coefficients....

The proprieties of the soil related to bank erodibility (erosion coefficients) are specified for regions in the river valley. The program establishes in which region the

eroding bank is located and therefore which values of the erosion coefficients must be applied.

Some boundary conditions are required to solve the equation of the water depth longitudinal profile. These conditions are the near-bank (left bank) ware depth excess from its reach-averaged value and its gradient at the upstream boundary.

To solve the equation of tangential velocity profile, the required boundary condition is the near-bank velocity excess with respect to its reach-averaged value at the upstream section.

The reach-averaged values of the velocity and water depth are computed with the Chézy formula.

The program can be calibrated by five coefficients. These coefficients weigh the influence of: channel curvature on the bed shear stress direction (α_1), the sloping bed on the sediment transport direction (E), secondary flow convection (σ), flow-induced bank erosion (E_u) and bank retreat due to the cohesive failure (E_h) (the erosion coefficients are therefore treated as calibration coefficients).

Miandras has been tested computationally for the prediction of initiation and further development of meanders. Some other case studies were carried out (Bloom, 1996).

Numerical tests were carried out on initiation and further developments of meanders from the initial conditions of the Straight Flume Experiment by assuming erodible non-cohesive banks (Crosato, 1990).

This model is applicable to those channels which are characterized by the four following situations: neither aggradation nor degradation of the bed; an approximately constant width; shallow water; relatively slow bank erosion processes. It means the typical meandering rivers with vegetated floodplains, cohesive banks.

A limitation is due to the assumption that neither the development of bed topography is influenced by bank erosion, nor the latter is influenced by the presence of alternate bars migrating downstream, which is the case with most of meandering rivers. The occurrence of meander cut-offs is not taken into account for the development of the model, but cut offs can be introduced during the computations.

Meander migration models have a numerical errors related to the computation of the local channel curvature and to the procedure of adding and deleting computational points as the river planform evolves (Crosato, 2006).

The methods adopted to reduce these errors may influence size, form and migration rate of the developing meanders. Cubic spline interpolations and curvature smoothing (at different degrees) are some of the methods for reducing this error.

3.4.2-Summary

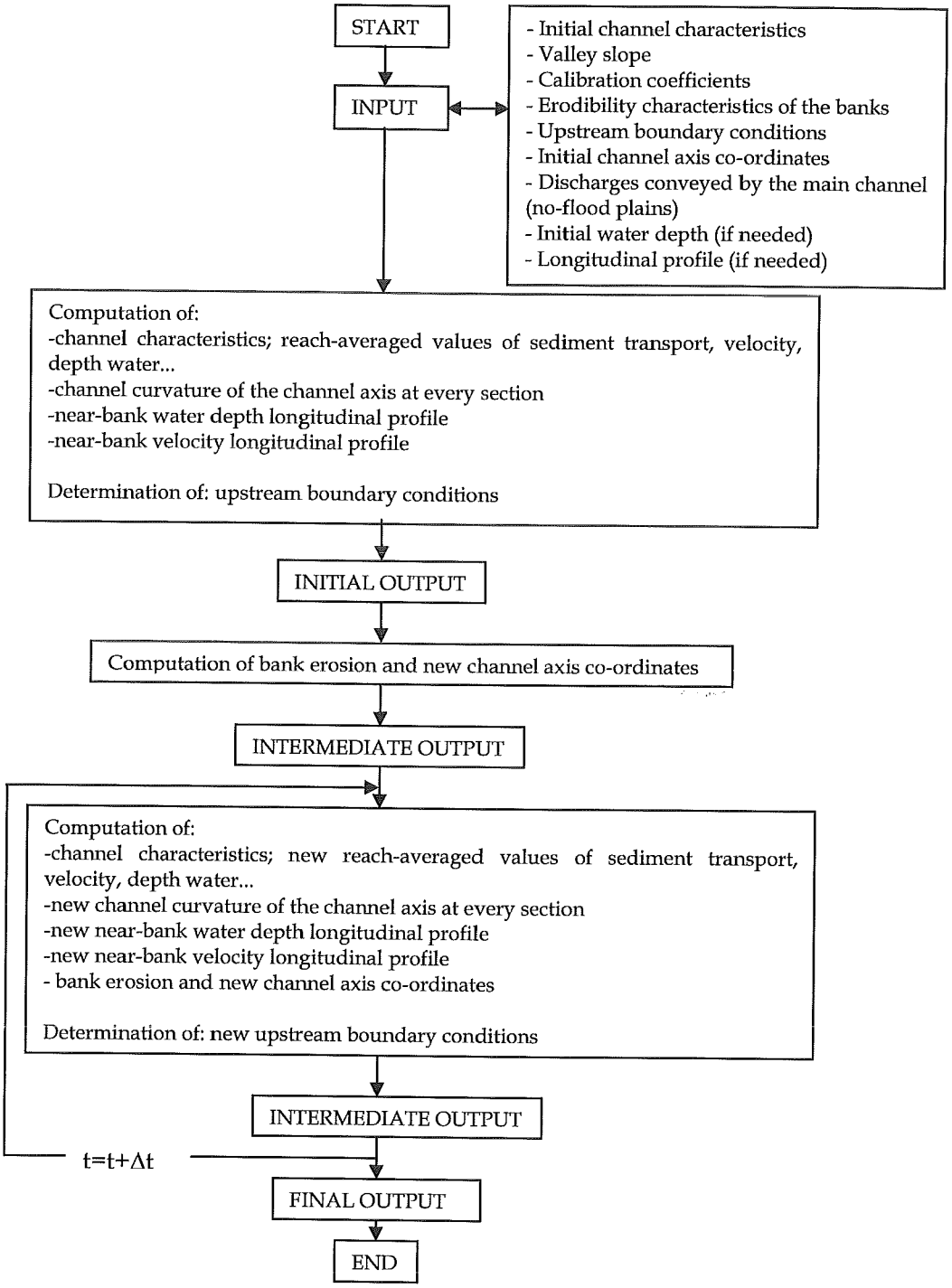

Figure 3.5: Flow-chart of Miandras (Crosato, 1990)

4- Historical analysis based on aerial photographs

Aerial photographs are analysed in order to obtain the planform planimetry evolution of the Geul river. Available photographs are from 1935, 1965, 1983, 1992 and 2003.

Some other parameters, as the width of the river, the discharge and the presence of trees along the river banks, are also studied to understand the historical planimetric changes.

In order to work with aerial photographs and get the real coordinates of the past and current position of the river, the photographs have been georeferenced using the program ArcMap and a detailed map of the region LIMBURG (1:25.000). They have also been rectified.

During this process some errors have been introduced in the coordinates of the points describing the channel centreline. The first error is the one inherent to pictures. The article "Accuracy assessment of georectified aerial photographs: Implications for measuring lateral channel movement in a GIS" (Hughes et al., 2005), explains that spatial errors in digital imagery (including scanned aerial photos) is inevitable and can impart inaccuracies in measurements of lateral channel movement.

A second error is given by the measurement of the real coordinates. Using a map of the Limburg region (1989) the coordinates of some specific points present in the pictures (as crossroads) have been measured. That step introduces a new error due to the inaccuracies of working with a ruler.

We have to find these points on the photographs and attributing the measured coordinates to them. This entails another error, because of the inaccuracy to point the picture at exactly the same place as where the coordinates were obtained. Subsequently, the program does an approximation of the values introduced, which adds a new error.

The georectification applied to the photographs after georeferencing can also introduce errors (rotation, deformations...).

Finally, a maximum error for all the pictures of 6 m is obtained. In general, this error is acceptable. Aerial photos can be consistently georectified with an accuracy of approximately ± 5 m, with a 10% chance of a greater error ("Accuracy assessment of georectified aerial photographs: Implications for measuring lateral channel movement in a GIS" (Hughes et al., 2005)).

Due to this error, the study of the erosion rate will be inaccurate. Planimetric changes less than 6 m will be of the order of the location error.

4.1- Aerial photographs

Aerial photos provided by the land register of Emmen for the area of the river are shown in this section. The Figures 4.1-4.5 are focussed on the study area of the Geul river.

On the photos we can observe channel and trees position.

Figure 4.1: Aerial photograph of the Geul river in the study area, 1935

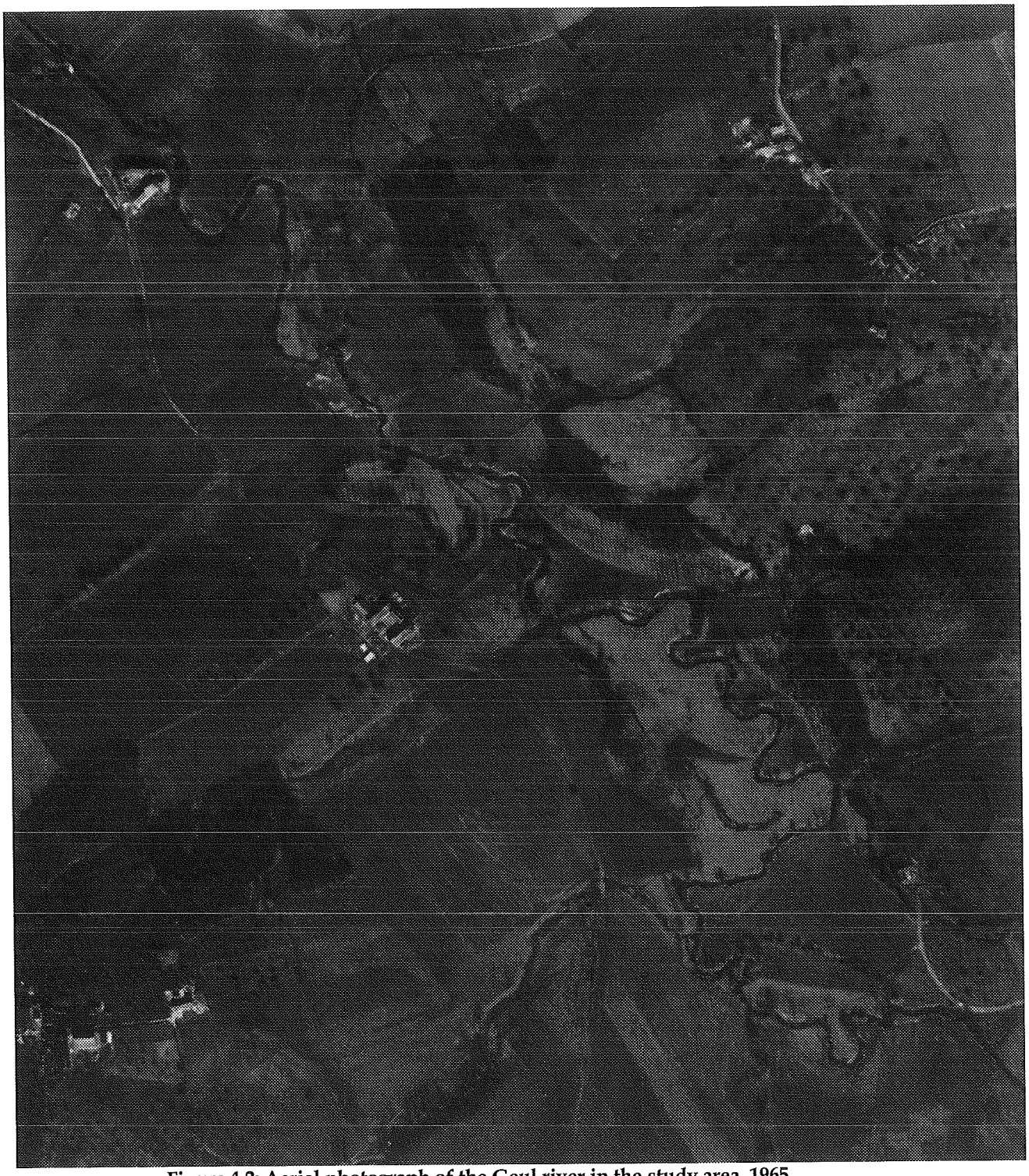

Figure 4.2: Aerial photograph of the Geul river in the study area, 1965

Figure 4.3: Aerial photograph of the Geul river in the study area, 1983

Figure 4.4: Aerial photograph of the Geul river in the study area, 1992

Figure 4.5: Aerial photograph of the Geul river in the study area, 2003

4.2- Presence of trees

Three kinds of trees can be found along the river banks: poplar trees, willow trees and alder trees.

Poplar trees don't grow naturally in this zone (Figure 4.6). They were planted along some stretches of the river, near the banks to delay the erosion as a provisional solution. These trees are very useful to deal with the erosion because they grow very fast and they have very deep roots.

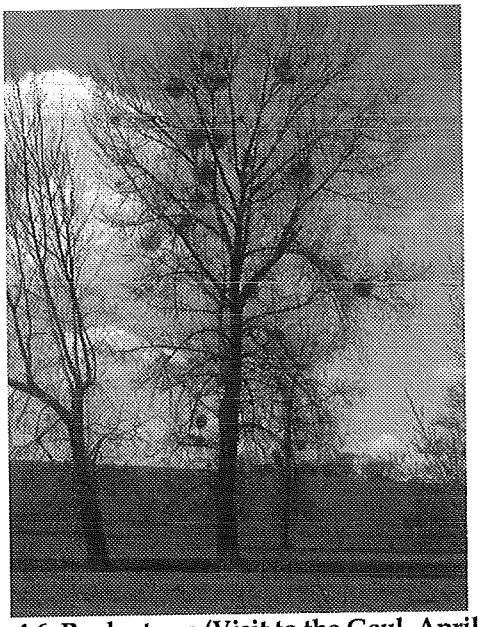

Figure 4.6: Poplar trees (Visit to the Geul, April 28th)

Willow trees and alder trees grow naturally near this river. They have deep roots which allow them to survive river migration and stand into the river.

Sometimes, a scour hole is developing on the upstream side of one of these trees, which grows as erosion takes place. The hole expands until the bank is eroded all around the tree (Figure 4.7). Then the tree stands isolated in the river without any connection to the riverbank (Figure 4.8).

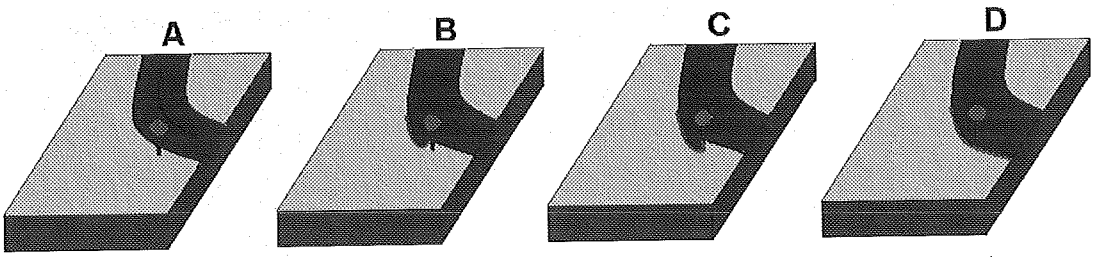

Figure 4.7: Representation of erosion phases around a tree by surrounding (Spanjaard, 2004)

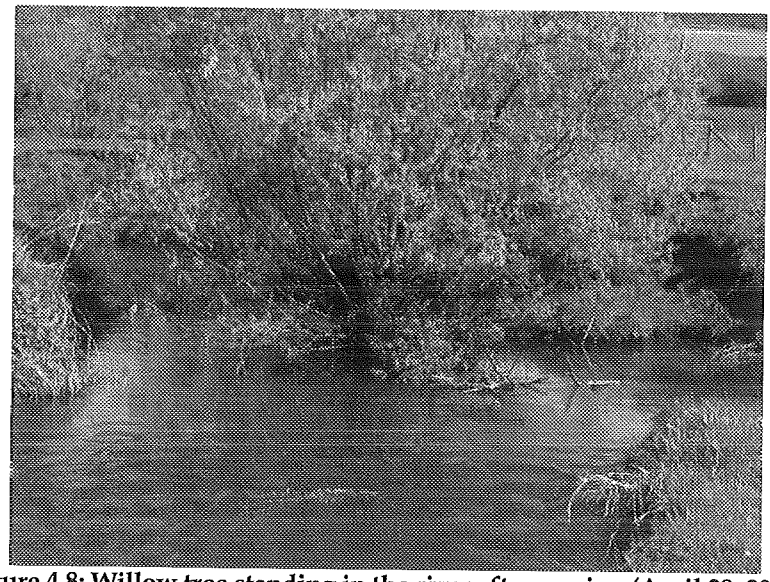

Figure 4.8: Willow tree standing in the river after erosion (April 28, 2006)

As the river keeps migrating, the bank behind the tree is further eroded and sedimentation on the opposite bank continues. The trees in the river seem to be moving from one bank to another, although it's not the trees but the bank who is migrating.

In this case, the bottom of the trees is sometimes covered by sedimentation (Figure 4.9).

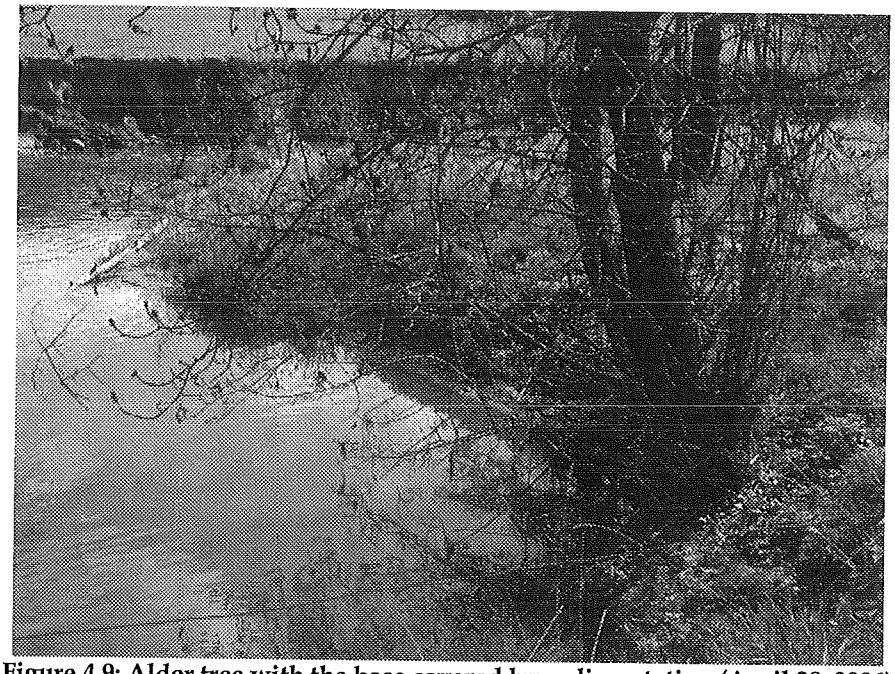

Figure 4.9: Alder tree with the base covered by sedimentation (April 28, 2006)

Neither alder nor willow trees have any effect on bank protection. For that reason, this analysis will be focused on the poplar trees.

We can observe where poplar trees are planted on aerial photos. In general they are situated on the outer side of the bend, where erosion takes place; some trees are also planted along straight stretches.

The following sections deal with the analysis of presence and effects of poplar trees along the banks of the Geul river. At first the bank erosion rates are estimated.

4.3- Erosion rate

To obtain the value of the erosion rate, the positions of the bank through the years are compared with one another. The distances between the first photo (1935) and the others are obtained by measuring the movement of the bank at the bend apex and at straight reaches.

To carry out the analysis, four periods are distinguished. Observing the results of this analyse, we decided to ignore the values of 1992, because in all the section the distance of the movement was less than 6m, which is within the inaccuracy range of the photos (Table 4.1). For position differences that are smaller than 6 m, the analysis is not possible because we don't really know what happened. Then the analysis is finally focussed on three periods.

Nine sections are chosen to carry out the analysis (Figure 4.10).

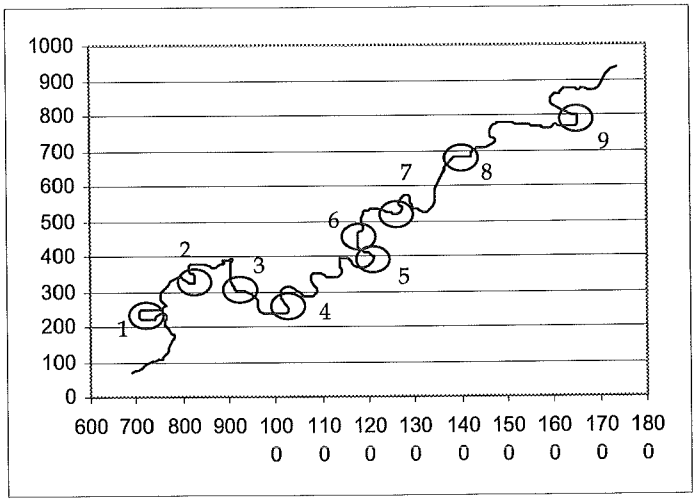

Figure 4.10: Study sections where erosion rate is analysed

At these sections, bank migration is analysed. The movement compared with bank position in 1935 is measured (Table 4.2).

	1965	1983	1992	2003	
Section 1	-	8.96	12.98	19.07	Apex
Section 2	12.33	18.41	21.86	25.68	Apex
Section 3	8.18	13.77	13.95	16.29	Straight stretch
Section 4	8.33	13.88	13.99	16.29	Downstream apex

Section 5	14.84	20.16	26.99	32.38	Apex
Section 6	7.02	13.68	16.42	16.75	Straight stretch
Section 7	-	43.92	50.82	60.48	Apex
Section 8	5.68	10.64	14.15	17.85	Straight stretch
Section 9	6.95	12.24	16.98	19.97	Apex

Table 4.2: Bank movement (m) compared with channel situation in 1935

We observe high values, i.e. section 6. A migration of about 60m is a large movement, but it takes place during a long period (68 years; erosion rate of 0.9 m/y). The erosion rate for each period, differentiating between straight stretches and curved stretches, has to be considered in a range (± 6 m) of values due to the error from the photos.

Analysis of erosion rate in a curved stretch

Analysing only the sections corresponding to bends, erosion rate is obtained by the distance between one year and the previous taking into account the period length. Values are given in meters/year.

A final interval for the bank retreat is found, taking into account the range of the error (Table 4.3).

The error introduced has been calculated as:

$$\frac{6\ \text{m}}{\text{Duration of the period (years)}}$$

	1935-1965	1965-1983	1983-2003
Section 1		0.19	0.51
Section 2	0.41	0.34	0.36
Section 5	0.49	0.30	0.61
Section 7		0.92	0.83
Section 9	0.23	0.29	0.39
Average (m/y)	0.38	0.41	0.54
Error (m/y)	±0.2	±0.33	±0.3
Range of bank retreat (m/y)	**0.18-0.58**	**0.08-0.74**	**0.24-0.84**

Table 4.3: River movement (m) and erosion rate (m/y) in bends

The erosion rate has increased during these periods of time. The previous idea was that the erosion rate should decrease because of the trees. This different behaviour from the expected one can be explained by the trees position. They were not planted just in the edge of the bank, but some meters away from the river. This fact allows the river to keep on migrating.

Analysis of erosion rate in a straight stretch

The same method used to analyse the erosion rate in the bends is used also in this case (Table 4.4).

	1935-1965	1965-1983	1983-2003
Section 3	0.27	0.31	
Section 4	0.28	0.31	
Section 6	0.23	0.37	
Section 8	0.19		0.36
Average (m/y)	0.24	0.33	0.36
Error (m/y)	±0.2	±0.33	±0.3
Range of bank retreat (m/y)	**0.04-0.44**	**0-0.66**	**0.06-0.66**

Table 4.4: River movement (m) and erosion rate (m/y) along straight channels

Erosion rate along straight reaches of the river is less important than at the bends. It increases also with time. Not many trees were planted along straight stretches.

4.4- Planform river evolution and analysis of erodibility

To observe the evolution of the river, the coordinates of the river channel have been found for four years: 1935, 1983, 1992 and 2003.

The photo from 1965 is not used in this analysis, because it is the one that presents the maximal error (6m).

The analysis of the planform evolution is done by comparison of the coordinates of the centreline of the river for different years. From aerial photos and using the program ArcGis, the coordinates have been taken by hand, which is another source of error. On the photos, the top of the trees and their shadow are sometimes covering the channel position. Given that the centreline position cannot be observed, an estimation of the position is done in some parts.

Also in this section, the erodibility is studied. The migration of the river in one direction or another is related to the erodibility of the bank and by the local values of flow velocity and water depth. The erodibility is influenced by many factors, like the presence of trees or the proximity to hills. The river is situated near a hill in the right side (according to the flow direction) and many trees are present between the river and the hill which decreases the erodibility of the bank.

The river has been divided in four parts to better observe the evolution. The position of trees (green lines) is also represented in the following Figures 4.11, 4.12, 4.14 and 4.15.

River stretch 1

In the figure 4.11 we can observe 2 bends which have a strange evolution (indicated with a circle).

For the first indicated bend, looking at the pictures, we can observe:

Period 1935-1965	The curved stretch tents to a straight shape
1983	The bend has been cut-off; instead of the bend there is a straight channel
Period 1992-2003	The curved shape can be observed again. During this period the bend increases.

The second indicated bend decreases gradually until almost disappearing in 2003.

The evolution of these two bends could be explained because of the cut-offs.

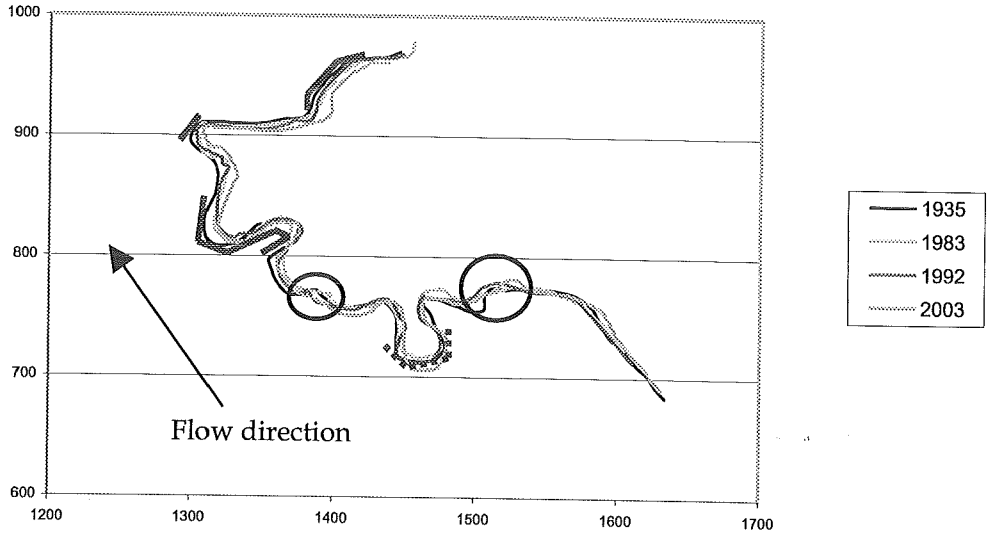

Figure 4.10: First part of the studied stretch

Dark green lines represent poplar trees planted to counteract bank erosion. The non continuous line means isolated poplar trees, which have little influence on bank protection. Light green lines show the position of trees which don't have any effect on bank protection.

Poplar trees have effectively suppressed bank erosion. In the zones where poplar trees were planted (after 1935), the erosion along the outer bank has stopped.

In the downstream reach of this stretch, we can observe that the river tends to migrate upstream for 1983, 1992 and 2003.

River stretch 2

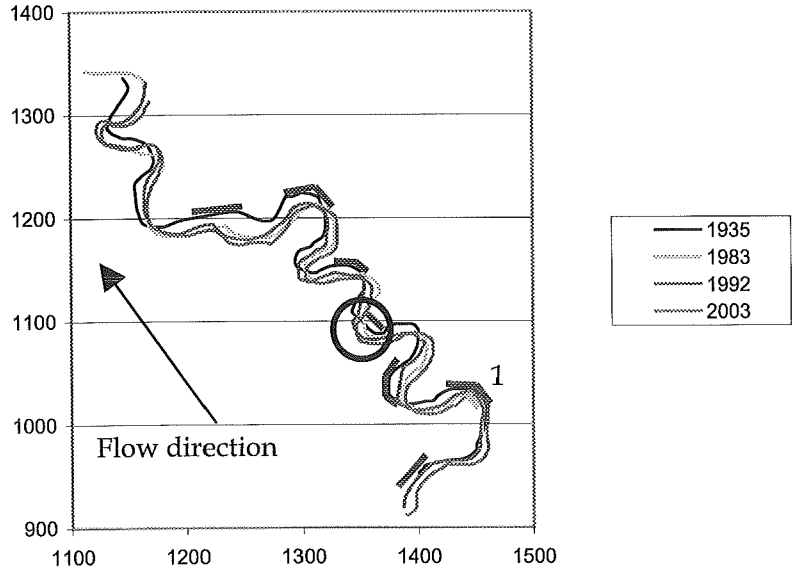

Figure 4.12: Second part of the studied stretch, Geul river

The upstream migration can also be observed in river stretch 2 (Figure 4.11). Upstream migration can be due to several reasons. One reason is that the point bar is formed before the apex of the bend. To verify the point bar situation, it's necessary to use the program Miandras, which gives the evolution of the planform including the new point bars.

The river tends to migrate towards the hill, which is situated on the right side of the river. It means that this bank is more erodible. The reason for that could be the groundwater flow from the hills to the river and also through the valley, following the direction of the river (downstream). It makes the bank less stable (discussion with Ronald van Balen, VUA).

Upstream migration has also been observed by de Moor (2006) in bend 1, but not along all the stretch.

The position of the point bar, downstream of the bend apex (Spanjaard, 2004; and field observations, 2006), means that the river migrates downstream.

Since upstream migration on the Geul river is not observed on the field, it can be explained by a rotation of the photos. Rectifications done by ArcGis change the photos in order to put them in the most accurate position. One of these changes is the rotation of the image.

A rotation for the photo of 1935 could explain the upstream migration observed on the river stretch 2 and also on the downstream reach of river stretch 1.

The section indicated with a circle is analysed further (Figure 4.13).

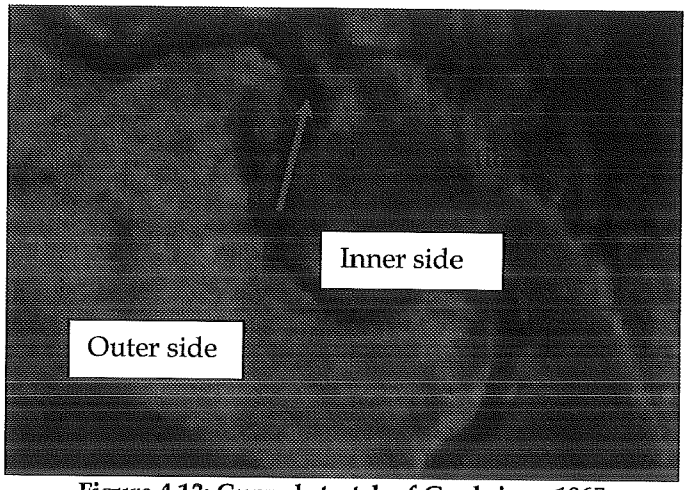

Figure 4.13: Curved stretch of Geul river, 1965

From the photo of 1935 we can see that erosion took place on the inner side of the river. To combat this bank erosion, trees were planted along the inner bank. Then, the river changed its behaviour (we can see the difference in the photo of 1965) and the erosion occurred on the outer part.

At present, erosion takes place at the outer side and the inner side is affected by accretion and a row of poplar trees is situated in the middle of the bank.

River stretch 3

In Figure 4.14 we also observe upstream migration, at the upstream part of the river stretch 3. This might also be a consequence of the error introduced by the rectification.

In section 1 upstream migration due to the rotation is still observable. This end extends following the flow direction and not eroding the outer side.

In section 2 and 3 erosion takes place at the outer side of the bend and we can observe how the bend develops by extending itself. The error produced by the rectification done by ArcGis also affects this reach. River migrate downstream, but the planform movement is too high (erosion rate higher than 3m/y between 1935-2003)

In the section 4, there is a bend corresponding to 1935. This curved stretch tends to become straight. In 2003 there is no curve in that place anymore.

Due to the important influence of the error on the coordinates of that stretch, this part won't be taken into account for model calibration.

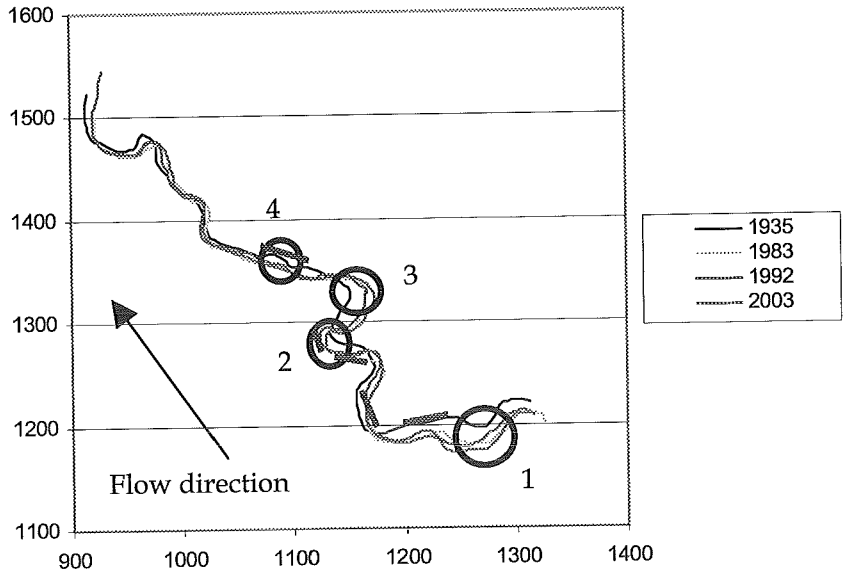

Figure 4.14: Third part of the studied stretch, Geul river

River stretch 4

In Figure 4.15 we can observe the presence of trees on the outer side of the bend that reduce the erosion in that place. Then, there is again an upstream migration, maybe a bit increased by the error.

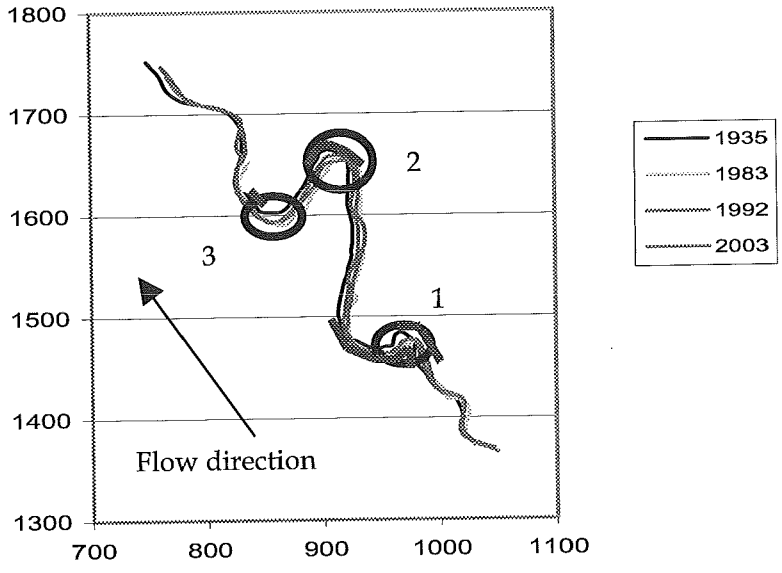

Figure 4.14: Fourth part of the studied stretch, Geul river

In the section 1 (Figure 4.15), due to presence of trees erosion reduces downstream the apex of the bend.

Upstream migration is also observed along the stretch between sections 1 and 2.

In section 2 and 3, the effect of the trees is also observable. There is no more erosion in the outer side where they are planted but in the inner side.

In section 2, trees prevent the erosion on the outer side. From width analysis (See Section 4.5) we get that width increases on this bend, which implies that erosion has to take place on the inner bank (point bar). This explains the movement on the centreline through the inner bank (upstream migration).

Conclusions:

The accuracy error (6 m) has the same order of magnitude as the channel width (8 m). Planform changes obtained from aerial photos can be considered doubtful.

Geul river is too small to carry out a river migration analysis based on these aerial photos.

4.5- Width evolution

Seven sections of the river have been analysed to be able to know how the river width has developed with time (Figure 4.15). Values are obtained by measuring the width in the apex of some bends and in straight stretches.

The values obtained from the photos are:

	1935	1965	1983	1992	2003	Position
Section 1	5,91	7,10	8,34	9,23	8,39	Apex
Section 2	4,64	5,94	6,97	7,31	8,14	Straight reach
Section 3	6,15	6,39	6,57	7,37	8,80	Downstream apex
Section 4	7,19	8,44	7,31	9,61	12,27	Apex
Section 5	4,33	3,22	3,95	5,62	6,79	Straight reach
Section 6	4,53	7,41	-	8.81	12.85	Apex
Section 7	-	7,63	7,95	8,24	9,38	Apex

Table 4.5: Width evolution during the period 1935-2003 obtained from the aerial photos

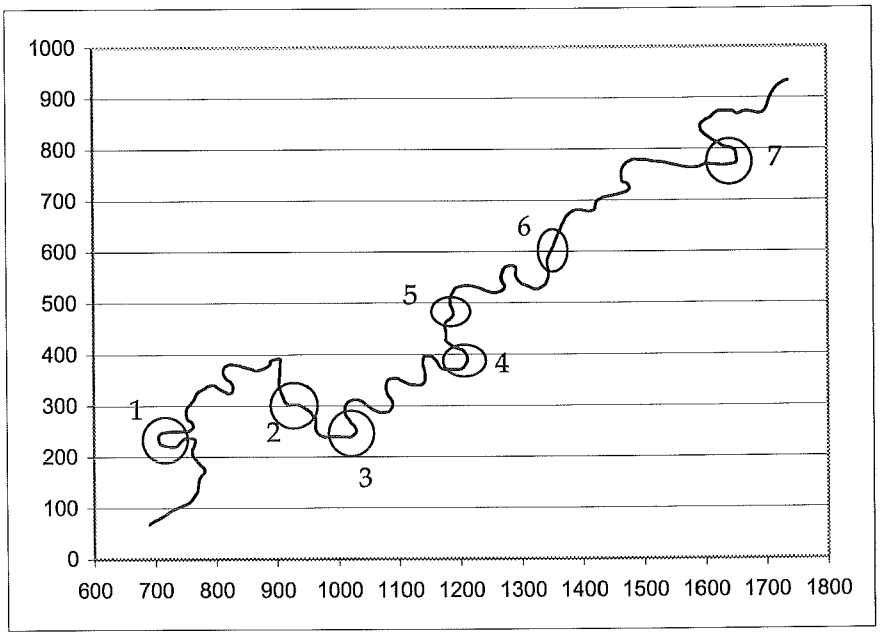

Figure 4.15: Section of the river in which the width has been analysed

Observations:

Section 1:

Width increases from 1935 to 1992 inside the bend.

At the inner side a point bar has been formed; it has grown especially between 1992 and 2003. At the outer side some trees were planted before 1983, which reduced the erosion rate. This explains the reduction of the channel width between 1992 and 2003.

Section 2

The width has increased from 1935 to 2003. The increasing rate was higher at the beginning (1935-1965). Also in this stretch of the river some trees were planted before 1983.

Section 3:

Some trees were planted along both sides of the river after 1935; for that reason, the variation of the width is negligible.

After 1983, the trees along the outer side of the bend have been surrounded by the water and at present time they are situated inside the channel. This means that there are no trees to contrast bank erosion anymore. As Table 4.5 shows, the channel width has increased more after the trees are in the channel.

Section 4

In 1935 there were trees along the inner side of the end, but not along the outer side of the bend, where erosion took place.

Observing the values, the width increases between 1935 and 1965, but then it reduces until 1983. After that, from 1983 to 2003, the width tends to increase.

The decrease from 1965 to 1983 doesn't follow the increase patterns observed in the other sections.

Section 5:

The width increases regularly; the increase in more important during the first part of the period.

Section 6

It's possible to observe that channel width in that section decreases from 1935 to 1965. The reason could be that some trees had been planted along the outer side which reduced the erosion rate, but sedimentation continued in the other side.

As in section 3, at present time trees are surrounded by the river. Also the width has increased considerably, after 1983; which can be due to the fact that trees didn't have any effect on erosion anymore.

Section 7:

River width increases little by little. The increase is higher between 1992 and 2003.

According to these observations, the river width tends to increase in the studied area.

There are some reasons that might explain this. One reason is the influence of the discharge. If the average discharge changes with time, the width of the channel can be affected.

Another reason is removal of the bank protection, done after 1988, that allows to increase the channel width.

5- Historical analysis based on data

5.1- Discharge evolution

Discharge data are obtained form the "Water Roer en Overmaas", from the University of Liège. The data consists of the daily discharge values from 1969 to 2002.

Data vary from 0 to 36m³/s (Figure 5.2). Discharges higher than 30 m³/s have occurred three times during this period (33 years). This means that this phenomenon has a frequency of 1 every 14 years.

The year-averaged discharge values are shown in the Table 5.1 and represented in the Figure 5.1.

1969	1.15	1977	0.79	1986	1.79	1994	1.65
1970	2.56	1979	2.17	1987	2.47	1995	1.72
1971	0.82	1980	2.21	1988	2.03	1996	0.9
1972	0.99	1981	2.62	1989	1.49	1997	1.1
1973	1.34	1982	1.94	1990	0.8	1998	1.79
1974	1.81	1983	2.11	1991	0.95	1999	2.03
1975	1.25	1984	2.32	1992	1.28	2000	1.89
1976	0.61	1985	1.62	1993	1.58	2001	2.33
						2002	2.26

Table 5.1: Discharge year average-values

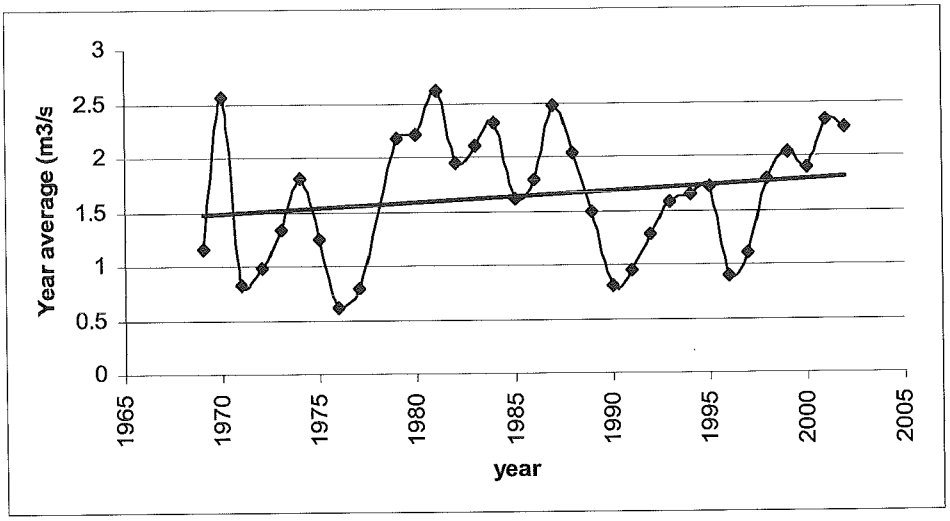

Figure 5.1: Representation of the discharge year-average

In section 4.5, width evolution is linked with the variation of the discharge. In the Figure 5.2, we observe that the year-average value of the discharge tends to increase

with time (the trend line shows it). So, it can effectively be one of the reasons for the increasing behaviour of the channel width.

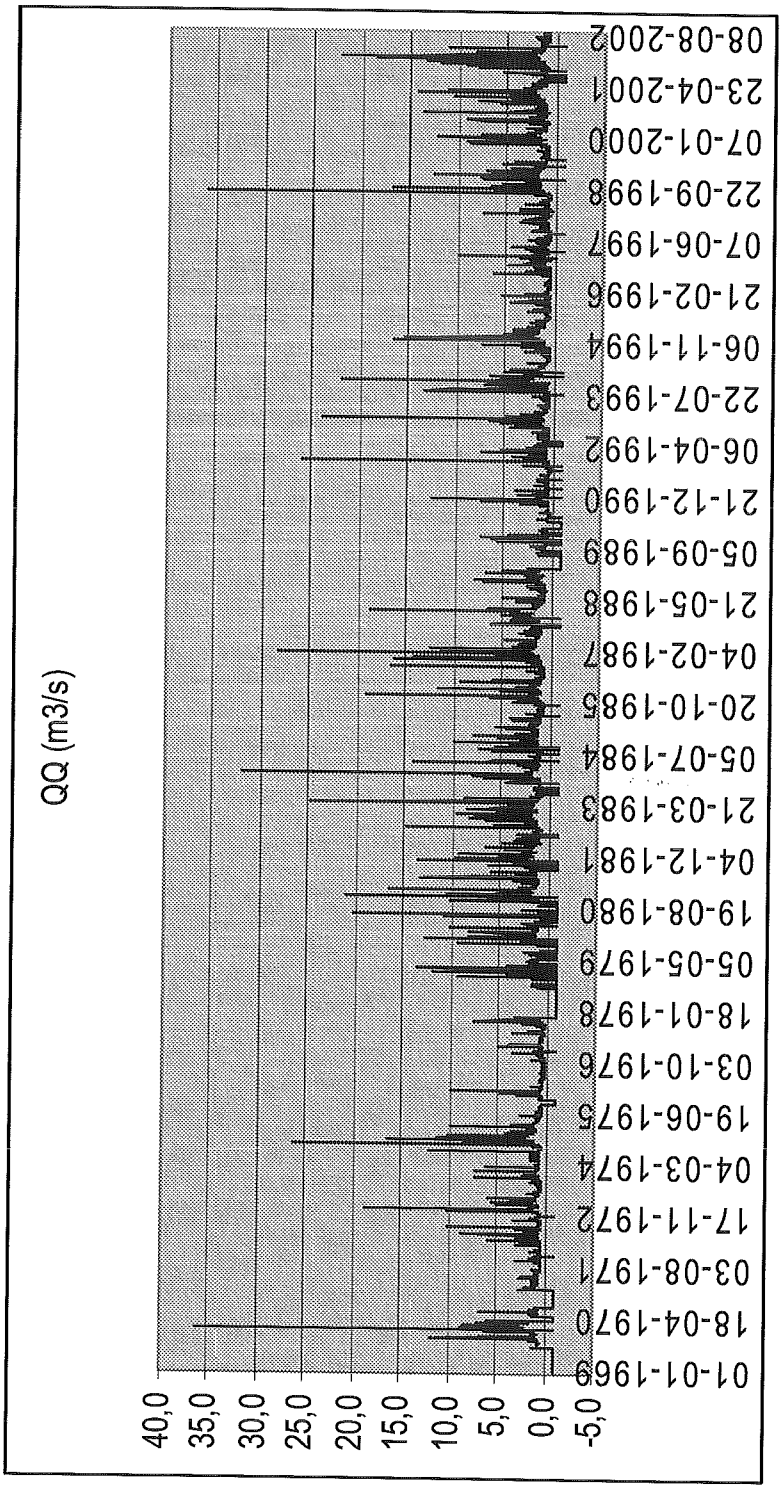

Figure 5.2: Discharge evolution from 1969 to 2002 (University if Liège)

6- Input data

In this chapter, a description and a discussion of the input data are made for certain parameters. The choice of the best values has been an iterative process since some of those parameters are interdependent.

6.1- Valley slope

The following map from "Consultancy for environmental management and research" (2000) shows the topography of the catchment area, and also the different slope gradient classes. The black mark shows the zone the studied area.

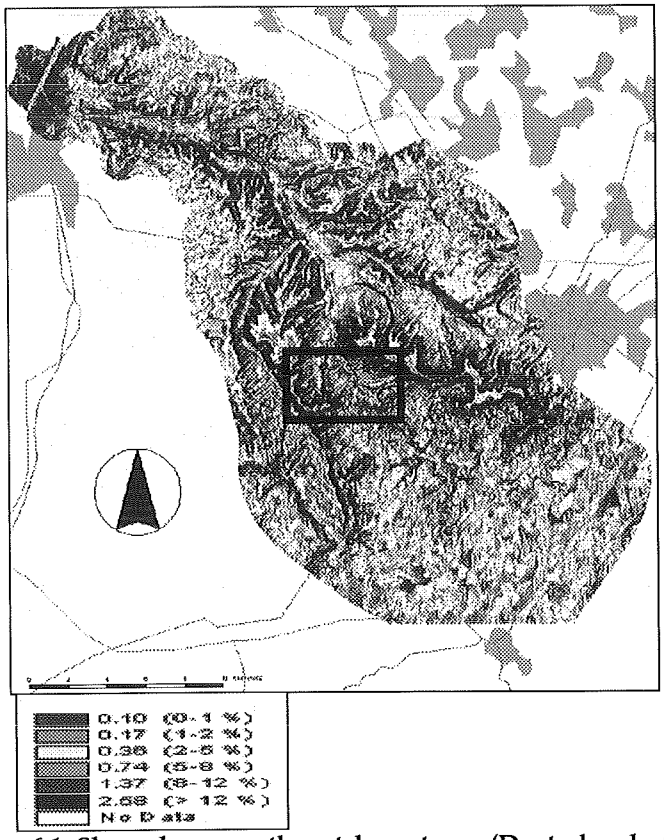

Figure 6.1: Slope classes on the catchment area (Dautrebande, 2000)

Using this map, we obtain a slope value between 0 and 0.01 m/m.

As explained in Section 2.1, the valley gradient of the whole river decreases from 0.02 m/m near the source to 0.0015 m/m at Itteren. Derived from a digital elevation model, the valley slope gradient in the area is **0.004m/m** (de Moor, 2004).

6.2- Water depth at bankfull stage

Channel depth of the Geul river varies from 2 to 2,5m (Chapter 2). Thus, water depth at bankfull discharge also varies in that range.

6.3- Chézy coefficient

A reasonable value of the Chézy coefficient for rivers like the Geul is 20 $m^{1/2}/s$ (based on expert opinion).

6.4- Discharge

Miandras works with a formative discharge. This is often chosen as a bankfull discharge. However, higher values of the discharge might be used. In this case the water flowing on the floodplains shouldn't be able to change the morphology of the river channel. This remains true as long as the velocity on the flood plains is very low.

Discharge is derived from the discharge data of "Waterboard Roer en Overmass".

Generally bankfull discharge occurs once every 1,5 or 2 years (discussion with de Moor).

6.4.1-Formative discharge based on sediment motion

The discharge has to be capable of moving the armour layer on the channel bed; otherwise it can not act as a formative discharge.

The discharge is checked on its capacity for removing the observed armoured layer having a 5 cm grainsize. To carry this out, Shields-parameter is studied. This number let us know if there is any motion on the river or not for some given parameters.

These parameters are shown in Table 6.1:

Grainsize	0.05 m	Grainsize of the armoured layer that formative discharge have to move D_*=1256
Channel width	8 m	Averaged width based on the results of de Moor (2006)
Chézy number	20 $m^{1/2}/s$	See 6 .3

Table 6.1: Parameters used to obtain the bankfull discharge

Studies done by de Moor (2006) show that the most realistic width to simulate the study area is 8 m.

Shields (1936) determined the critical value of θ (Shields-parameter) which determines the beginning of the movement and it depends on the grain attributes and the flow patterns near the bottom. Using the Shields diagram for the motion start moment some values are obtained:

$$\theta_{cr} = \frac{0.24}{D_*} \qquad \text{if } 1 < D_* \leq 4$$

$$\theta_{cr} = \frac{0.14}{D_*^{0.64}} \qquad \text{if } 4 < D_* \leq 10$$

$$\theta_{cr} = \frac{0.04}{D_*^{0.1}} \qquad \text{if } 10 < D_* \leq 20$$

$$\theta_{cr} = D_*^{0.29} \qquad \text{if } 20 < D_* \leq 150$$

$$\theta_{cr} = 0.055 \qquad \text{if } D_* > 150$$

with $D_* = (\frac{\Delta g}{\nu^2})^{\frac{1}{3}} D$, with $\Delta = \frac{\rho_s - \rho}{\rho}$

where ρ_s : material density (2650 kg/m³)
ρ : water density (1000 kg/m³)
ν : water viscosity

For values of θ below the critical value no sediment transport will occur. This value is calculated as:

$$\theta = \frac{u_0^2}{C^2 \Delta D_{50}} \qquad \text{with } u_0 = \frac{Q}{\sqrt{Bh}}$$

in which C : Chézy coefficient
D_{50} : grainsize

The river bed slope is also needed to obtain the water depth value (h). It's calculated as:

river bed slope= valley slope/ sinuosity

Based on the results of de Moor (2004), the study area has a sinuosity of 1.67 and a valley slope of 0.004 m/m (See Section 6.1). River bed slope value is 0.0024 m/m.

Discharge (m³/s)	$\theta_{critical}$	θ	Sediment motion
19	0.055 ($D_* > 150$)	0.052	no
20		0.054	no
21		0.055	-
22		0.058	yes

From Shield's parameter analysis, the formative discharge is 22 m³/s.

The water depth corresponding to this discharge is 2 m. Taking into account that the channel depth is 2-2.5 m, the formative discharge is also considered as bankfull discharge.

To check the bankfull discharge frequency, values are arranged from bigger to the smaller one (Figure 6.2). Discharge values are represented as a function of their frequency.

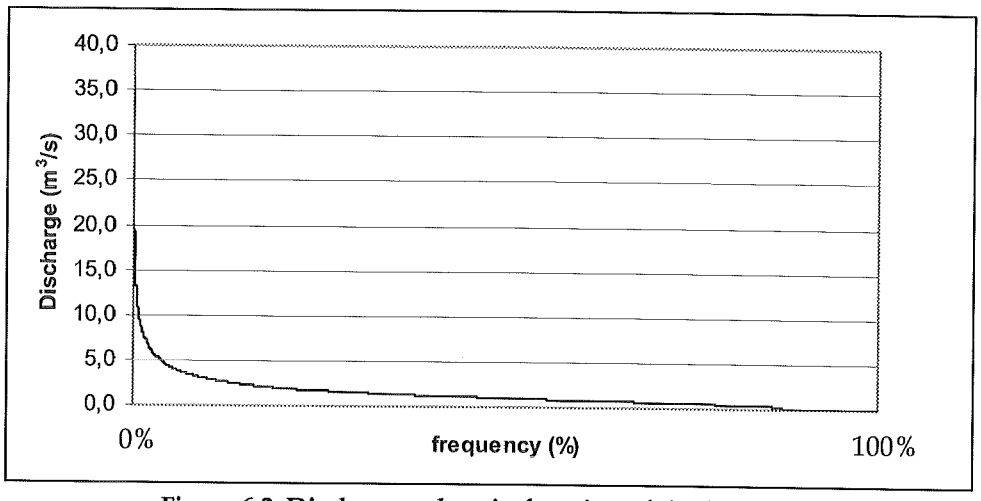

Figure 6.2: Discharge values in function of the frequency

A phenomenon that occurs every day during the period of 33 years (12325 days) has a frequency of 100%.

The frequency of bankfull (formative) discharge is 2 years (as de Moor analysis, 2004).

Corresponding to a frequency of once every 1.5 years, the discharge is 19m³/s (Figure 6.3).

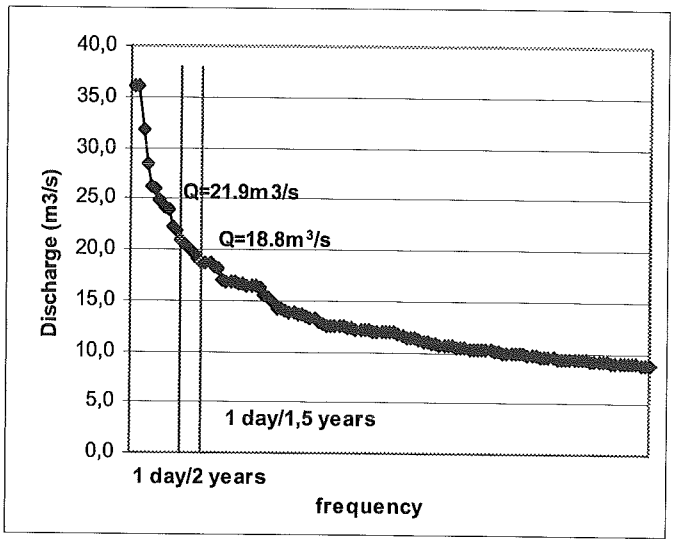

Figure 6.3: Representation of bankfull discharge frequency

In order to observe the influence of the discharge on the planform evolution, some tests are done for a period of 10 years. In Miandras the period length is 5 days because the frequency of bankfull discharge is one day every two years.

The used values are: 22 (formative discharge), 30 and 36 m^3/s (maximum observed during the period 1969-2002) (See Appendix B).

6.5- Channel width

The Geul river has some different channel-forming widths varying from 8 m to more than 15 m. These widths are a function of the local curvature. In the straight stretches, width channel is about 8 m and it raises to 15.5 m (maximum) in the bends (Figure 6.4).

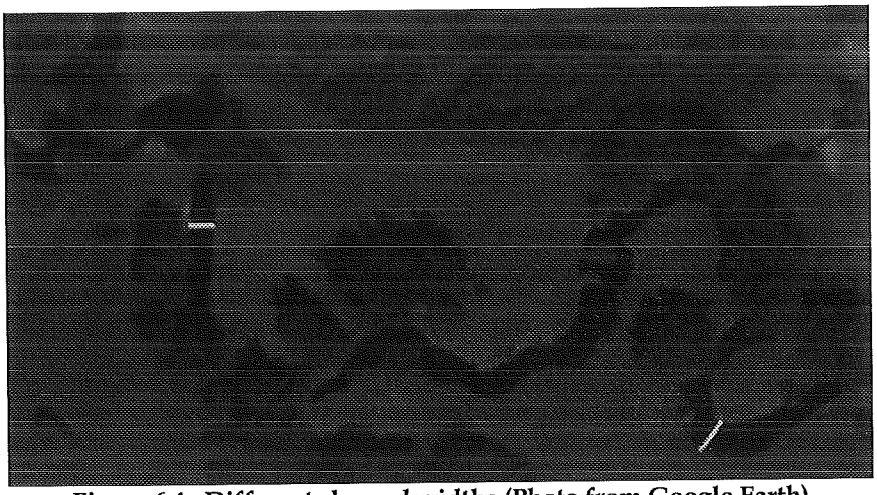

Figure 6.4 : Different channel widths (Photo from Google Earth)

Predictions made by VUA (de Moor, 2006) used two different width values to carry out the computations: 8 m and 15.5 m. The results show that the 8 m width is the most realistic value along the study area.

The mathematical model assumes that channel width is constant in time and space. For this reason, an optimisation of the channel width is done (Section 7.3). The values used are: 8, 11.75 (the averaged from the minimal and the maximal value) and 15.5 m.

6.6- Grainsize

In order to determine the existing grainsize carried by the river, material on the bed and on the point bars is analysed.

Some samples have been taken from several point bars of the Geul river (Spanjaard, 2004). The analysis showed that sediments are constituted by two members:

a fine fraction and a coarse fraction. The D_{50} of each fraction can be obtained using the following distributions (Figure 6.5):

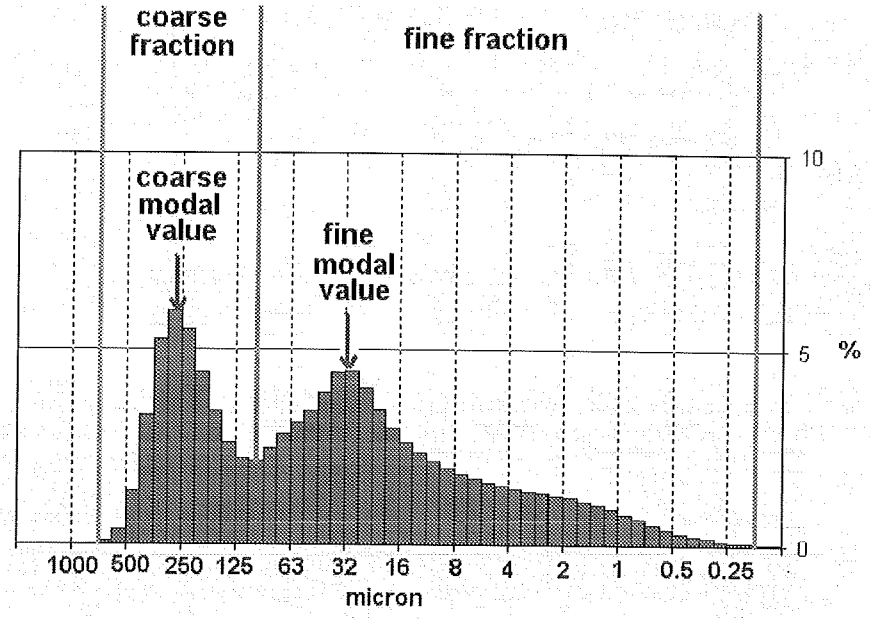

Figure 6.5: Grainsize distribution of the banks (Spanjaard, 2004)

The fine modal value is around 32 micron and the coarse modal value is about 250 microns. The modal value of the bank material is taken as 250 microns (0,00025m).

The fine fraction present on the point bars of the river can be observed in Figures 6.6 and 6.7.

The grain diameter of bed material has been fixed by the University of Liège (Belgium) by making counts/plots of the gravel in the bed of the river. They observed a clear pattern of downstream decreasing D_{50}. The median grainsize of the bed load that they obtained varies from 45mm (near Gulpen) to 52mm (near the Dutch- Belgium border, where the study area is located). A value of 50mm is taken as the grainsize in the bed.

The river bed appears armoured with the largest grainsize forming the top layer and protecting the smaller ones underneath.

The active gravel layer (moved material during high discharges) is supposed to have an average thickness of 10-15 cm (from the study held by the University of Liège of a river with similar characteristics to the Geul river).

The relevant grainsize for the study is the one that contributes to form the point bar (coarse and fine material).

The value used for the simulations is 0.025 m. This value is the average between the modal value of the coarse fraction of the bank material (250 microns) and the one corresponding to the bed material (5 cm).

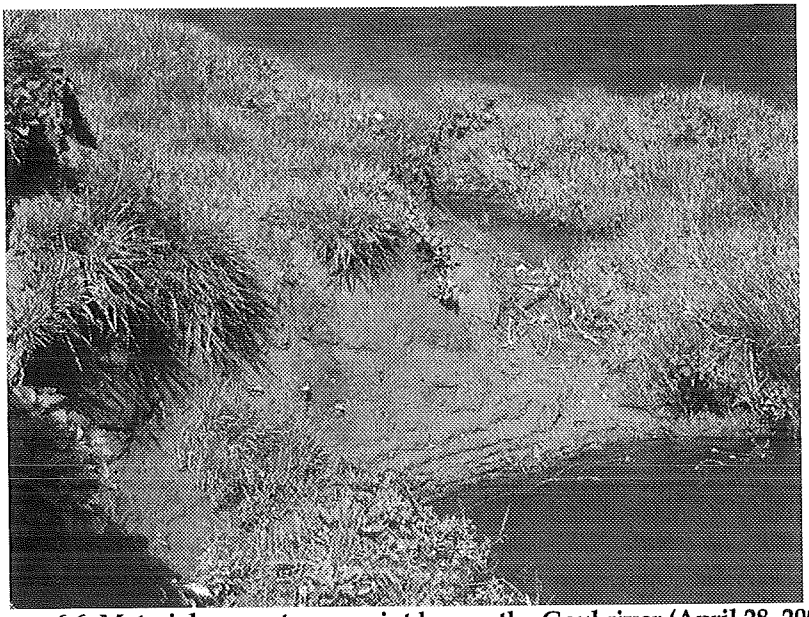

Figure 6.6: Material present on a point bar on the Geul river (April 28, 2006)

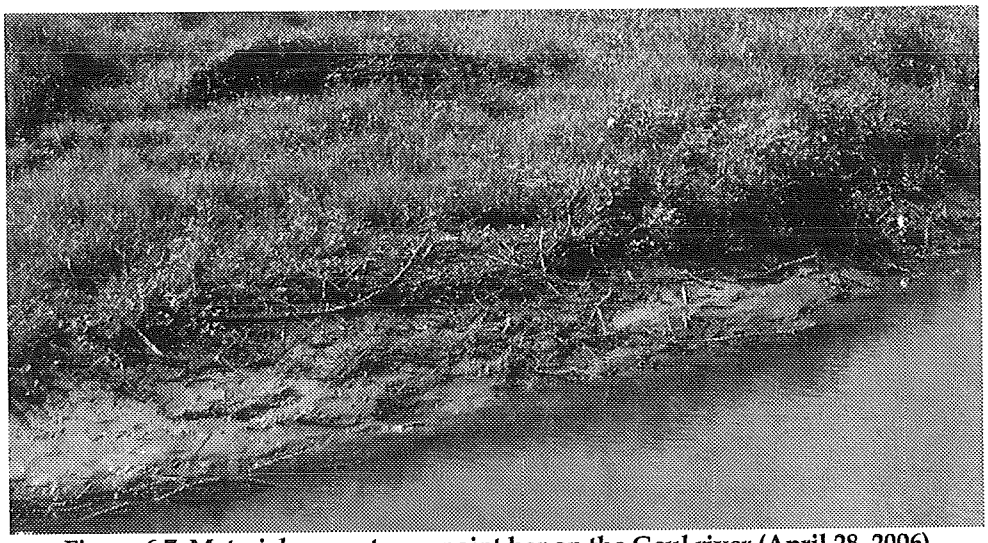

Figure 6.7: Material present on a point bar on the Geul river (April 28, 2006)

The program Miandras is useful to observe different behaviours of the river when using different values for the grainsize (D_{50}).

The results of this analyse are reflected in Appendix C.

7- Optimization of the model parameters

In this chapter some parameters are analysed by calibration. To obtain a correct prediction, the model has to be calibrated several times and validate.

Using the input data described in the previous chapter, values are discussed and a comparison is made to analyse the influence of these parameters on planform changes, sediment transport, erosion rate....

For each calibration, Miandras is run for a steady-state situation and then, for a time adaptation situation. The first run computes bed deformation at the initial time; the second one gives the results for planform evolution.

7.1- Choice of the sediment transport formula

Three formulas can be used in the program to calculate the sediment transport rate. Depending on the grainsize chosen one formula is better than the other ones. For coarse sediment, Meyer-Peter & Muller (M-P & M) and power low formulas are recommended; Engelund & Hansen formula is used for fine sediments.

Power low formula is chosen to simulate the sediment transport because of the grainsize chosen (0.025m - coarse sediment).

Power low formula is a simplified formula to get a quick insight of the morphological behaviour:

$$s = mu^b \qquad [1]$$

The value of b varies from 3 to 5 (excluding 3). For the formula of Engelund and Hansen (fine sediments) b is equal to 5 and for the formula of M-P & M can be determined as follows:

$$b = \frac{3}{1 - \frac{0.047}{\psi}} \qquad [2]$$

The value of b=4 is kept for this analysis.

Coefficient m only influences the rate of sediment transport and does not affect the flow and bed topography profiles. A value of 0,0001 is adopted.

7.2- Optimisation of the channel width based on the location of bank erosion

The model assumes a constant channel width and therefore only a single value can be used. In order to obtain the most realistic situation two analyses are done. Both analyses are evaluated for three width values: 8, 11.75 and 15.5 m.

The first analysis consists of the study of the centreline migration.

The second one compares the bank erosion shown by centreline movement with the bank erosion results obtained by Spanjaard (2004).

7.2.1-Comparison at the present situation

Centreline coordinates obtained by Miandras are compared with the coordinates of 2003 (from the aerial photos). The analysis is done for a period of 2 years (one day in the program) and using the three possible width values.

The comparison consists of observing where the migration occurs when the width values are changing.

B=8 m (Figure 7.1)

We can observe that centreline migrates at bends and also along the straight stretches even if the movement is not very important.

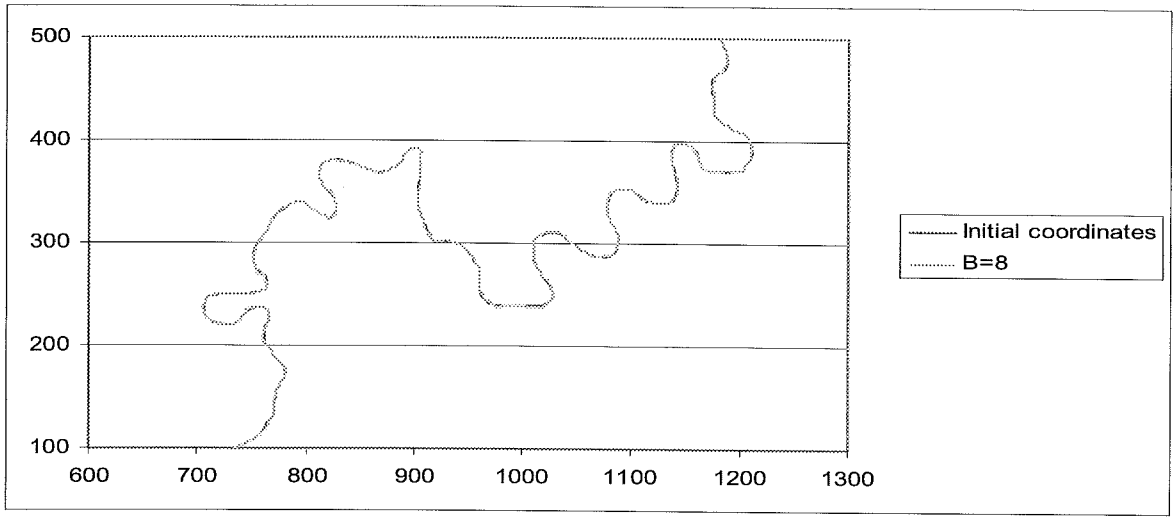

Figure 7.1: Comparison between actual coordinates (2003) and coordinates obtained by Miandras (B=8m ; Q=22m3/s)

B=11.75 m (Figure 7.2)

Migration is less important than in the previous case. It is only observable in a few bends, and it is not along the straight stretches.

B=15.5 m (Figure 7.3)

As in the previous case, erosion is only easily observable at bends.

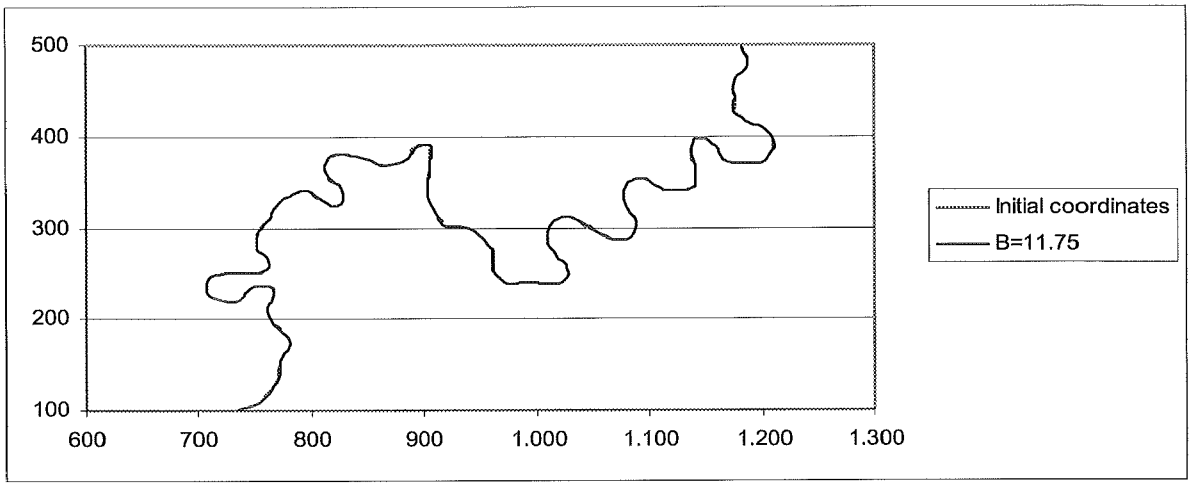

Figure 7.2: Comparison between actual coordinates and coordinates obtained by Miandras (B=11.75m ; Q=22m3/s)

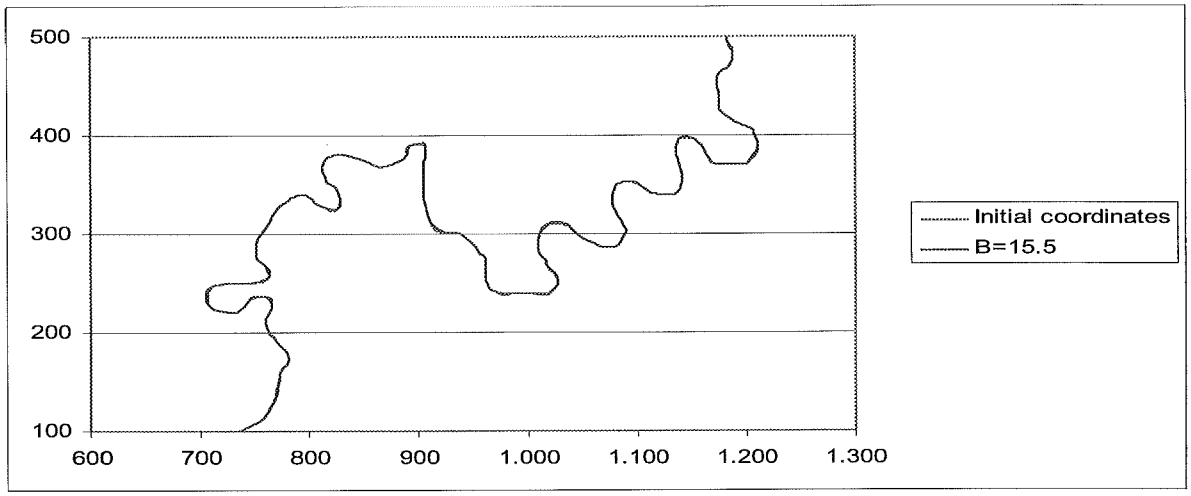

Figure 7.3: Comparison between actual coordinates and coordinates obtained by Miandras (B=15.5m ; Q=22m3/s)

From these analyses, migration obtained with an 8 m width best represents the real erosion, because river migration occurs at the bends and along straight stretches.

7.2.2-Comparison with the results from VUA

This consists of comparing the planform evolution obtained with the program with the Spanjaard's results (2004) (Figure 7.4).

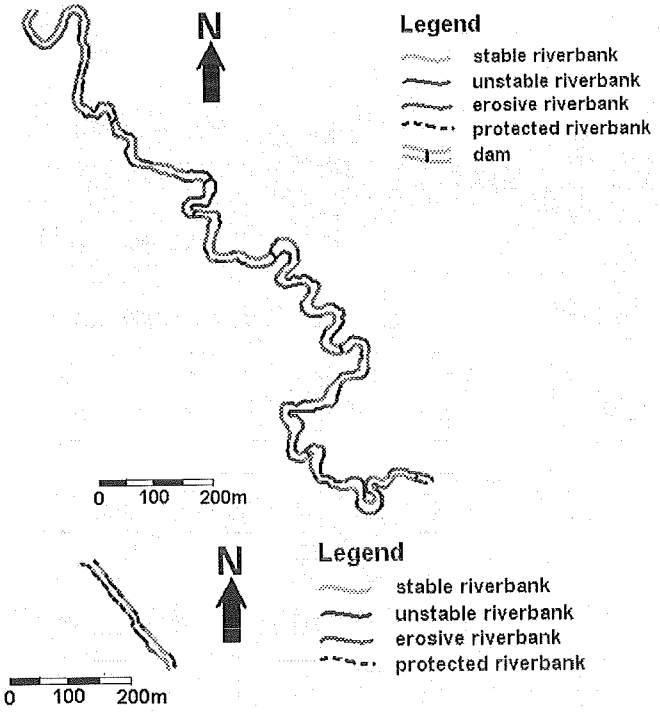

Figure 7.4: Schema of erosion (Spanjaard, 2004)

From his work, we observe the position of the erosive banks, and these positions are compared with the zones where the program Miandras computes the river migration.

Three types of river banks are represented on the figure, depending on its stability. Stable banks are fully vegetated and they haven't suffered any substantial erosion for a long time.

Unstable banks are partly vegetated because the exposed sediment is not constantly removed and they have not been strongly eroded for a few years.

Erosive banks are steep, unvegetated banks where the sediment is fully exposed; these banks experience intensive scour which also causes frequent mass failure by undercutting and oversteepening of the banks.

Miandras results are obtained after 10 years. The river migration for the different channel width values are shown in Figures 7.5, 7.6 and 7.7.

B=8 m (Figure 7.5)

Along straight stretches, centreline migration occurs very close to erosive banks position.

Generally, centreline migration at bends takes place downstream of the erosive banks of Spanjaard's results.

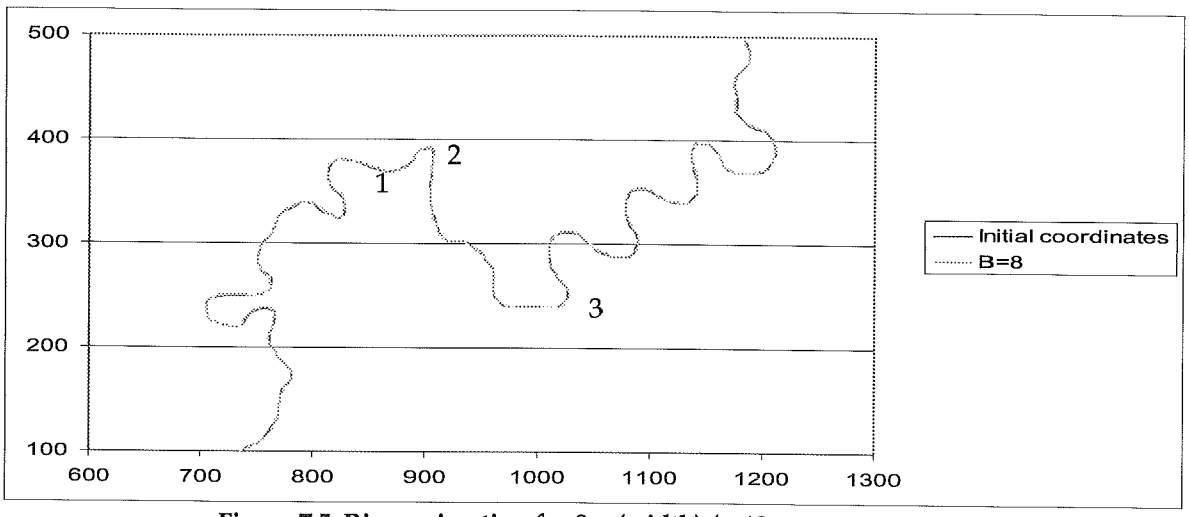

Figure 7.5: River migration for 8m (width) (t=10 years; Q=22m³/s)

B=11.75 m (Figure 7.6)

Centreline movement at the bends occurs downstream of the indicated erosive banks, as in the previous case.

In bends 1, 2 and 3, the centreline evolution obtained by Miandras does not follow the behaviour described in Figure 7.4. River at bends 1 and 2 doesn't migrate and at bend 3, the migration is quite important (no erosion in Figure 7.4).

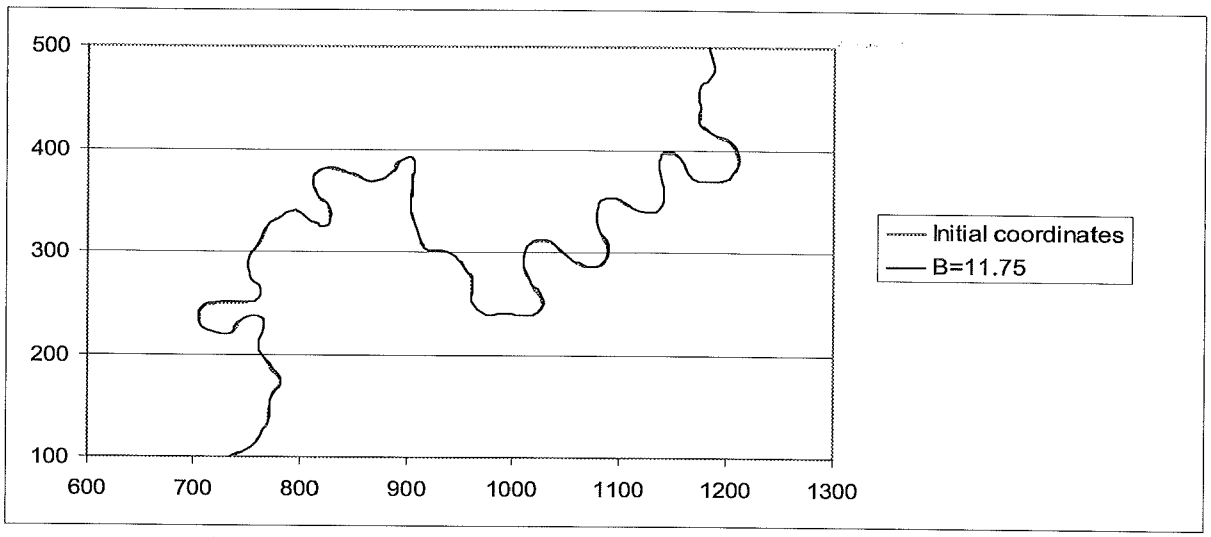

Figure 7.6: River migration for 11,75m (width) (t=10 years; Q=22m³/s)

B=15.5 m (Figure 7.7)

River migration at bends is also downstream of the apex, as in the other two cases. Erosion obtained by the program takes place along the entire bend so that it overestimates bank erosion.

River migration along the straight stretches doesn't correspond to erosive bank position.

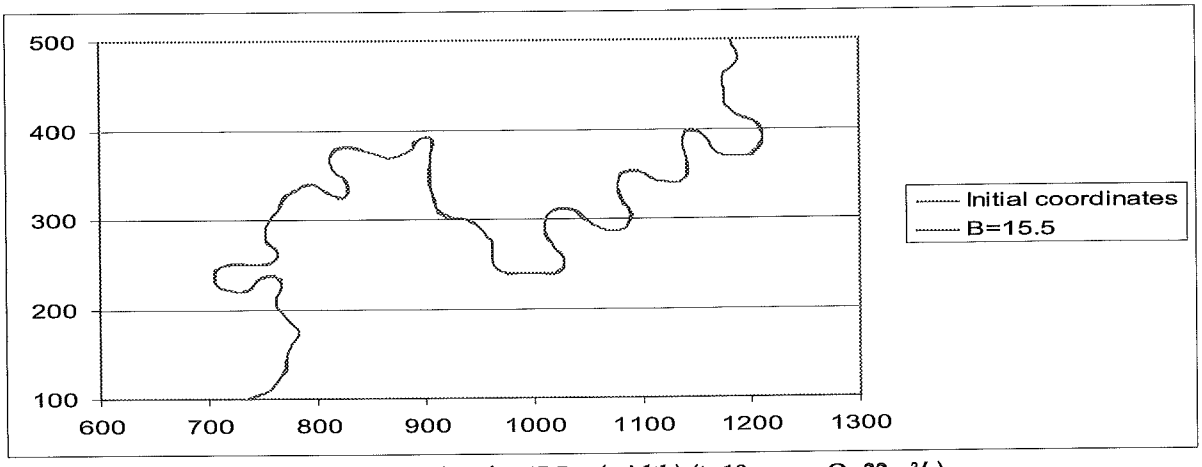

Figure 7.7: migration for 15.5m (width) (t=10 years; Q=22m³/s)

In conclusion, the migration obtained for 8 m width is the closest to his result. Following these analysis, the value of **8m** is kept for future simulations.

Bed profile evolution is compared for the three cases in Appendix D.

7.3- Calibration of flow parameters and coefficients

The influence of some flow parameters on the bed profile is studied for a steady-state situation, assuming erodible banks.

These parameters are: α_1 (coefficient weighing the effects of channel curvature on bed shear stress direction), E (coefficient weighing the effects of transverse bed slope on the sediment transport direction) and σ (coefficient weighing the secondary flow momentum convection).

7.3.1-Coefficient weighing the effects of the channel curvature on bed shear stress direction, α_1

This coefficient is introduced in the equation for the angle between the bed shear stress direction and the main flow direction, in which it weighs the deviation of bed shear stress due to the curvature of the channel.

As first estimation, this coefficient can be calculated as follows:

$$\alpha_1 = 0{,}10 * (\frac{h_0}{D_{50}})^{0.3}$$

This value varies from 0,4 to 1,2. In case that with the values of the data introduced the result is smaller than 0,4, the latter is used as a value of this coefficient. If the value obtained is inside the range, the result from the first approach is used.

7.3.2-Coefficient weighing the effects of transverse bed slope on the sediment transport direction, E

This coefficient is introduced in the angle equation. The study is focused on the angle between sediment transport direction and main flow direction.

$$f(\theta) = \frac{0,85}{E}\sqrt{\theta}$$

in which θ : Shields parameter
f(θ) : weighing function of the influence of the sloping bed

The value of E has been derived from flume tests. The advised values are:
- for experimental flumes : $E \cong 0,5$
- for rivers: $E \cong 1,0$

The coefficient can be estimated (first attempt) by the following equation:

$$E = 0,10(\frac{h_0}{D_{50}})^{0.3}$$

The value for rivers (E=1.0) is used to carry out the simulations.

7.3.3-Coefficient weighing the secondary flow momentum convection, σ

This coefficient is introduced in the flow equation, multiplying (2-σ) and the transverse friction term. Its value can affect the prediction of the flow and bed deformation: an increasing value of σ entails an increase of computed flow deformations. This value is usually assumed to be between 2 (no transverse friction) and 4. With σ>2 the effect is comparable to the secondary flow momentum convection.

To estimate this value a relation has been obtained with a theoretical approach:

$$\sigma = 1 + 90\frac{C}{\sqrt{g}}(\frac{h_0}{B})^2$$

Using these values of the input data, values for this coefficient bigger than 4 are obtained. For this reason, a value of 4 will be during the simulations.

7.4- Calibration of erosion coefficients

Calibration coefficients are the erosion coefficients introduced by the erosion law.

In some cases, erosion can only be due to the effects of the near-bank flow. If so, the value for the flow-induced bank erosion coefficient can be found through:

$$E_u = \frac{\Delta n_y}{u_0 \Delta t_y} \qquad [1]$$

If bank instability also affects bank erosion, the value for the coefficients is:

$$E_u = \frac{1}{2}\frac{\Delta n_y}{u_0 \Delta t_y}$$

$$E_h = \frac{1}{2}\frac{\Delta n_y}{h_0 \Delta t_y}$$

$\frac{\Delta n_y}{\Delta t_y}$ is the bank retreat (space/time)

These coefficients are analysed using the value of bank retreat obtained by VUA and from the aerial photos analysis. The results give an idea about the order of magnitude for the coefficients.

7.4.1-Erosion coefficients based on the erosion rate used in VUA

A first attempt to calculate the coefficients has been done using the value given by the analysis of Spanjaard (2004). Using the position of the trees near the river bank, the erosion rate was studied in two points. The results were 0.37m/y and 0.6m/y.

The first simulation is done with the average value (approximately 0.5m/y). The values obtained for the erosion coefficients during a period of two years (discharge value of $22m^3/s$) are:

Δn_y (m/y)	E_u	E_h
0.5	$4.194e^{-06}$	$2.91e^{-06}$

7.4.2-Erosion coefficients based on the erosion rate using aerial photographs

The averaged value for the maximal erosion rate in curved stretches obtained from the aerial photos (Section 4.2) is now used to calculate the erosion coefficients.

Δn_y (m/y)	E_u	E_h
0.72	$5.87e^{-06}$	$4.07e^{-06}$

Theoretically, Eu is more important than Eh. This fact has to be analysed during the calibration.

Higher Eu means that bank erosion occurs because of the flow. If Eh is more important, erosion is caused by bank failure because of its instability.

7.4.3-Calibration of erosion coefficients based on the present observation on location of bank erosion

In order to determine the importance on the erosion of these two coefficients, a calibration has been carried out. The calibration consists of changing the values of the

coefficients and analysing the influence of these changes in order to obtain the value that gives the closer results to the real situation.

The analysis is focussed on the variation of water depth and velocity, obtained from the output files of Miandras. When these parameters are positive, the erosion takes place in the left bank; if their values are negative, the erosion occurs in the right bank.

When the test is focussed on the flow-induced coefficient (E_h=0), the parameter to be studied is the velocity variation. When the study is focussed on the bank instability (E_u=0), the variation of water depth is the parameter studied.

The flow-induced coefficient is related to the downstream migration. It means that as this parameter grows, downstream migration is higher. The bank instability influences the extension of the bend and upstream migration.

Water depth and velocity variation are analysed in eight sections of the river (Figure 7.10) and compared to Spanjaard's results (2004) to verify if the program computes the erosion at the same place than field observations.

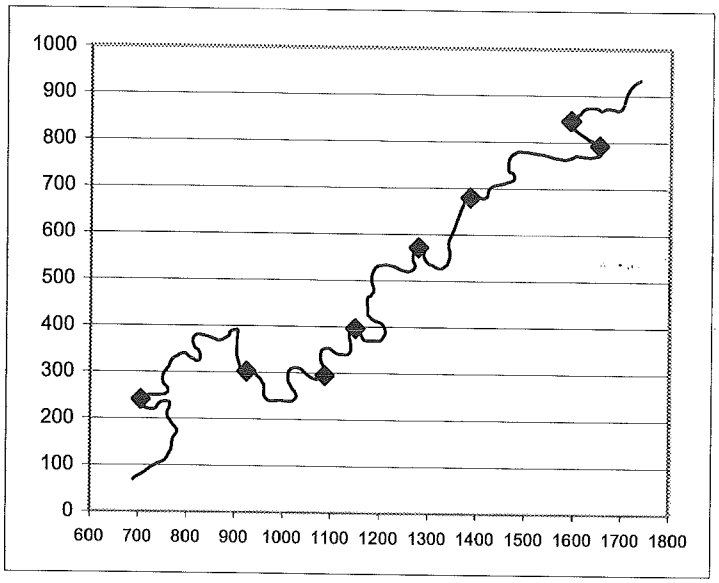

Figure 7.10: Sections where the erosion coefficients are studied

Section	1	2	3	4	5	6	7	8
Side of the river	left	right	right	left	left	left	left	left
Water depth and velocity variation sign	+	-	-	+	+	+	+	+

The range of values to analyse Eu and Eh is 1e-07 to 1e-05, in both cases.

Using this range, for seven out of the eight sections, the sign of water depth and velocity variation correspond to those on the scheme. Section 7 is the only one that doesn't correspond. We observe that erosion takes place in the inner side of the bend

because of the presence of the trees (Chapter 4). Miandras can not simulate this because it's a factor that the program doesn't take into account.

Some values of Eu and Eh are studied in order to obtain the most accurate values with the real situation.

The first test consists of giving the comparable value to both parameters; then, Eu is considered higher than Eh; and finally, Eh values is higher than Eu (Figure 7.11 and 7.12).

The most accurate result is obtained by using Eu=4e-06 and Eh=6e-06. This means that bank erosion on the Geul is due to bank instability.

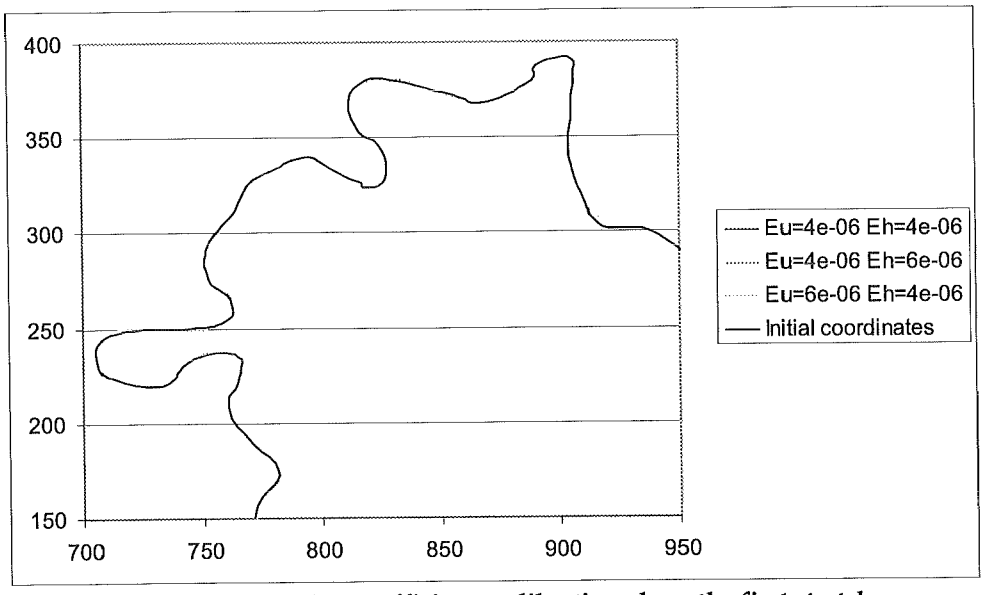

Figure 7.11: Erosion coefficients calibration along the first stretch

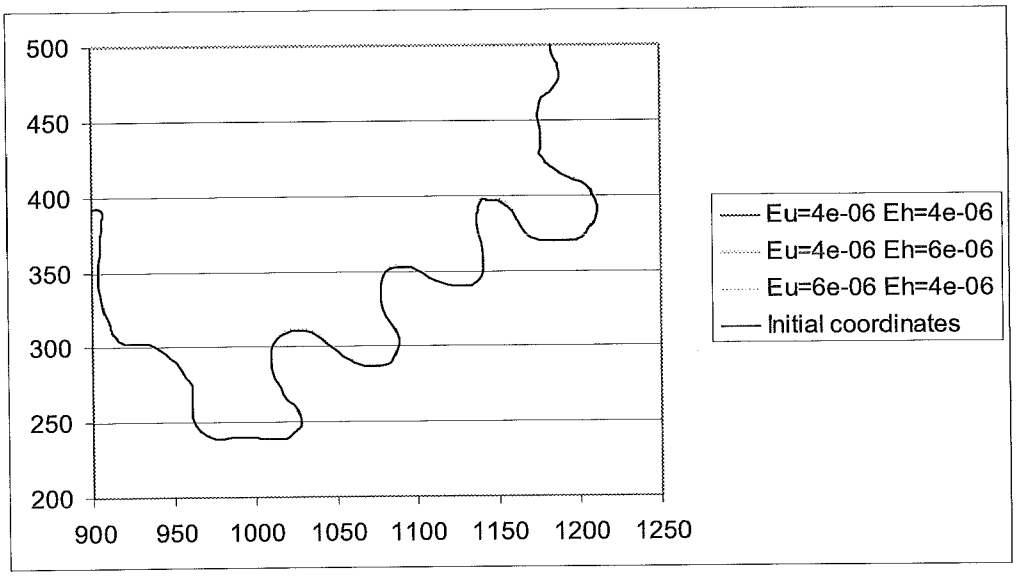

Figure 7.12: Erosion coefficients calibration along the second stretch

Before carrying out the prediction, these values have to be calibrated and validated with the coordinates obtained from the aerial photos.

The new calibration (Chapter 9) will consist of studying the values of Eu and Eh and, if needed, finding new values. The fact that bank instability erosion coefficient is more important in the Geul river than flow-induced erosion coefficient is kept.

7.5- Summary of the flow parameters optimized after calibration

	Range of value	Value after calibration
Valley slope (m/m)	0.0015-0.02	0,004
Discharge (m^3/s)	0-36	22
Width (m)	8-15.5	8
Reach- averaged water depth (m)	2-2.5	2
Grainsize (m)	0.00025-0.05	0,025
Reach-averaged velocity (m/s)		1.38
Chézy coefficient ($m^{1/2}/s$)		20
α_1	0.4-1.2	0,4
E	0.5-1	1
σ	2-4	4
E_u		$4e^{-06}$
E_h (s^{-1})		$6e^{-06}$

Table 7.1: Flow parameters after calibration

With the values obtained after the flow parameters calibration, the influence of the valley slope and the Chézy number on bed profile evolution is analysed in Appendix E and Appendix F.

8- Study of upstream migration

We observe from the aerial photos that the river seems to migrate upstream (Section 4.4). A numerical study is done to check if also Miandras predicts upstream migration for the Geul river.

In order to verify the upstream migration an analysis of the point bar position is done. Point bars are formed upstream of the apex bend if the river migration is upstream. Then studying their position we can get to know the migration direction.

To study the point bar position, two analyses can be carried out. The first one is the comparison between the position obtained by Miandras and the results obtained by Spanjaard (2004). The second one consists of the evaluation of the position using the aerial photos. In some cases, point bars and the evolution of their position can be observed on the photos. However, the available photos don't give any useful information about the position, for that reason, only the first analysis is done.

8.1- Upstream migration in Miandras

The mathematical model can be analysed from the point of view of the prediction of the point bar position.

The phase lag s_p between the maximum bend deformation (centre of the point bar) position and the maximum channel curvature (bend apex) location is calculated with the characteristic parameters of the Geul river based on the analysis performed by Crosato (1990). If the s_p value is negative, it means that the point bar is situated upstream of the apex, in which case the river migrates upstream.

In order to calculate the point bar shift it's necessary to describe the variation of the amplitude of water depth deformation along the longitudinal direction, s. For that a second-order differential equation is used. In that equation the source term is a function of the curvature and of local parameters.

$$a_1 \frac{\partial^2 H}{\partial s^2} + a_2 \frac{\partial H}{\partial s} + a_3 H = b_1 \frac{\partial^2 \Gamma}{\partial s^2} + b_2 \frac{\partial \Gamma}{\partial s} + b_3 \Gamma \qquad [1]$$

in which

$$a_1 = 1$$

$$a_2 = \frac{1}{\lambda_s} - \frac{b-3}{2\lambda_W}$$

$$a_3 = \frac{1}{\lambda_s \lambda_W}$$

$$b_1 = -\frac{h_0}{k_B}(b-1)$$

$$b_2 = Ah_0{}^2 k_B - \frac{(2-\sigma)(b-1)h_0}{2\lambda_W k_B}$$

$$b_3 = \frac{Ah_0{}^2 k_B}{\lambda_W}$$

The rest of the values are described in Chapter 3.

Then the phase lag is calculated as follows (Crosato, 1990):

$$s_p = \frac{1}{K}\arctan\left(\frac{Kb_2(-K^2a_1 + a_3) - Ka_2(-K^2b_1 + b_3)}{(-K^2b_1 + b_3)(-K^2a_1 + a_3) + K^2a_2b_2}\right) \qquad [2]$$

with : K : wave number = 2π/L.

The values used for the required parameters are:

Bankfull discharge (m^3/s)	22
River bed slope (m/m)	0.0024
C ($m^{1/2}/s$)	20
B (m)	8
D_{50} (m)	0.025

The result of equation [2] is a positive value, which means that the point bar is situated downstream of the apex and, thus, the river migrates downstream.

To carry out further analyses, the parameters are evaluated for a range of possible values:

Parameter	Interval	Phase lag evolution
Q (m^3/s)	19-36	When discharge increases, the value of the phase lag also decreases
i (m/m)	0.0001-0.004	When slope decreases, also the value of the phase lag also decreases
C ($m^{1/2}/s$)	9.5-20	When the Chézy number decreases, the value of the phase lag also increases
B (m)	8-15.5	When channel width increases, the value of the phase lag also decreases
D_{50} (m)	0.00025-0.05	When the grainsize decreases, the value of the phase lag also decreases

By doing several tests with these values to evaluate the possibility to migrate upstream, we always get a positive result for the phase lag. Miandras can not compute an upstream migration for this river.

8.1.1-Example of the influence of flow parameters on the point bar position: Discharge

Point bar positions can be obtained by running the program Miandras. This comparison is focussed on one part of the stretch.

Miandras is run to observe how point bar positions vary as a function of the discharge (Appendix B).

We can observe that point bars are formed downstream of the apex or at the apex. When the discharge increases, point bars are situated closer to the apex bend.

8.2- Comparison with the results from VUA

From the results obtained by the VUA analysis (Figure 8.2), three different kinds of point bars can be observed: active, vegetated and non-active. The analysis is focussed on the active point bars.

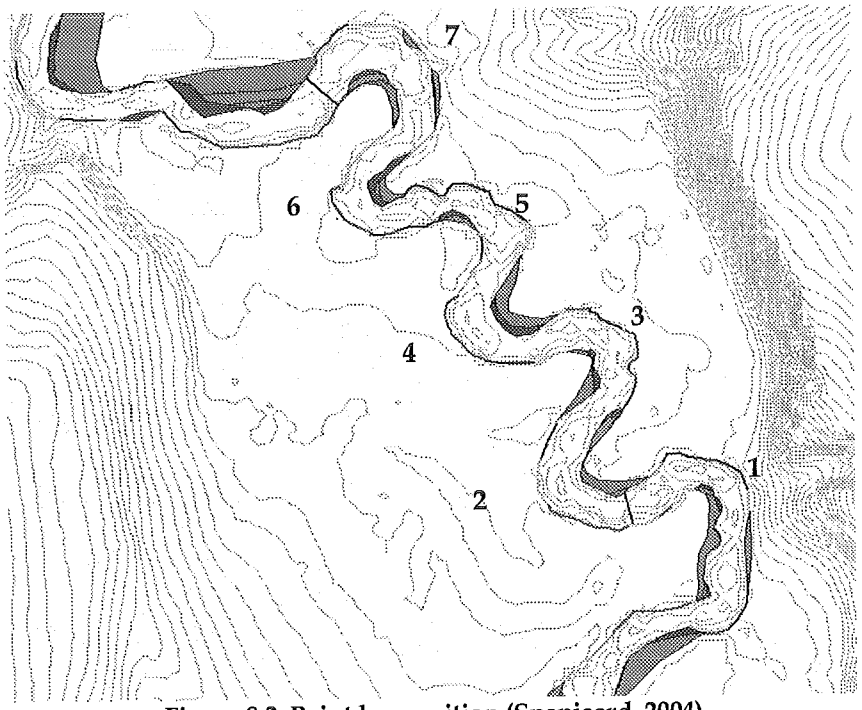

Figure 8.2: Point bar position (Spanjaard, 2004)

In bend 1, there is a non-active point bar situated upstream of the apex, and the active one is more or less situated at the apex.

Bend 2 also presents a non-active point bar upstream of the maximum curvature, but there's no evidence of active point bars.

The point bar corresponding to bend 3 tends to move towards the position of the apex of the bend although there is an important non-active point bar upstream.

Point bars in bend 4 (non-active and active) are situated in the apex position. For bends 5, 6 and 7 active point bars take place downstream of the apex of the bend. Bend 6 also presents a non-active point bar at the apex.

A vegetated and a non-active point bars are observed at bend 7. The non-active point bar is located upstream of the apex, and the vegetated takes place at the apex, as the active point bar.

From Figure 8.2, we can observe evidences of upstream migration in the past, but not in the actual situation. Nowadays, the river tends to migrate downstream.

This means that photos might not be representative of the river migration due to errors. Both Miandras and present-trend observations indicate downstream migration.

As said before, the Geul river is a small river to be studied by aerial photos analysis because of its tiny channel width.

9- Calibration and validation of the erosion coefficients based on aerial photographs

9.1- Calibration

First of all, to carry out the prediction another calibration has to be done using the coordinates from aerial photos. The period considered for this calibration is 1935 - 1992 (57 years). The coordinates of 1935 are introduced in the program Miandras and computed with the parameters calibrated before (Table 7.1).

From the aerial photos upstream migration is obtained (Chapter 4) but it is not verified by field observations (Chapter 8). For this reason, the calibration and validation of flow parameters can not be carried out.

In order to obtain the most accurate values for the erosion coefficients, the following analysis is not focussed anymore on all the stretch.

This new analysis is focussed on the cut-off indicated in Figure 9.1 (Section 1). Nowadays, we know that this bank (where the bend has almost been cut off) has a width of less than 5 m. In 1935, the width was of around 20 m. The condition that new erosion coefficients need to accomplish is that bank width has to be bigger than 5 m in 1992.

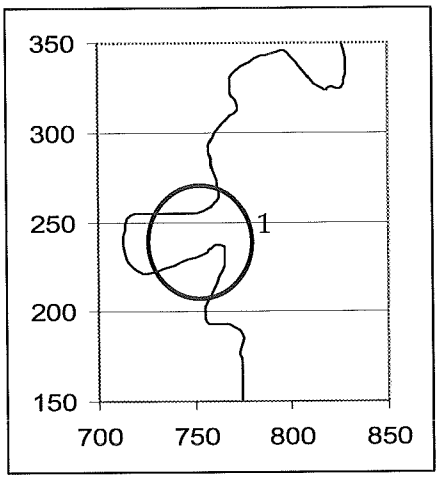

Figure 9.1: Study sections for erosion coefficients calibration (coordinates from 1935)

Using the erosion coefficients calibrated above, the program gives some problems because of the velocity.

After some testing, the most accurate values that keep that condition are:

Eu =1.5e-07 ; Eu=6e-06

The sign of water depth and velocity evolution is analysed as done in Section 7.4.3. The erosion given by the new coefficients occurs in the same side as described by Spanjaard (2004).

Coordinates of 1992 obtained by Miandras and from the 1992 aerial photos, are represented in Figure 9.2.

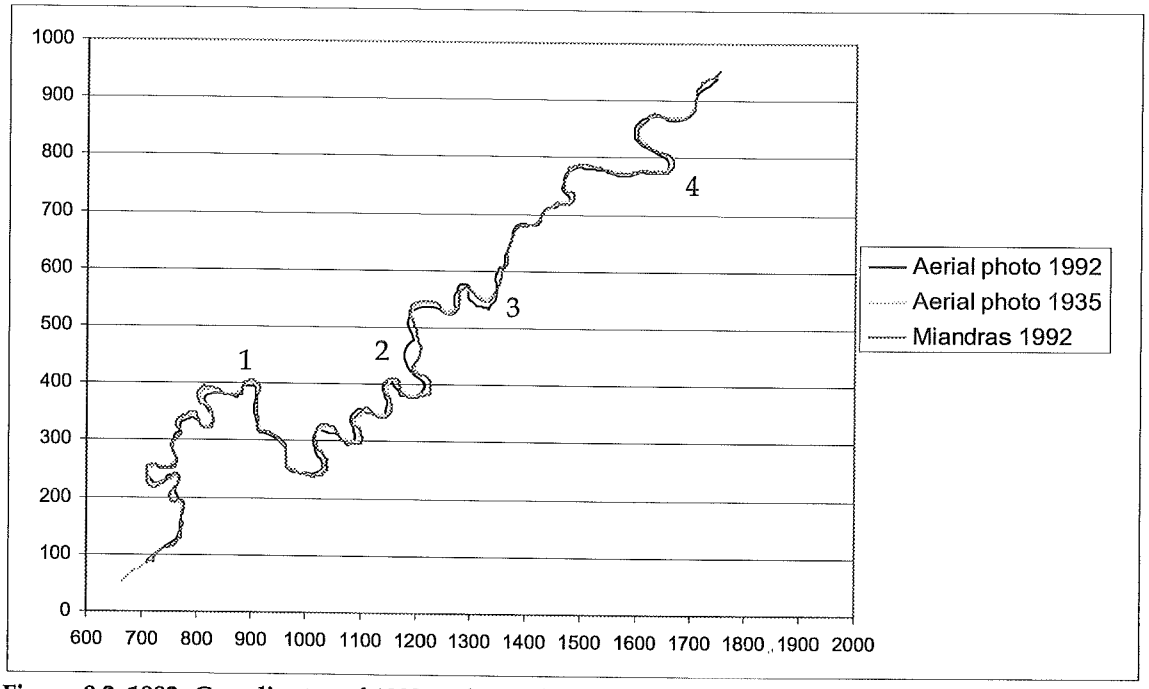

Figure 9.2: 1992- Coordinates of 1992 and 1935 (based on aerial photos) and coordinates obtained by Miandras

In this figure the coordinates of 1935 are also represented to observe the river development according to Miandras simulation.

We can observe that the two river locations in 1992 are very different because of the error.

Migration is not anymore analysed but bank erosion.

The most remarkable differences between the coordinates from the aerial photos and the simulated planform by Miandras are (Figure 9.2):

- bend 1: due to the presence of trees it is eroding on the inner bank of the bend (right bank).

-bend 2: in the real situation erosion extends the bend following the flow direction; Miandras can not compute that phenomenon. It is affected by upstream migration (error).

- bend 3: aerial photos coordinates show higher erosion than obtained by Miandras. It is also affected by upstream migration

- bend 4: as in bend 2, some trees protect the outer bank; its presence causes erosion in the inner part on the bend.

Further analyses using a non-uniform erodibility are also carried out. Upstream migration can not be reached even changing the erodibility of just one side. Concerning to bends that are eroded on the inner bank, the erodibility variation can not reproduce it; it can only reduce the extension of the bend.

For bend 3, where the erosion is more important than in other bends, when the erodibility of that zone is changed new coordinates don't get closer to the coordinates from the aerial photos, because the stretch also migrates upstream.

The results of the non-uniform erodibility are not successful either.

9.2- Validation

The studied period to carry out the validation is 1992-2003 (9 years). Coordinates of 2003 obtained by Miandras and the ones from the aerial photos are represented in Figure 9.3.

In that case differences between the coordinates are not as important as before because the period of time is shorter, so the migration is smaller

If we observe the stretch characterized by upstream migration in aerial photos, the coordinates simulated by Miandras tend also to migrate downstream.

The section calibrated in Figure 9.1 is validated here. We observe that the neck width is less than 5 m.

Coordinates of bend 1 from the aerial photos show that the bend is eroded on the outer bank (before it was in the inner bank). It can occur because during the period 1992-2003 trees seem to have been removed (aerial photo of 2003). It can also be a consequence of the error present on the photo analysis.

Concerning to bend 2 the river has the same behaviour: an extension of the bend that can not be reproduce by the program.

Erosion in bend 3 is more approximated in that period, because the coordinates from aerial photos (1992 and 2003) are also closer. If the evolution of 1992 to 2003 (obtained by Miandras) is observed, we can appreciate that it has hardly moved.

Finally bend 4, according to Miandras, goes on eroding on the right bank (outer bank) but not in the observed direction in the aerial photos (upstream migration, on the inner bank).

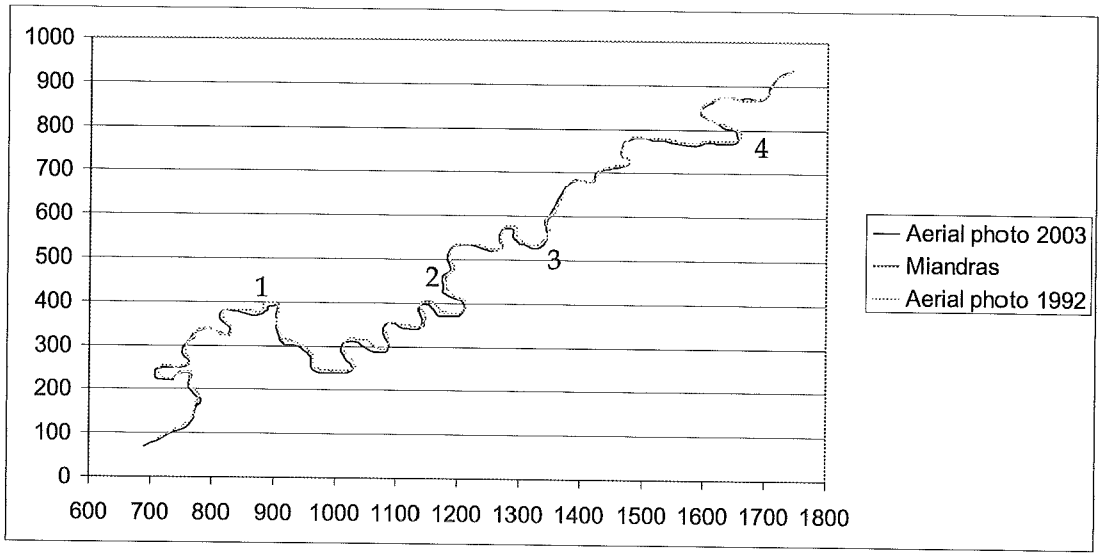

Figure 9.3: 2003- Real coordinates and coordinates obtained by Miandras

10- Conclusion and discussion of the planimetric changes

A long-time prediction of the river migration cannot be properly made because the model has been neither calibrated nor validated.

To carry out a prediction in the future, it is important to verify that the chosen parameters can reproduce the river behaviour in the past. The errors in the coordinates obtained by the aerial photos make this impossible.

The large errors present on the aerial photos mean that the Geul is too small to be analysed with this method. For this kind of studies, the aerial photos would have to be more accurate.

Despite these inaccuracies, some useful results have been obtained. The effect of the bank erosion protection has been verified, with the increasing trend of the bank erosion and the channel width.

From the analyses done during this work, we get to know that the model tends to reproduce river planform changes in the present situation as observed in the studies carried out by the VUA.

Miandras is not capable of simulating the upstream migration indicated by the aerial photos, but the accuracy of this observation is doubted, because it does not comply with the field observations of VUA.

The good agreement between Miandras results and the VUA-data for the shorter term (a few years) shows that channel deformations in this type of river can be predicted using Miandras.

The analyses show that bank erosion along the Geul river is not just influenced by flow parameters, but also by geological properties. Groundwater is an important factor to take into account in bank stability analyses.

Bank erosion along the study area of the Geul river has been influenced by the presence of trees. At present, the influence of these trees is decreasing because no more of them are being planted. The river migration might therefore change back to the behaviour observed in the past.

11- References

Books

Blom, A. 1997. "Planform changes and overbank flow in meandering rivers. The river Allier". Master's research project. TU Delft.

Crosato, A. 1990. "MIANDRAS. Meandering river migration". Delft Hydraulics.

Crosato, A. 1990. "Simulation of meandering river processes". TU Delft.

Dautrebande, S., J.G.B. Leenaars, J.S. Smitz & E. Vanthournout. 2000. "Pilot project for the definition of environment-friendly measures to reduce the risk for flash floods in the Geul river catchment". European Commission-DG Environment.

De Vriend, H. 2005. "CT 5311. Lecture notes. River dynamics".

De Vriend, H. 2005. "CT 3340. Lecture notes. River Engineering".

Dijkstra, J.T. 2003. 'The influence of vegetation on scroll bar development". Master's research project. TU Delft.

Elliot, C. 1983. "River meandering. Proceedings of the Conference Rivers". American Society of Civil Engineers.

Gregory, K.J. 1977. "River channel changes". British Geomorphical Research Group.

Jansen, P.Ph et al.1979. "Principles of River Engineering. The non-tidal alluvial river". Delftse U.M. III.

Mount, J. F. 1995. "California Rivers and Streams. The conflict between fluvial process and land use - Chapter 4: The shape of a river". The University of California press.

Robert, A. 2003. "River Processes". Oxford University Press. Arnold

Seminara, G. & Blondeaux, P. 2001. "River, Coastal and Estuarine morpho-dynamics". Springer (New York).

Spanjaard, G. 2004. "Recent erosion and sedimentation processes in the Geul river". Master's research project. Vrije Universiteit Amsterdam.

Topogrphische Dienst. 1989. "Grote provincie atlas 1:25000. Limburg". Wolters-Noordhoff Atlasprodukties.

Articles

Blanckaert, K., de Vriend, H.J. 2003. "Secondary flow in sharp open-channel bends". J. Fluid Mech, vol. 498, pp. 353-380.

Blanckaert, K., de Vriend, H.J. 2003. "Nonlinear modelling of mean flow redistribution in curved open channels". Water resources research, vol. 39, no. 12, 1375.

Baptist, M. et al. 2005. "Modelling the influence of vegetation on the morphology of the Allier, France". Final COST 626 meeting in Denmark, pp 15-22.

Baptist, M. et al. 2005. "Modelling the effects of vegetation on flow and morphology in rivers". Arch. Hydrobiology. Suppl. 155/1-4, pp. 339-357.

Camporeale, C. et al. 2005. "On the long-term behaviour of meandering rivers". Water resources research, vol 41, W12403.

Chen, D., Duan J.D. 2006. "Simulating sine-generated meandering channel evolution with analytical model". Journal of Hydraulic Research Vol. 44, no. 3, pp. 363-373.

Darby, S. et Thorne, C., 1996. "Simulation of widening and bed deformation of straight sand-bed rivers. I : Model development". Journal of hydraulics Engineering.

Darby, S. et Thorne, C., 1996. "Simulation of widening and bed deformation of straight sand-bed rivers. II : Model evaluation". Journal of hydraulics Engineering.

Darby, S. et Thorne, C., 1996. "Development and testing of riverbank-stability analysis ". Journal of Hydraulic Engineering.

Darby, S., Gessler, D. and Thorne, C., 1999. " Computer program for stability analysis of steep, cohesive riverbank". Earth Surface Processes and Landforms 25, 175-190 (2000).

Darby, S. et al., 2002. "Numerical simulation of bank erosion and channel migration in meandering rivers". Water resources research, Vol. 38, n. 9.

De Moor, J. et al. 2006. "Simulating meander evolution of the Geul River (the Netherlands) using a topographic steering model" (Submitted). Earth Surface Processes and Landforms.

Duan, J., 2005. "Analytical approach to calculate rate of bank erosion". Journal of Hydraulic Engineering.

Hooke, J.M., 2003. "Cutoffs galore!: occurrence and causes of multiple cutoffs on a meandering river". University of Portsmouth.

Hughes, M., McDowell, P., Marcus, A. 2005. "Accuracy assessment of georectified aerial photographs: Implications for measuring lateral channel movements in a GIS". University of Oregon, USA.

Lagasse, P.F. et al. 2004. "Methodology for predicting channel migration". National Cooperative Highway Research Program. Project 24-16.

Lancaster, S., Bras, R. 2000. "A simple model of river meandering and its comparison to natural channels". John Wiley & Sons, Inc.

Lanzoni, Federici & Seminara, 2005. "On the convective nature of bend stability". River, Coastal and Estuarine morphodynamics, 2005

Mengoni, B. and Mosselman E., 2005. "Analysis of riverbank erosion processes: Cecina river, Italy". River, Coastal and Estuarine Morphodynamics.

Simon, A. et al. , 2000. "Bank and near-bank processes in an incised channel". Geomorphology 35 (2000) 193-217

Van Houter, F. et al., 2003. "Modelling planform changes of braided rivers". H. R. A. Jagers

Zolozzi, G. et al. 2004. "Experimental observations of upstream overdeepening". Università di Genova, Italy.

Internet

http://users.aber.ac.uk/rra3/processes_of_bank_eorsion.htm

http://www.paleocurrents.com/castle_rock/docs/mendering_river.ttml

Appendix A Site Visit - April 28th 2006

The visit to the river was focussed on the observation of the bank erosion process and the presence and effect caused by the trees. The visit has been very useful to understand the important effect of the trees on the erosion process and also to distinguish the different types of erodibility along banks.

Erosion process

On the visited stretch, we can observe very erosive banks and also straight stretches protected by poplar trees.

Different processes of erosion have been observed. They are shown in the following pictures.

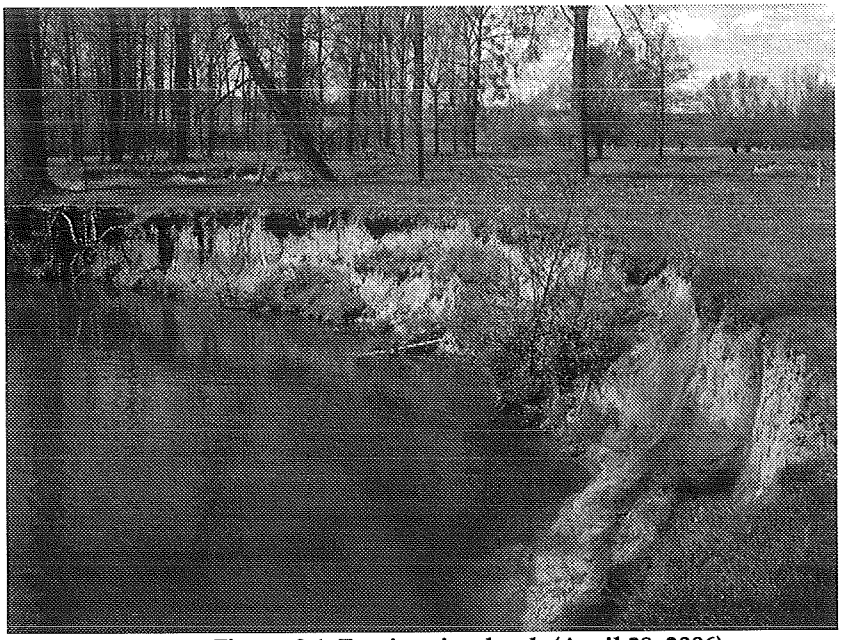

Figure 0.1: Erosive riverbank (April 28, 2006)

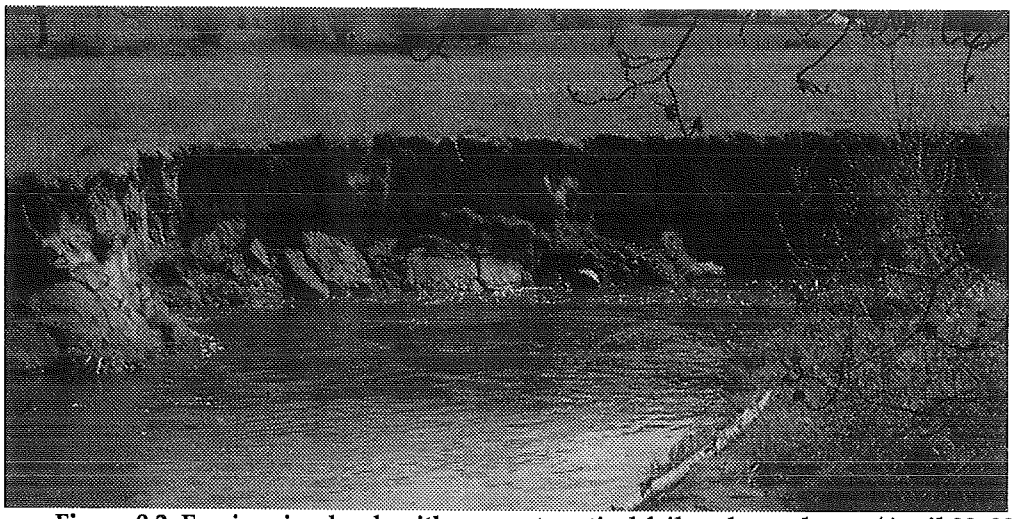

Figure 0.2: Erosive riverbank with a recent vertical failure by undercut (April 28, 2006)

The following picture shows a mass failure by sliding. The flow was eroding the bank and it fell following a sliding surface. This failure happened long time ago since we can observe the vegetation has covered all the area.

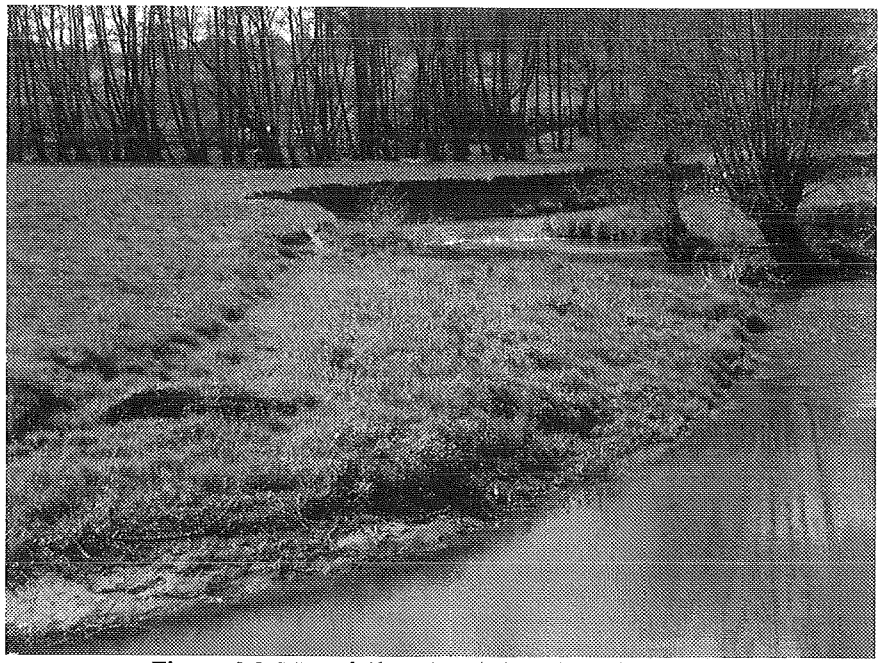

Figure 0.3: Mass failure by sliding (April 28, 2006)

An example of erodible banks is shown in Figure 0.4. Two years ago, there was a pipe (red line in the figure) buried in the ground. Then, because of the erosion on this bend, the tube had to be removed because the bank in which it was located had been completely eroded (Discussion with de Moor). It's still possible to observe the entrances of the pipe.

Figure 0.4: Image of a very erodible bank (April 28, 2006)

In one bend of the river, the flow has caused the vertical failure of one part of the riverbank, as shown in Figure 0.5. This kind of erosion causes a division of the flow. A new flow appears flowing in circles, which causes stronger erosion on one part of the bank. As the erosion on the bank gets stronger, the circular flow gets more powerful.

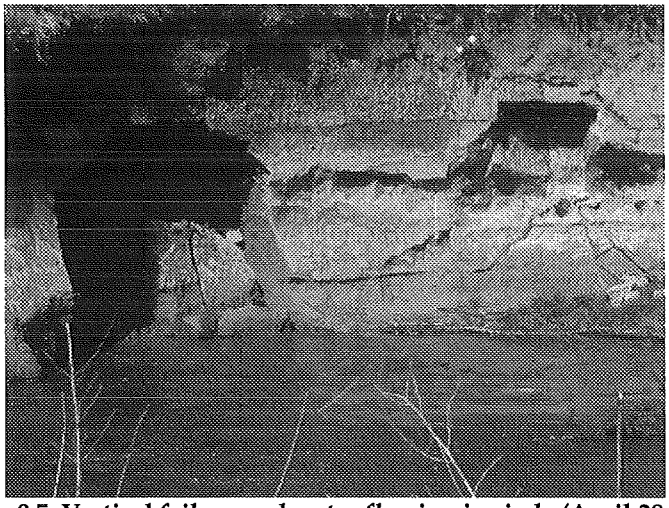

Figure 0.5: Vertical failure and water flowing in circle (April 28, 2006)

In some parts of the river, black-grey areas can be observed (Figure 0.6). This colour comes from the zinc contamination which affected the river during the 19th century. Mining activities in the Belgian part of the catchment let out zinc on the water that was absorbed by the ground.

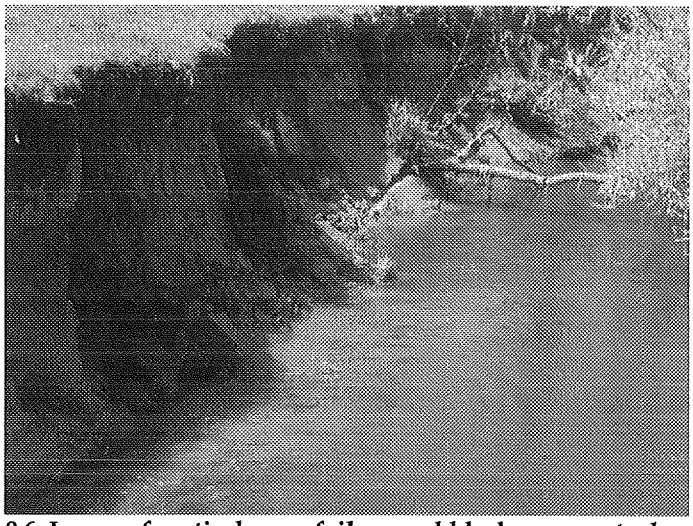

Figure 0.6: Image of vertical mass failure and black-grey parts due to zinc contamination (April 28, 2006)

Vegetation

During the visit the three kinds of trees have been observed: poplar trees, willow trees and alder trees.

Poplar trees are planted along some stretches of the river, in rows near the banks (Figure 0.7). In zones where banks are protected by these trees, we can observe that erosion gets stronger between them. Finally the river surrounds them and they can't survive river migration and they fall down.

Figure 0.7: Poplar trees protecting banks from erosion (April 28, 2006)

To avoid the danger generated by fallen trees, some of them have already been cut (Figure 0.8).

Figure 0.8: Poplar tree surrounded and undercut by the river but still protecting banks, and a poplar tree already cut (April 28, 2006)

Before their fall, trees are undercut by the river. They still have an effect on bank stabilisation just in the place where they were planted because of its roots (Figure 0.9).

Figure 0.9: Poplar tree surrounded by the river with an incipient scour hole upstream (April 28, 2006)

Willow trees and alder trees grow naturally near this river. They have deep roots which allow them to survive to river migration.

In Figure 0.10, a willow tree can be observed on the bank. It won't fall; it will finally survive, resting in the middle of the river because of the scour hole developed around it (Section 4.1).

A willow tree on the river channel after the erosion of the bank can be observed in Figure 0.11. This tree is a bit inclined, like the one in Figure 0.10. Anyway it has survived.

In Figure 0.12, we can also observe a willow tree which keeps itself standing thanks to its deep roots but it is almost fallen. In this picture we can also observe the presence of two poplar trees. Between them (where the willow trees are situated) the erosion is less important than in other parts of the stretch, as for example just before the first poplar tree (actually the flow is flowing in the other direction of the picture, so the eroded part is downstream of the tree).

The erosion downstream can also be caused by the fallen of the bank in the other side of the river. We can observe a part of the bank in the water, with vegetation, that means that the bank has collapsed.

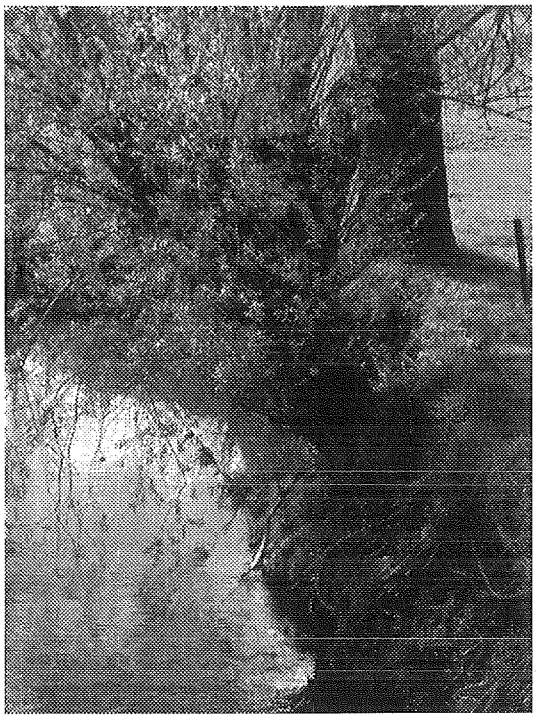

Figure 0.10: Willow tree on the bank (April 28, 2006)

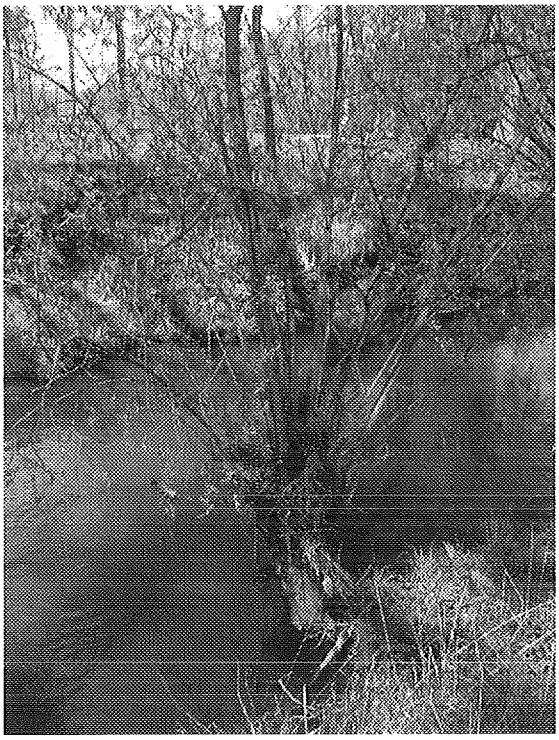

Figure 0.11: Willow tree already in the river (April 28, 2006)

Figure 0.11: Straight stretch with willow tree almost fallen and a failure of the bank (April 28, 2006)

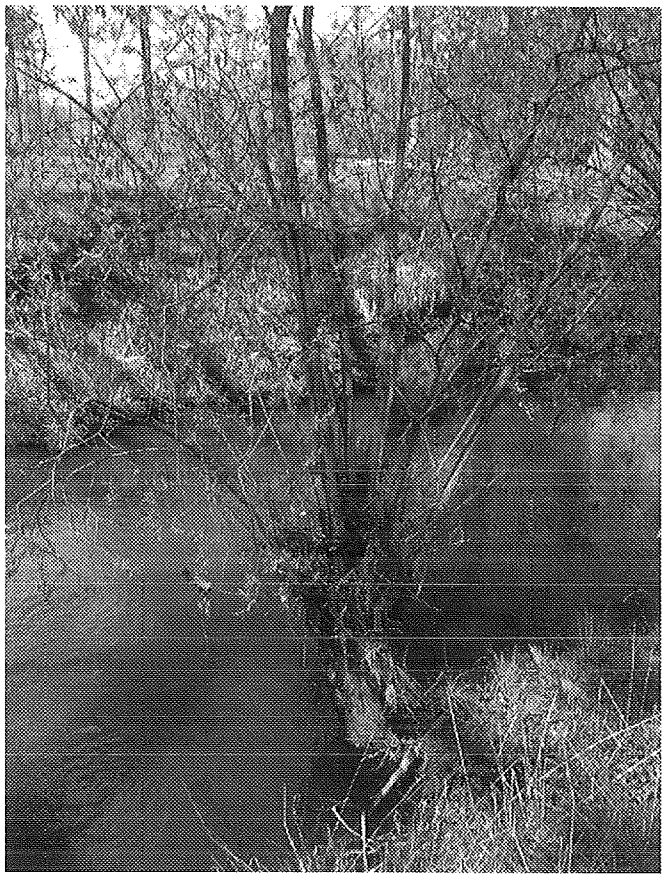

On the river plain, an odd species for this region can be observed: the zinc violin (viola calaminaria) (figure 0.14). This flora is typical from ground with zinc. They have appeared in that zone because of the contamination explained before.

Nowadays, the populations of zinc violin are decreasing due to river migration and also to the dilution of contaminated sediments.

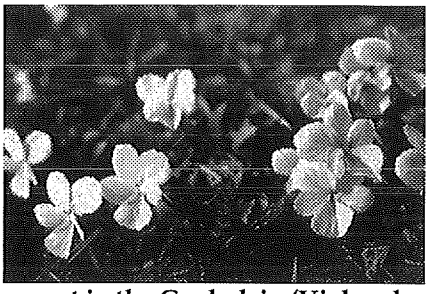

Figure 0.14: Zinc flora present in the Geul plain (Viola calaminaria) (April 28, 2006)

Appendix B Study of the discharge influence on planform evolution and bed profile evolution

Discharge (m^3/s)	Averaged water depth (m)	Averaged velocity (m/s)
22	1,99	1,38
30	2,44	1,53
36	2,76	1,63

We can observe that the water depth for the last case is higher than the channel depth (2-2,5 m), which means that the water flowing on the flood plains can't change the channel morphology. Only the other two cases are studied in this section.

	Discharge (m^3/s)	Width (m)	Grainsize (m)	Chézy number ($m^{1/2}/s$)	Duration of study (years)
Run 1	22	8	0.025	20	10 (5 days)
Run 2	30				

Planform evolution

Run 1

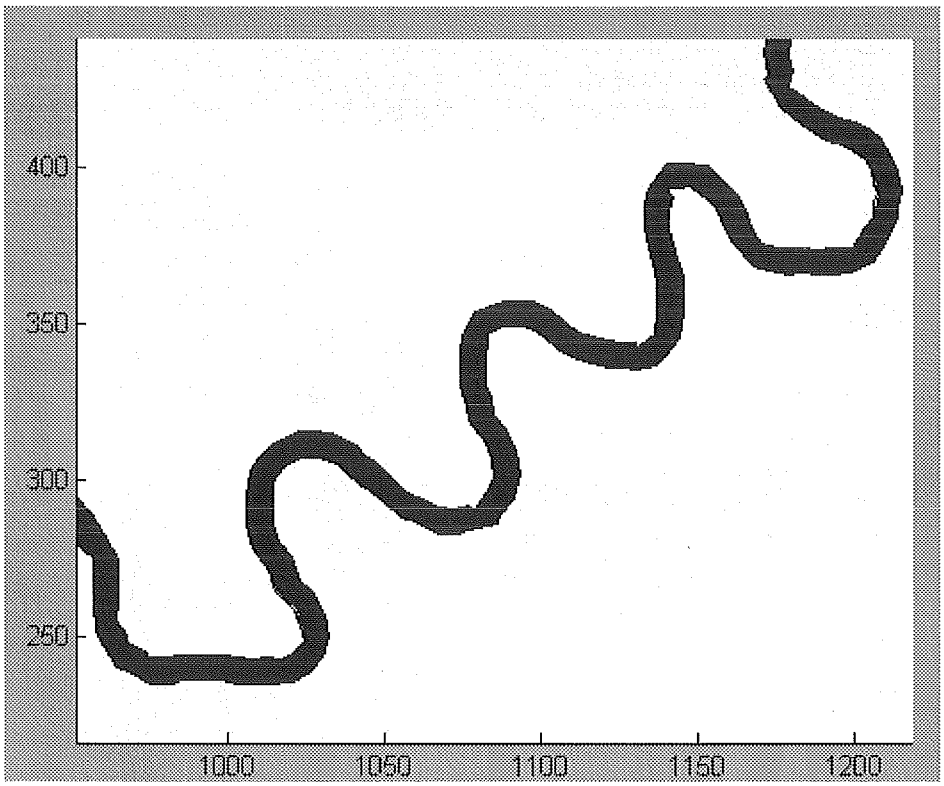

Run 2

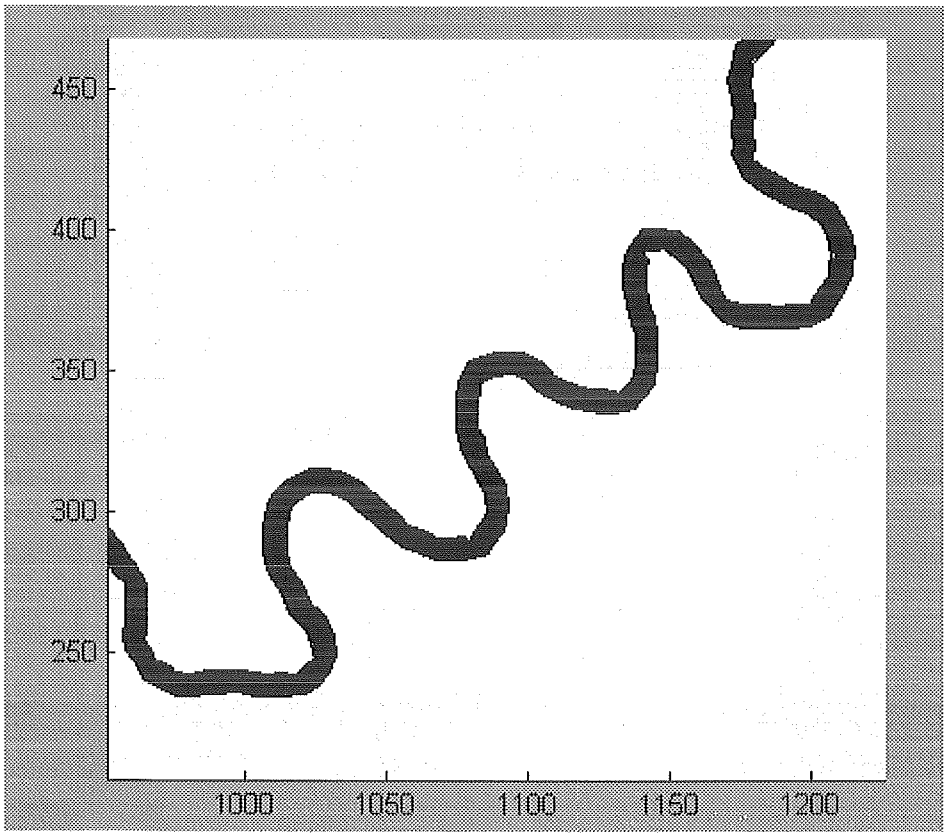

Channel planform has been analysed with an erosion rate of 0,5 m/y (Spanjaard, 2004). We can not appreciate channel planform changes because of the channel width.

The comparison of river migration can not be done.

Bed profile after 5 days

An analysis of the bed evolution after 5 days (10 years) is also carried out to compare the sediment transport. The position of point bars and the depth of the pools are observed.

Generally, point bars are located downstream of the apex of the bend for a discharge of $22m^3/s$, whereas, for a higher discharges, point bars are formed closer to the apex and sometimes even at the apex.

We can also observe that for the first case, more point bars are formed. When the flow is more powerful (higher discharge), it can transport bigger particles and carry the smaller ones further. For the second case, point bar might be formed more downstream.

Pools depth is also different in both situations. The deepest value in the first case is 2,45 m; in the second one is more than 3 m. More discharge implies that the helical flow is more important and thus, stronger erosion on the banks (also on their bottom).

Run 1

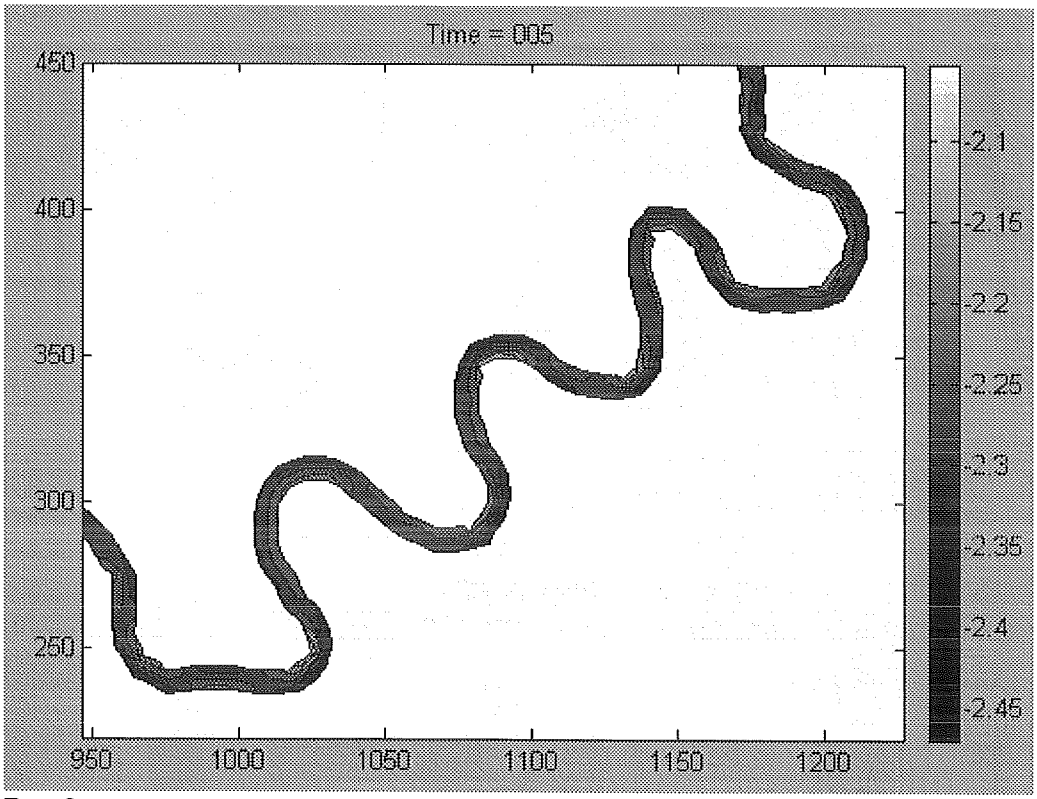
Time = 005
450
400
350
300
250
950
1000
1050
1100
1150
1200
-2.1
-2.15
-2.2
-2.25
-2.3
-2.35
-2.4
-2.45

Run 2

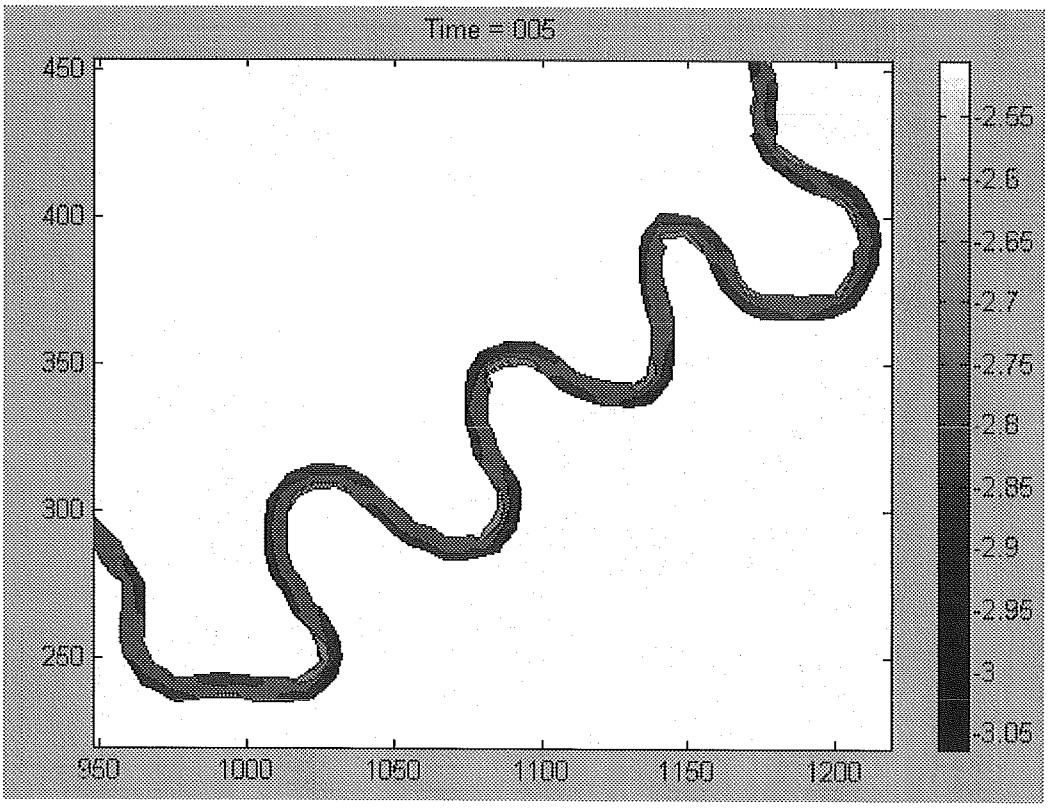
Time = 005
450
400
350
300
250
950
1000
1050
1100
1150
1200
-2.55
-2.6
-2.65
-2.7
-2.75
-2.8
-2.85
-2.9
-2.95
-3
-3.05

Appendix C Study of the influence of grainsize

	Grainsize (m)	Discharge (m^3/s)	Width (m)	Chézy number ($m^{1/2}/s$)	Duration of study (years)
Run 3	0.05	22	8	20	10 (5 days)
Run 4	0.025				
Run 5	0.00025				

For Run 3 and 4 the formula chosen to simulate the sediment transport is the power low formula. For Run 5, Engelund & Hansen formula is used.

The value of the coefficient weighing the effects of channel curvature on bed shear stress direction is also changed in the last case.

Planform evolution

Run 3

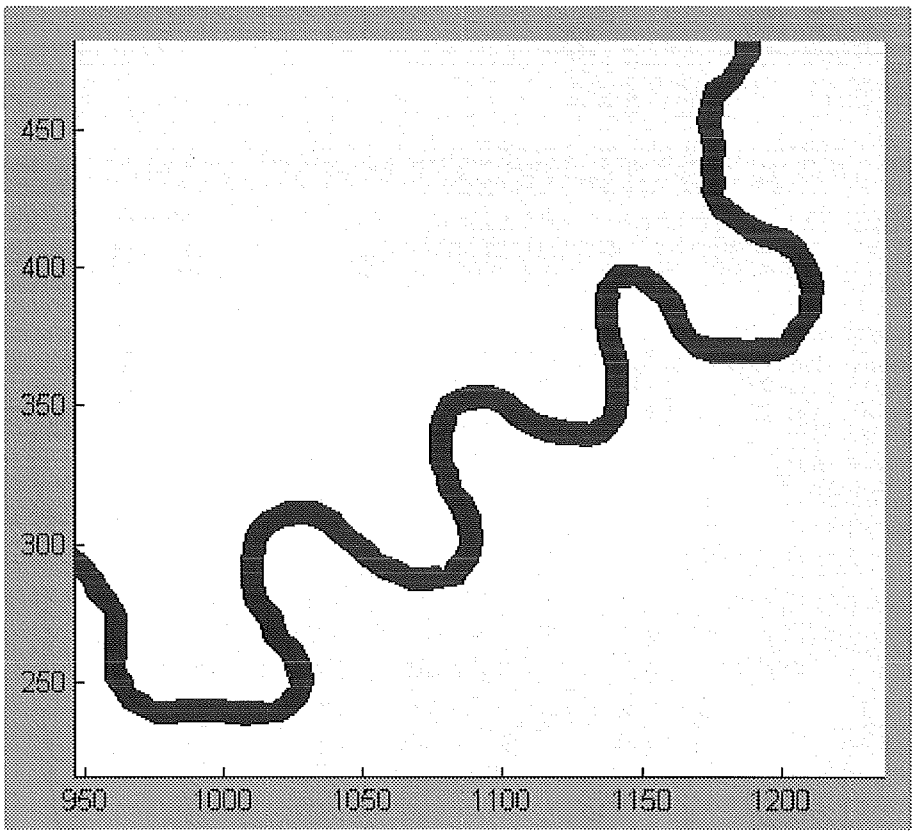

Planform changes for a grainsize of 5 and 2.5 cm is almost negligible. As said before, the river migration is small compared to the channel width and the evolution can not be appreciated.

Run 4

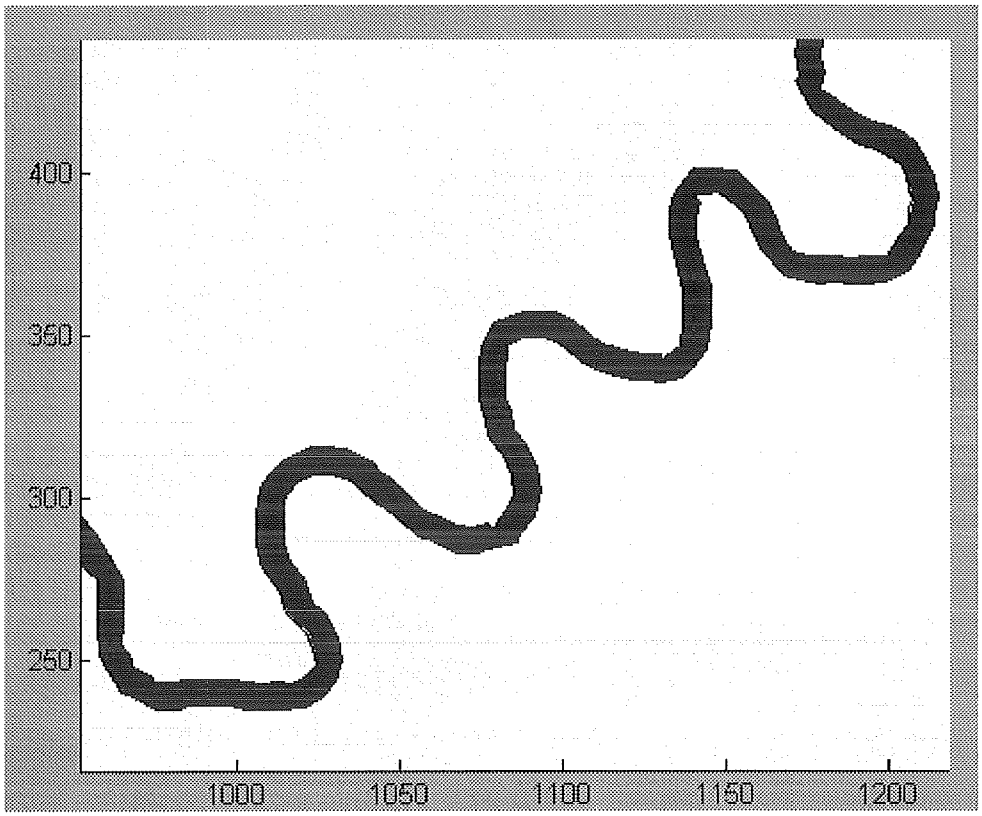
400
350
300
250
1000
1050
1100
1150
1200

Run 5

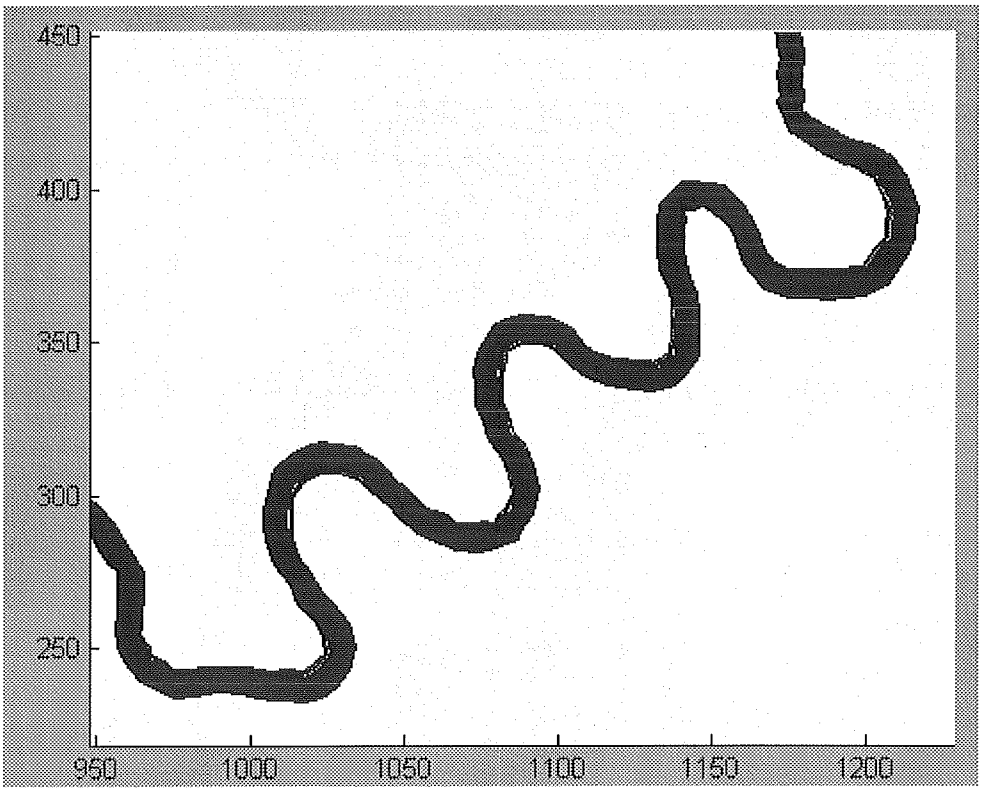
450
400
350
300
250
950
1000
1050
1100
1150
1200

When river banks are formed by fine sediment (D_{50} = 250 microns), they are more erodible.

For that case we can observe river migration especially at the apex of the bends.

Bed profile after 5 days

With a decreasing grainsize, we can observe that the formed point bars are bigger and more numerous. They are located downstream of the apex of the bend, for the three cases, but slightly closer to the apex (or at the apex) for the finest material.

The river is deeper with smaller grainsize because the banks and the river bed can be eroded easily. In the last case, pools have a depth of more than 3 m, while for the other cases is around 2.5 m.

The value of the formative (and bankfull) discharge (22m^3/s) has been calculated for a grainsize of 5 cm, in armoured bed. This layer with bigger particles protected the smallest ones located in the deepest layers. For Run 5, this layer does not exist, so there is no protection for the fine sediment layer. The river bed is more sensible to erosion.

Run 3

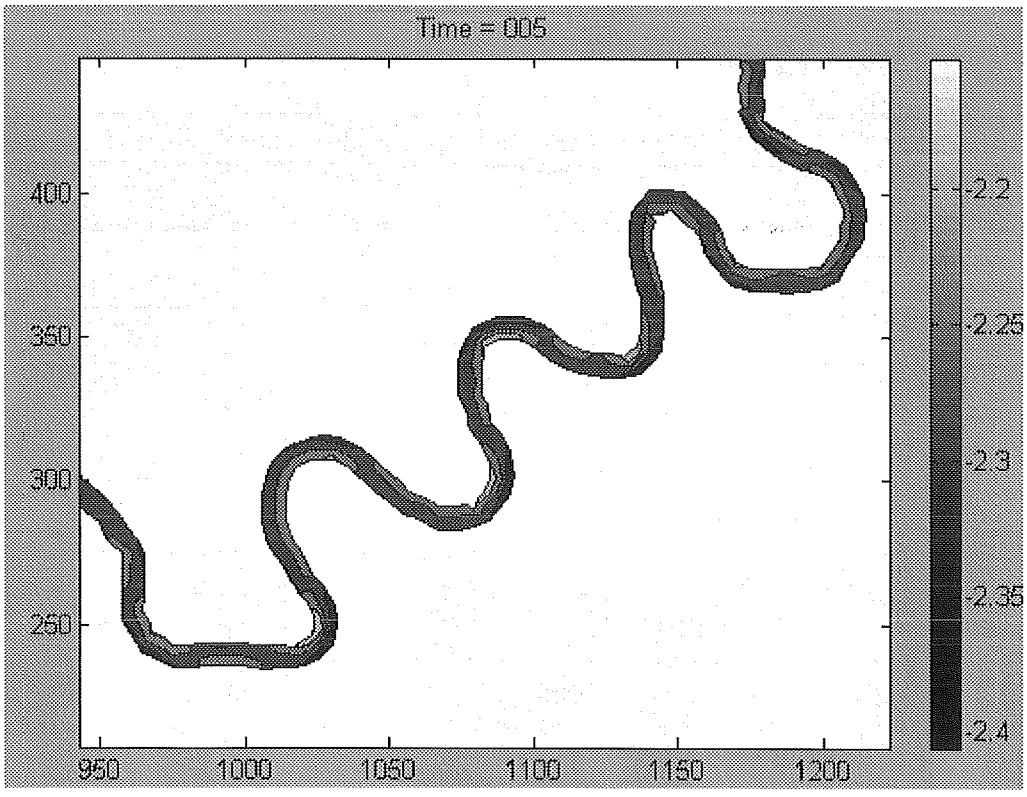

Run 4

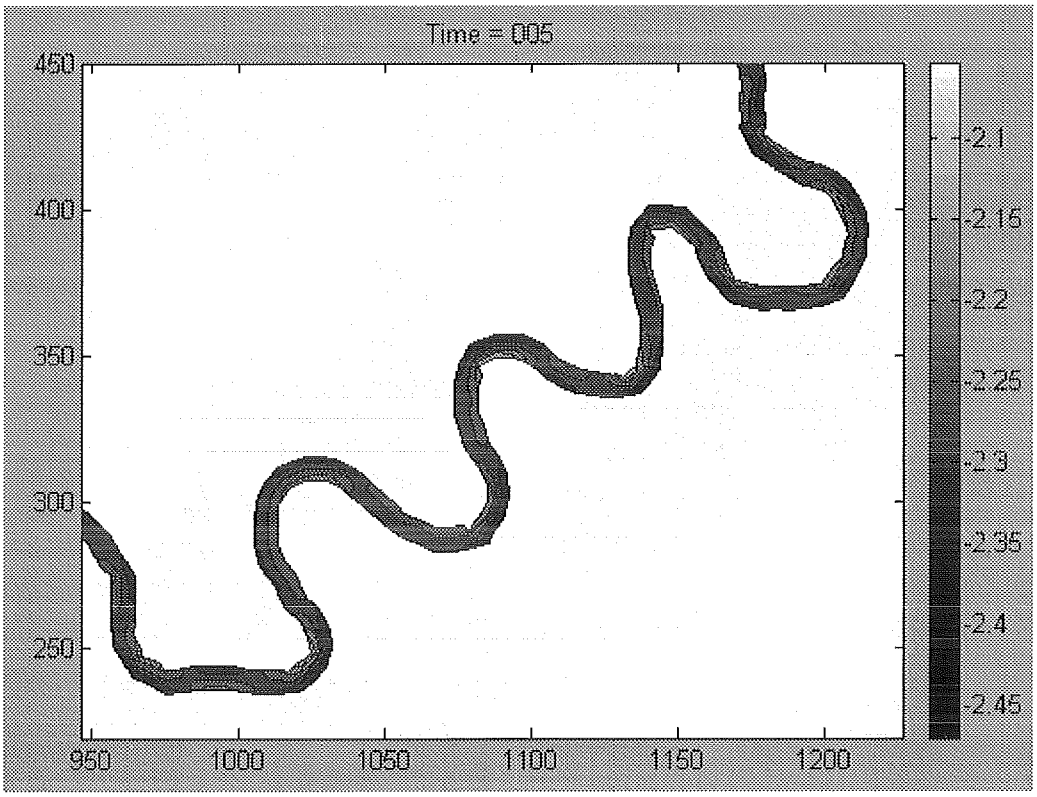
Time = 005
450
400
350
300
250
950
1000
1050
1100
1150
1200
-2.1
-2.15
-2.2
-2.25
-2.3
-2.35
-2.4
-2.45

Run 5

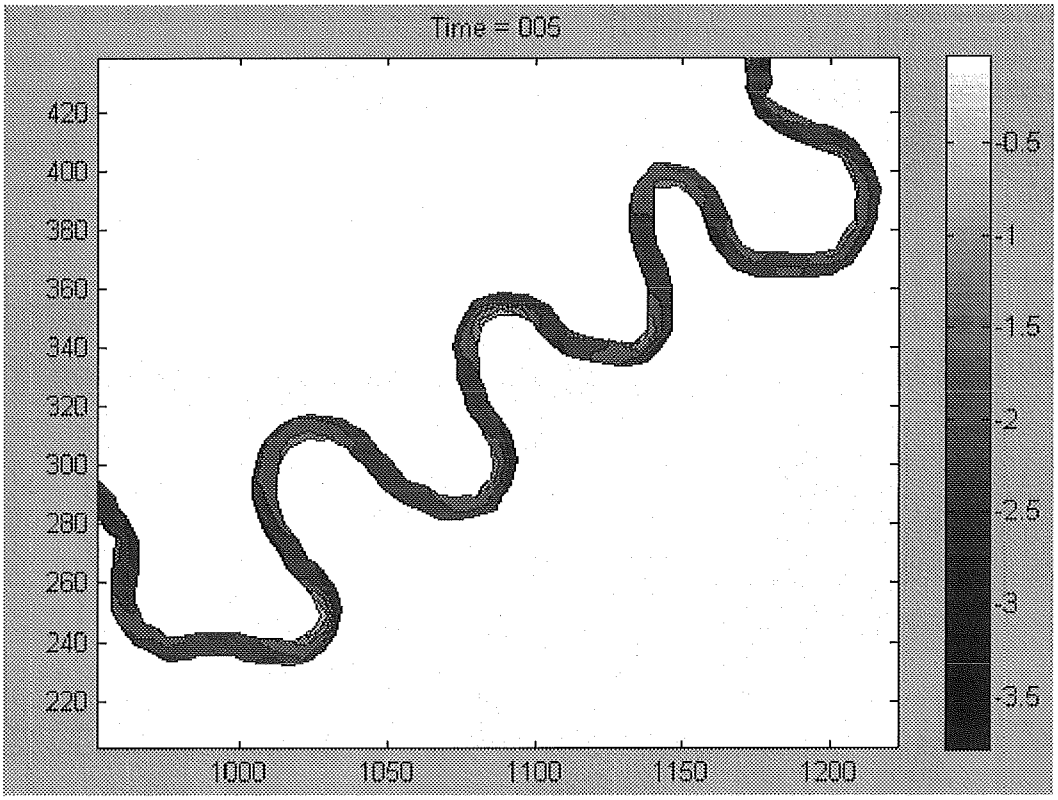
Time = 005
420
400
380
360
340
320
300
280
260
240
220
1000
1050
1100
1150
1200
-0.5
-1
-1.5
-2
-2.5
-3
-3.5

Appendix D Study of the channel width influence on bed profile

	Width (m)	Discharge (m^3/s)	Grainsize (m)	Chézy number ($m^{1/2}/s$)	Duration of study (years)
Run 5	8	22	0.025	20	10 (5 days)
Run 6	11.75				
Run 7	15.5				

Bed profile after 5 days

Run 5

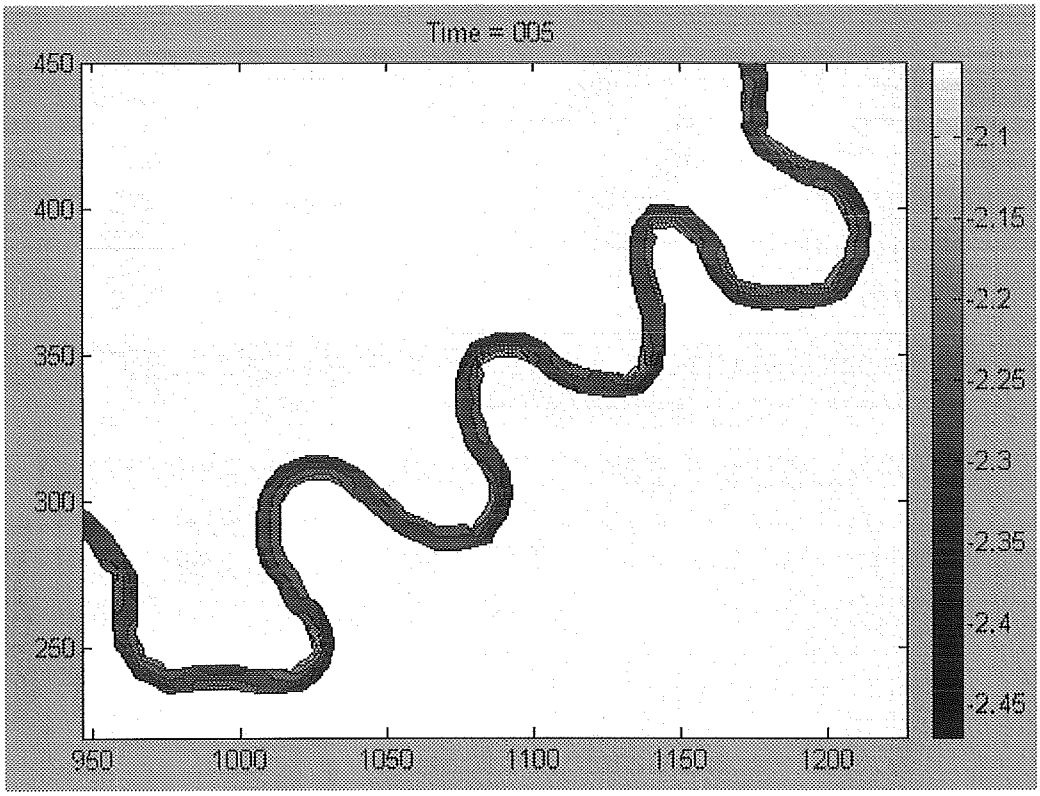

We can observe that point bars are bigger as the width increases and also less deep. They are located closer to the apex of the bend for the last case (15.5 m). As river is wider, migration tends to be less downstream.

For the formative discharge (22 m^3/s), water depth decreases with the width.

Width (m)	Water depth (m)	Depth-averaged velocity (m/s)
8	1.99	1.38
11.75	1.54	1.21
15.5	1.28	1.11

For the last two cases, formative discharge doesn't correspond to bankfull discharge, because of the depth.

Pools depth is smaller when width increases.

Run 6

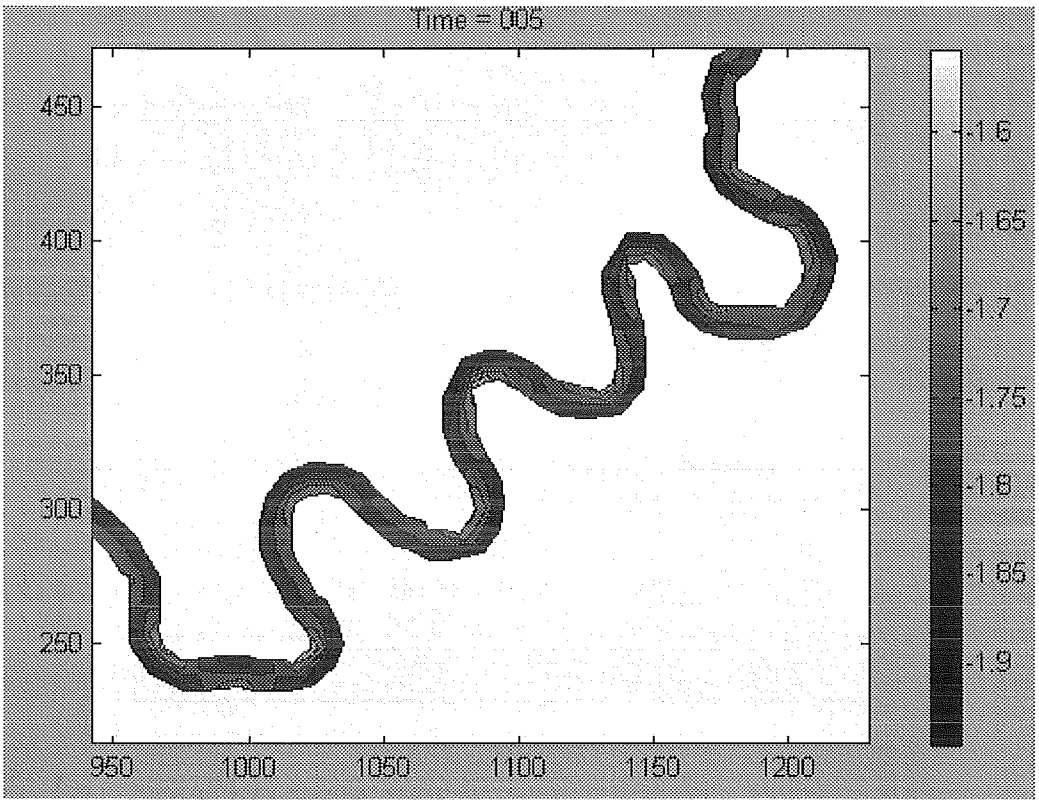
Time = 005
450
400
350
300
250
950
1000
1050
1100
1150
1200
-1.6
-1.65
-1.7
-1.75
-1.8
-1.85
-1.9

Run 7

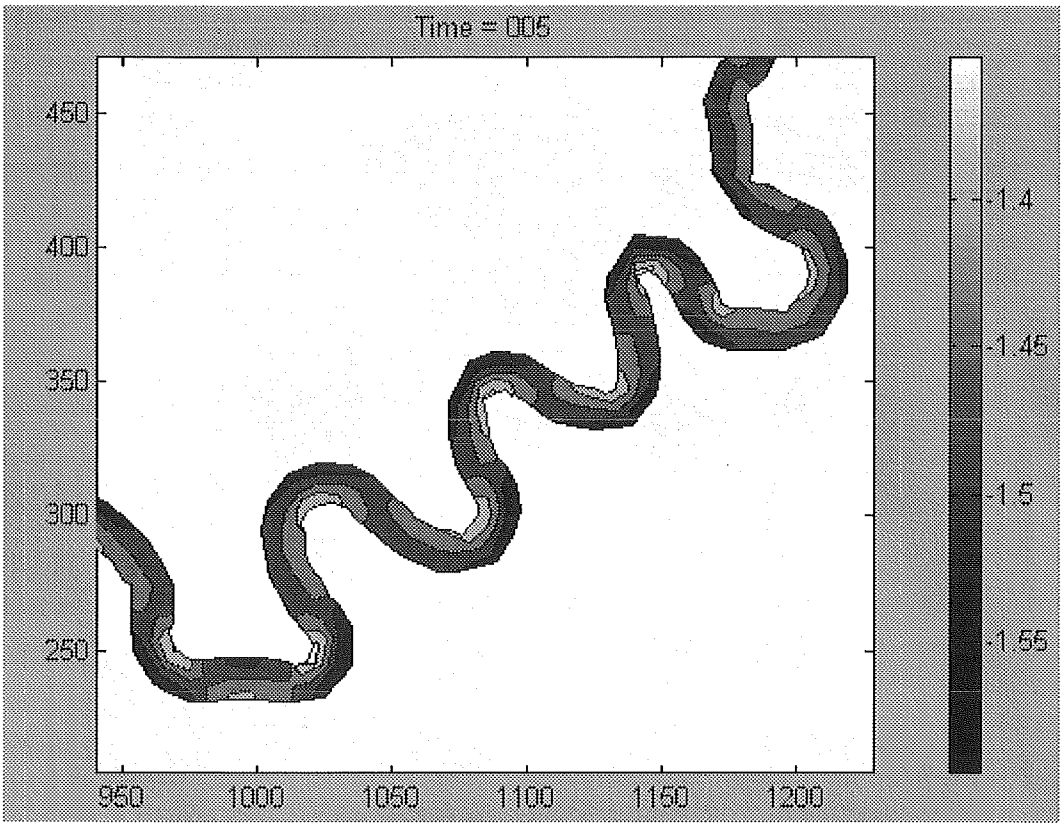
Time = 005
450
400
350
300
250
950
1000
1050
1100
1150
1200
-1.4
-1.45
-1.5
-1.55

Appendix E Study of the valley slope influence on the bed profile

	Valley slope (m/m)	Width (m)	Discharge (m^3/s)	Chézy number ($m^{1/2}/s$)	Duration of study (years)
Run 8	0,0001	8	19	20	10 (5 days)
Run 9	0,004				
Run 10	0,01				

Planform evolution

Valley slope (m/m)	Water depth (m)	Averaged velocity (m/s)
0,0001	6,81	0,40
0,004	1,99	1,38
0,01	1,47	1,87

Bed profile after 5 days

Run 8

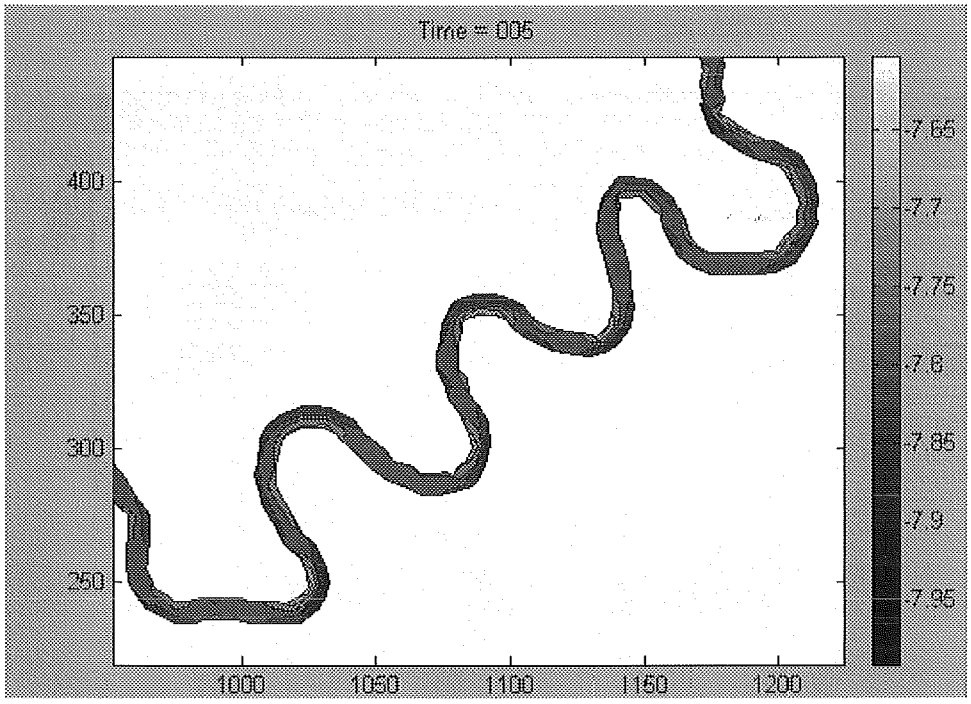

For the first case, water depth is higher than channel depth, which means that the flow floods the plains.

For the higher slope, formative discharge doesn't correspond anymore with bankfull discharge.

Presence of point bars decrease when the slope increases. They are located closer to the apex of the bend for smaller slopes. Pools are deeper for the first case, and pool depth decreases for steep slopes.

Run 9

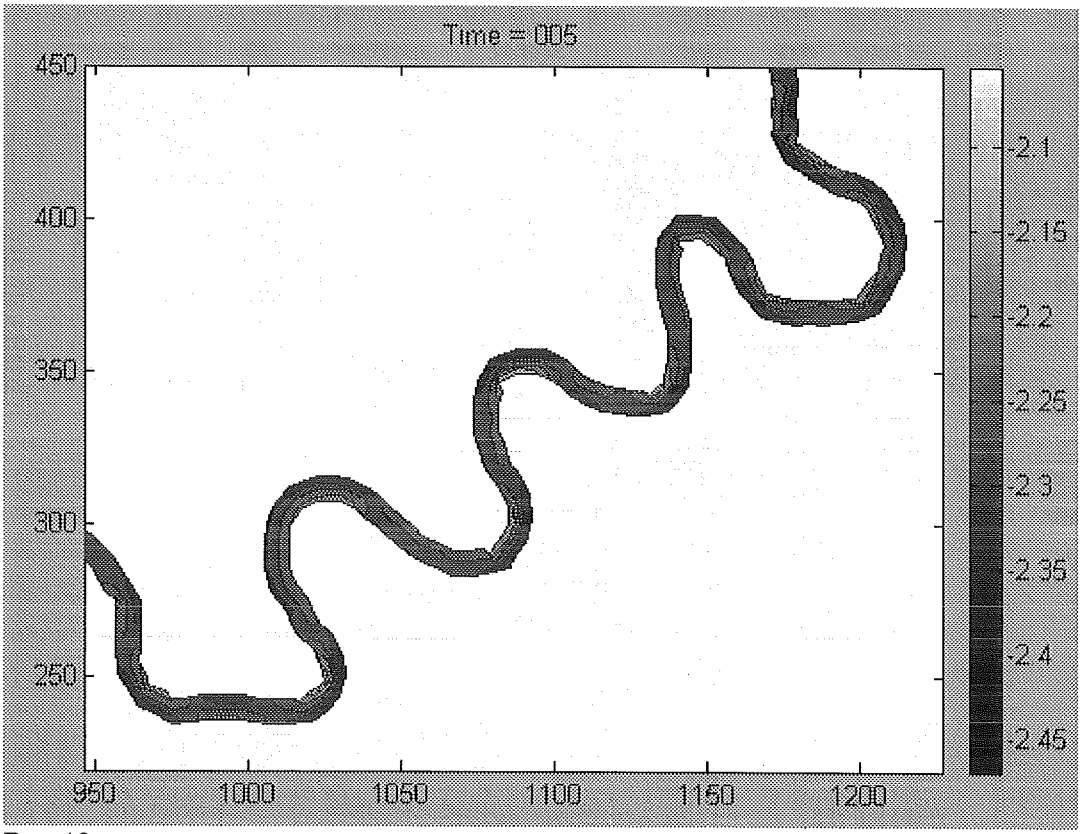
Time = 005
450
400
350
300
250
950
1000
1050
1100
1150
1200
-2.1
-2.15
-2.2
-2.25
-2.3
-2.35
-2.4
-2.45

Run 10

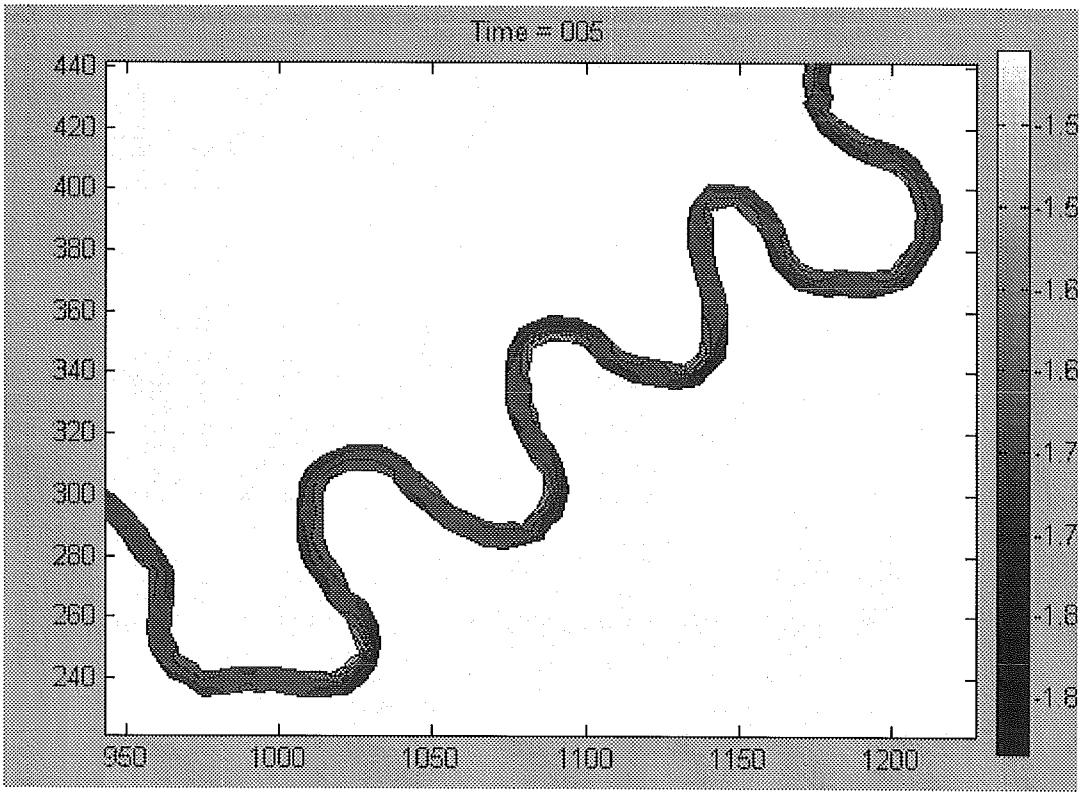
Time = 005
440
420
400
380
360
340
320
300
280
260
240
950
1000
1050
1100
1150
1200
-1.5
-1.6
-1.6
-1.6
-1.7
-1.7
-1.8
-1.8

Appendix F Study of the Chézy number influence on bed profile

	Chézy number ($m^{1/2}/s$)	Width (m)	Discharge (m^3/s)	Valley slope (m/m)	Duration of study (years)
Run 11	10	8	19	0,004	10 (5 days)
Run 12	20				
Run 13	30				

Planform evolution

Chézy number ($m^{1/2}/s$)	Water depth (m)	Averaged velocity (m/s)
10	3,16	0,87
20	1,99	1,38
30	1,51	1,81

For the third case, formative discharge and bankfull discharge are not equal because of the channel depth.

We can observe that velocity increases as the Chézy number increases.

Bed profile after 5 days

Run 11

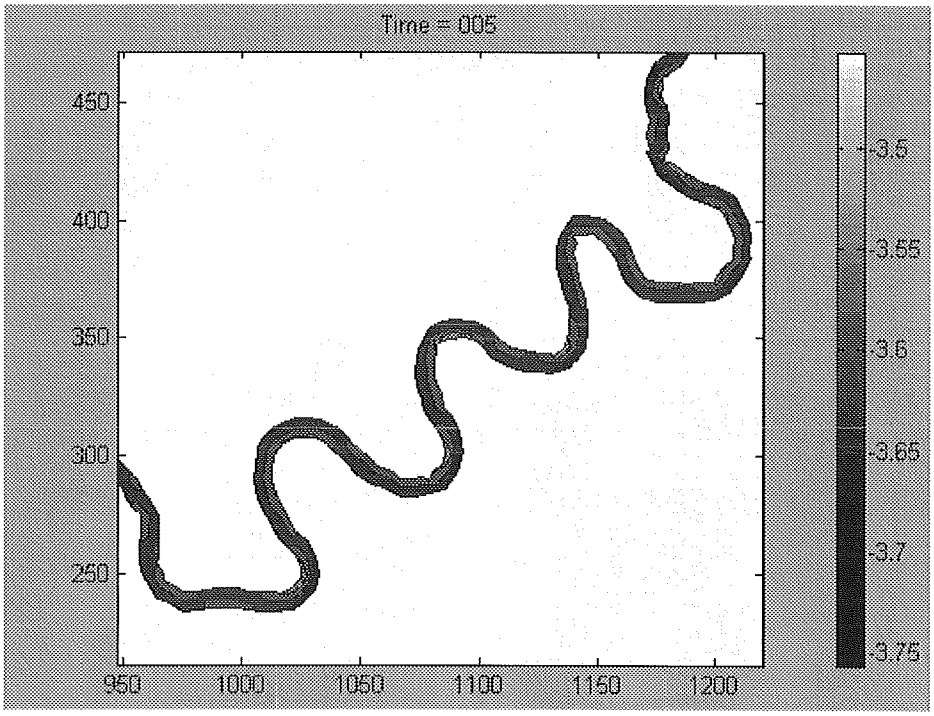

Point bar are more present on the second case (20 m $^{1/2}$/s). Velocity for smaller Chézy numbers is very small and few sediments are transported. Higher Chézy values imply higher velocities that might carry more materials downstream.

Their position is in the three cases downstream of the apex of the bend.

Run 12

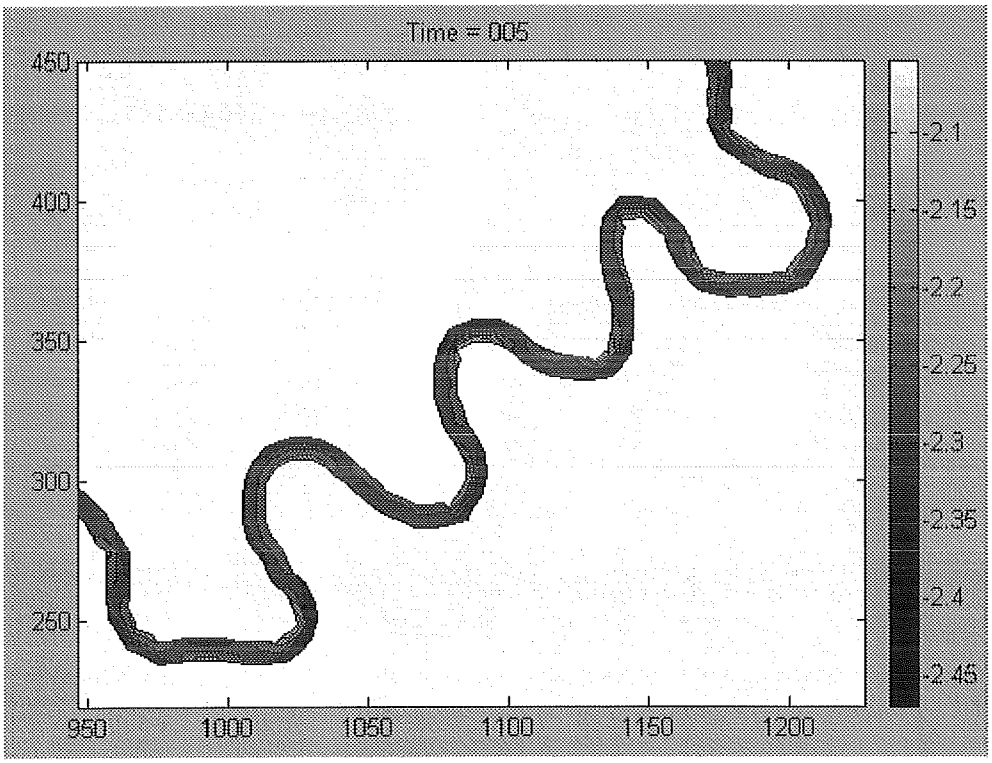

Run 13

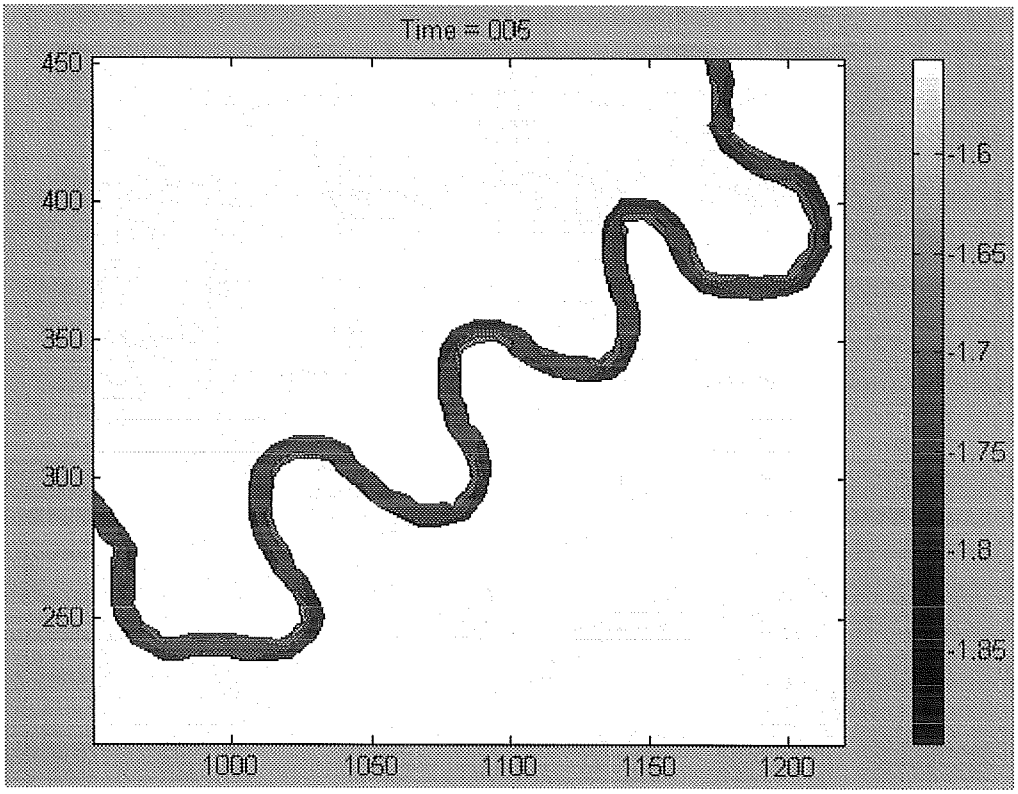
Time = 005
450
400
350
300
250
1000
1050
1100
1150
1200
-1.6
-1.65
-1.7
-1.75
-1.8
-1.85